



THE HONG KONG  
POLYTECHNIC UNIVERSITY

香港理工大學

Pao Yue-kong Library  
包玉剛圖書館

---

## Copyright Undertaking

This thesis is protected by copyright, with all rights reserved.

**By reading and using the thesis, the reader understands and agrees to the following terms:**

1. The reader will abide by the rules and legal ordinances governing copyright regarding the use of the thesis.
2. The reader will use the thesis for the purpose of research or private study only and not for distribution or further reproduction or any other purpose.
3. The reader agrees to indemnify and hold the University harmless from and against any loss, damage, cost, liability or expenses arising from copyright infringement or unauthorized usage.

If you have reasons to believe that any materials in this thesis are deemed not suitable to be distributed in this form, or a copyright owner having difficulty with the material being included in our database, please contact [lbsys@polyu.edu.hk](mailto:lbsys@polyu.edu.hk) providing details. The Library will look into your claim and consider taking remedial action upon receipt of the written requests.

**The Hong Kong Polytechnic University**  
**School of Nursing**

**Clinical Evaluation of Non-invasive Blood  
Glucose Measurement by Using Near Infrared  
Spectroscopy via Inter- and Intra-subject  
Analysis**

by

Lam, Chak Hing

A thesis

Submitted in partial fulfillment of the  
requirement for the degree of  
Doctor of Philosophy

September, 2008

## **CERTIFICATE OF ORIGINALITY**

I hereby declare that this thesis is my own work and that, to the best of my knowledge and belief, it reproduces no material previously published or written, nor material that has been accepted for the award of any other degree or diploma, except where due acknowledgement has been made in the text.

Signature

Lam, Chak Hing

# **Abstract**

## **Introduction**

Non-invasive blood glucose measurement through near infrared (NIR) is possible but its reliability is questioned. The aim of the thesis is to evaluate the reliability of non-invasive blood glucose measurement by using NIR spectroscopy.

## **Methods**

The experiments on glucose solutions provided positive results, which were followed by three clinical trials on healthy people and diabetic patients. The NIR transmittance method was applied on the first two clinical trials, while the NIR reflectance method was used on the last clinical trial, which was specifically designed for intra- and inter-subject comparisons. Partial least square (PLS) regression and preprocesses of piecewise, direct standardization (PDS) and Savitsky-Golay smoothing and differentiation (Savgol) were used for the glucose prediction and comparison.

## **Results and Discussions**

A higher predictability of NIR glucose measurement was found from the spectra of the intra-subject when compared with the inter-subject. The R correlation coefficient of prediction ( $R_p$ ) of inter-subject ranged from 0.73 to 0.80, while  $R_p$  of intra-subject were 0.90 to 0.94. The root mean square error of prediction (rmsep) ranged from 2.49 to 3.52mmol/l (inter-subject) and 1.49 to 2.10mmol/l (intra-subject). The  $R_p$  of intra-subject were 15 to 25% higher than that of inter-subject. The rmsep of

intra-subject was 43 to 74% lower than that of inter-subject. In addition, the results also supported the proportion that a larger calibration sample size to prediction sample size ratio provided a better prediction, in which  $R_p$  and  $rmsep$  could reach 0.92 and 1.71mmol/l, respectively, for 4:1 ratio (calibration sample size-to-prediction sample size). The Savgol preprocess was clinically proven to be suitable for the NIR spectroscopic reflectance measurement of human fingers. The NIR method provides an instantaneous measure to the glucose in blood. However, the method may be affected by physiological influences over long-term measurements.

## **Conclusions**

Non-invasive NIR blood glucose measurement was achievable for an instantaneous measure. The major effect for NIR spectroscopic measurement was the physiological difference. Therefore, the development should focus on intra-subject data acquisition which showed relatively low physiological influence. Sufficient sampling data for calibrations and prediction were also vital, with boosting by a suitable preprocess.

## **Acknowledgements**

I would like to acknowledge many individuals and groups who gave of their time and wisdom in my PhD study. Prof. Thomas K.S. Wong, Prof. Joanne W.Y. Chung and Dr. K. L. Fan provided their supervision and guidance during my study and provided helpful comments in the writing of my thesis. Thanks to the ASD team and Nigel for their initial technical support. I am indebted to Prof. P. L. Tang, Prof. Iris Benz and their teams for their expertise in biochemical tests and clinical trial advice.

I am especially grateful to Dr. Jennings who provided guidance on the mathematical analysis. I must thank Prof. David Jessops and Prof. Roger Watsons for their helpful comment on my thesis writing. I would like to thank the support from Integrative Community Health Centre and Princess Margaret Hospital for the recruitment of diabetic patients.

I am appreciative for the prayer support from the Barnabas Fellowship and Baptism class. I especially need to thank my parents and my two brothers for their support and understanding. I gratefully give thanks to my wife, Queenie Ma, who provides many great supports and patiently gives me opportunity to study.

## **Papers, Patents and Awards**

### **Accepted Paper with minor changes needed:**

1. **Lam SCH**, Chung JWY, Fan KL, Wong TKS: Non-invasive Blood Glucose Measurement by Near Infrared Spectroscopy: Machine Drift, Time Drift and Physiological Effect. Spectroscopy – Biomedical Applications.

### **Patents:**

1. Method for Predicting the Blood Glucose Level of a Patient Using a Near Infrared Spectral Scan (US Patent No.7,409,239 issued on 5 August 2008)

### **Awards:**

1. Bronze Medal, Non-Invasive Blood Glucose Meter - Qualitative Analysis, the 54th World Exhibition of Innovation, Research and New Technology, Brussels, Belgium, 2005
2. Jury Commendation and Gold Medal, Non-Invasive Blood Glucose Meter - Alpha Version for Quantitative Analysis, the 35th International Exhibition of Inventions, New Techniques and Products, Geneva, Switzerland, 2007

## Table of Contents

Abstract.....	ii
Introduction .....	ii
Methods.....	ii
Results and Discussions .....	ii
Conclusions .....	iii
Acknowledgements.....	iv
Papers, Patents and Awards .....	v
Table of Contents .....	vi
List of Figures .....	xiii
List of Tables .....	xvii
Chapter 1 Introduction .....	1
1.1 Preface .....	1
1.2 Glucose measurements .....	2
1.2.1 Non-invasive briefing .....	3
1.2.2 Non-invasive approach.....	4
1.2.3 Stage 1: Ground work among glucose solution.....	4
1.2.4 Stage 2: Studies among diabetics .....	5
1.2.5 Stage 3: Short-term measurement among non-diabetics .....	5
1.2.6 Stage 4: Longitudinal measurement for diabetics .....	5
1.3 Aims .....	6
1.4 Objectives.....	7
1.5 Research approach.....	8
1.6 Thesis organization .....	10
Chapter 2 Literature Review .....	14
2.1 Background .....	14
2.1.1 Diabetes prevalence .....	14
2.1.2 Diabetes classifications.....	14
2.1.3 Diabetes complications.....	17
2.1.4 Diabetes management.....	17
2.2 Blood glucose monitoring .....	18



2.2.1 Invasive.....	19
2.2.2 Semi-invasive .....	20
2.2.3 Non-invasive.....	21
2.3 Non-invasive blood glucose monitoring technologies .....	21
2.3.1 Fluorescence .....	22
2.3.2 Photoacoustic.....	22
2.3.3 Optical coherence tomography .....	24
2.3.4 Polarization changes .....	25
2.3.5 Raman spectroscopy .....	26
2.3.6 Mid-infrared.....	27
2.3.7 Near infrared.....	28
2.3.8 Summaries of the non-invasive approach for glucose measurement .....	29
2.4 Blood Glucose .....	30
2.4.1 Dietary carbohydrates.....	31
2.4.2 Mechanism of blood glucose regulation.....	31
2.4.3 Glucose .....	32
2.5 Skin tissue and finger structure .....	33
2.5.1 Finger.....	33
2.5.2 Human tissue .....	33
2.6 <i>In Vitro</i> clinical trials.....	34
2.7 <i>In Vivo</i> clinical trials .....	36
2.7.1 Oral glucose tolerance test.....	36
2.8 Other considerations.....	38
2.8.1 Machine drift and time drift consideration .....	38
2.8.2 Temperature consideration .....	39
2.8.3 Contact interface consideration .....	40
2.8.4 Location of the body.....	41
2.9 Calibration and prediction .....	43
2.10 Analytical method .....	44
2.10.1 Transmittance and reflectance .....	44
2.10.2 Absorbance .....	46
2.10.3 Beer-Lambert law .....	46

2.10.4 Partial least squares regression (PLS Regression).....	48
2.10.5 Nonlinear iterative partial least square (NIPALS) and SIMPLS.....	50
2.10.6 Clarke grid error plot .....	50
2.11 Conclusions .....	52
Chapter 3 Methods.....	54
3.1 Preprocess.....	54
3.1.1 The Savitsky-Golay smoothing and differentiation (Savgol).....	54
3.1.2 Piecewise direct standardization (PDS).....	56
3.1.3 Simple mean centred preprocess .....	57
3.2 Data analysis and presentation .....	58
3.2.1 PLS .....	58
3.3 Predictability .....	59
3.3.1 Rp correlation .....	60
3.3.2 Root mean square error of prediction .....	61
Chapter 4 Stage 1: Ground Work among Glucose Solutions .....	62
4.1 Glucose solutions test.....	62
4.1.1 Objectives .....	62
4.1.2 Apparatus and equipment .....	62
4.1.3 Materials/samples .....	64
4.1.4 Procedures .....	65
4.1.5 Characteristics .....	65
4.1.6 Analytical Techniques .....	66
4.2 Results .....	68
4.2.1 Glucose concentration measurement .....	68
4.2.2 Glucose solutions measurement on the same day .....	69
4.2.3 Glucose solution measurements on different days .....	73
4.3 Discussion .....	77
4.3.1 NIR absorbance and PLS.....	78
4.3.2 Overtones.....	80
4.3.3 Error and noise.....	81
4.4 Conclusions .....	83
Chapter 5 Stage 2: Studies among Diabetics .....	84

5.1 Clinical research on diabetic patients .....	84
5.1.1 Objectives .....	84
5.1.2 Apparatus and equipment .....	84
5.1.3 Subjects .....	85
5.1.4 Procedures .....	85
5.1.5 Characteristics .....	85
5.1.6 Analytical techniques .....	86
5.2 Results .....	87
5.2.1 Spectra .....	87
5.2.2 Prediction .....	89
5.2.3 Comparisons .....	92
5.3 Discussion .....	93
5.3.1 Simple mean-centred preprocess .....	95
5.3.2 Savgol Preprocess .....	96
5.3.3 PDS preprocess .....	97
5.3.4 Calibration and noise .....	98
5.4 Conclusions .....	99
Chapter 6 Stage 3: Short-term Measurement among Non-Diabetics.....	100
6.1 Non-diabetic subjects .....	100
6.1.1 Objectives .....	100
6.1.2 Apparatus and equipment .....	101
6.1.3 Subjects .....	101
6.1.4 Procedures .....	101
6.1.5 Characteristics .....	102
6.1.6 Analytical techniques .....	102
6.2 Results .....	103
6.2.1 Spectra .....	103
6.2.2 Predictions .....	104
6.2.3 Comparisons .....	110
6.3 Discussion .....	111
6.3.1 Spectra .....	111
6.3.2 Simple mean-centred preprocess .....	113

6.3.3 Savgol preprocess .....	114
6.3.4 PDS preprocess .....	115
6.3.5 Prediction amongst inter- and intra-subject .....	116
6.3.6 Physiology against time .....	117
6.3.7 Transmittance and reflectance NIR measurement .....	118
6.4 Conclusions .....	120
Chapter 7 Stage 4: Longitudinal Measurement for Diabetics .....	122
7.1 Diabetic clinical trial from a community clinic .....	122
7.1.1 Objectives .....	122
7.1.2 Apparatus and equipment .....	123
7.1.3 Subjects .....	124
7.1.4 Procedures .....	125
7.1.5 Characteristics .....	125
7.1.6 Analytical technique .....	128
7.2 Results .....	129
7.2.1 Prediction by PLS .....	133
7.2.2 Comparison and summary .....	139
7.3 Discussion .....	141
7.3.1 Reflectance against transmittance NIR spectroscopy .....	141
7.3.2 Pros and cons of using fingertips for NIR measurement .....	142
7.3.3 Consideration of the measurement on arms .....	143
7.3.4 Finger prick glucose meter .....	144
7.3.5 Measurement locations and blood effect .....	145
7.3.6 Force for the measurement area .....	145
7.3.7 Temperature effect .....	146
7.3.8 Physiological effect against Reliability .....	147
7.3.9 Spectral variations .....	148
7.4 Conclusions .....	149
Chapter 8 Evaluation of Preprocesses .....	150
8.1 Objectives .....	151
8.2 Predictions and comparisons .....	151
8.3 PLS prediction with simple mean centred preprocess .....	152

8.4 PDS preprocessing .....	153
8.5 Savgol preprocess.....	158
8.6 Discussion .....	162
8.6.1 Spectral variation.....	162
8.6.2 Simple mean-centred preprocess (SMCG).....	163
8.6.3 PDS.....	164
8.6.4 Savgol.....	164
8.7 Conclusions .....	165
Chapter 9 Evaluation of the Effect of Sampling Size Ratio of Calibration to Prediction .....	166
9.1 Objectives.....	166
9.2 Calibration size comparison .....	167
9.2.1 Calibration - large scale.....	167
9.2.2 Calibration - small scale .....	169
9.3 Discussion .....	176
9.3.1 Sampling size for calibration.....	177
9.3.2 Calibration .....	179
9.4 Conclusions .....	179
9.5 Future Work .....	179
Chapter 10 Physiological Evaluation by Inter- and Intra-subject.....	180
10.1 Objectives.....	180
10.2 Inter-subject glucose prediction .....	181
10.2.1 Results .....	181
10.3 Intra-subject glucose prediction .....	190
10.3.1 Results .....	190
10.4 Discussion .....	196
10.4.1 Intra- and inter-subject.....	196
10.4.2 Time drift and machine drift.....	198
10.4.3 Physiological effect .....	199
10.4.4 NIR spectra vs. body tissue .....	199
10.4.5 Effect of finger thickness.....	201
10.4.6 NIR spectra by PLS .....	202

10.4.7 Temperature effect.....	204
10.5 Conclusions .....	205
10.6 Future work .....	206
Chapter 11 Conclusions .....	207
11.1 Introduction .....	207
11.1.1 Objectives of each stages.....	208
11.1.2 Summary of significant results .....	210
11.1.3 Conclusions .....	211
Appendix A Apparatus and Equipment .....	A1
Appendix B Experiment and Clinical Trials Procedures .....	A11
Appendix C Temperature of Fingers .....	A15
References.....	I

## List of Figures

(In original colours)

Figure 2-1: D-Glucose Transformation .....	32
Figure 2-2: Skin and tissue cross-sectional structure .....	34
Figure 2-3: Light intensity passing through a sample; $I_0$ : incident light, $I_r$ : reflected light, $I_t$ : transmitted light, $I_e$ : light emitted and received to and from other source. ....	45
Figure 2-4: Light passing material with path length = $l$ .....	48
Figure 2-5: Clarke Grid Error plot .....	51
Figure 3-1: Block Diagram – PLS prediction with Savgol preprocess.....	55
Figure 3-2: PDS preprocessing for PLS application.....	56
Figure 4-1: Control Development’s NIR spectroscopy of NIR-128L-1.7-USB; 1: tungsten halogen light; 2: optical light stand; 3: optical white plate; 4: optical extension rods; 5: optical fiber; 6: USB cable; 7: spectrometer; 8: spectral reading program with computer .....	64
Figure 4-2: Block Diagram – Glucose concentration Analysis .....	65
Figure 4-3: Block Diagram - PLS prediction process of glucose solution concentration.....	66
Figure 4-4: NIR spectra – Glucose Solutions, Absorbance against wavelength (nm), Day 1, under room condition .....	69
Figure 4-5: Absorbance at 1180nm against glucose concentration, separated experiment in one hour; fit of Day 3a is close to fit of Day 3b.....	71
Figure 4-6: PLS prediction scatter plot, separated experiment in the same day within one hour; cross (x) = calibration; hollow (o) = prediction.....	72
Figure 4-7: Absorbance at 1180nm against glucose concentration, two experiments with a two-month separation.....	74
Figure 4-8: PLS prediction scattered plot, separated experiment in different days in two month – cross (x) = calibration; hollow (o) = prediction.....	75
Figure 5-1: NIR spectroscopy measurement process.....	86
Figure 5-2: Block Diagram – PLS prediction of the blood glucose levels from diabetic patient at a regional hospital.....	86
Figure 5-3: NIR spectra – ten diabetic subjects, absorbance against wavelength (nm); highly noises at 1381-1701nm caused by finger blocking the light transmission .....	88
Figure 5-4: Predicted against Actual Blood Glucose Level: (x) calibration, (o) prediction; data was arranged to an ascending order and preprocessed by simple mean-centered preprocess. ....	89

Figure 5-5: Predicted against Actual Blood Glucose Level: (x) calibration, (o) prediction; data was arranged to ascending order and preprocessed by simple mean-centered preprocess and PDS preprocess. ....	90
Figure 6-1: Absorbance against wavelength (Stage 3); high noises at 1381-1701nm caused by finger blocking the light transmission.....	104
Figure 6-2: Scatter plot of predicted glucose level against Finger Prick blood glucose level, where is treated by simple mean centered preprocess; full wavelength range was used, (x) calibration, (o) prediction. ....	105
Figure 6-3: Scatter plot of predicted glucose level against finger-prick blood glucose levels where glucose level had been sorted in ascending order and treated by simple mean-centered preprocess, full wavelength range was used, (x) calibration, (o) prediction.....	106
Figure 6-4: Scatter plot of predicted against finger prick blood glucose level, where spectra of full wavelength range were treated by simple mean-centered preprocess and Savgol preprocess; non-arranged data, (x) calibration, (o) prediction. ....	107
Figure 6-5: Scatter plot of the prediction against the finger-prick blood glucose level with a simple mean-centered preprocess and Savgol preprocess; glucose level had been sorted in ascending order, using wavelength 905 to 1380 nm, (x) calibration, (o) prediction. ....	108
Figure 6-6: Scatter plot of predicted against finger-prick blood glucose level with simple mean-centered preprocess and PDS preprocess, for full wavelength and non-arranged data, (x) calibration, (o) prediction.....	109
Figure 7-1: NIR spectroscopic probe measurement with customized finger mould	124
Figure 7-2: Finger prick against venous blood glucose level, forearm (Plasma Glucose), $R = 0.9$ , $rmse = 1.40mmol/l$ .....	129
Figure 7-3: Finger-to-finger glucose levels comparison by finger-prick glucose meter .....	131
Figure 7-4: Absorbance against wavelength (from left thumb of Subject 26, intra-subject) .....	132
Figure 7-5: Prediction scatter plot from the community clinic – Thumb, plot of all the predicted glucose levels together against the reference/finger-prick glucose level.....	134
Figure 7-6: Prediction scatter plot from the community clinic – index finger, plot of all the predicted glucose level together against the reference/finger-prick glucose level.....	135
Figure 7-7: Prediction scatter plot from the community clinic – middle finger, plot all the predicted glucose level together against the reference/finger-prick glucose level.....	136



Figure 7-8: Prediction scatter plot from the community clinic– ring finger, plot all the predicted glucose level together against the reference/finger-prick glucose level.....	137
Figure 7-9: Prediction scatter plot from the community clinic – little finger, plot all the predicted glucose level together against the reference/finger-prick glucose level.....	138
Figure 7-10: Intra-subject, R correlation coefficient of prediction (Rp) comparison .....	139
Figure 7-11: Intra-subject, on his/her 30 data sets, root mean square error prediction (RMSEP) comparison. ....	140
Figure 8-1: Bar chart of R correlation coefficient of prediction comparison, Rp; PLS with simple mean-centered preprocess for the intra-subject.....	152
Figure 8-2: Bar chart of root mean square error of prediction, rmsep; PLS with simple mean-centered preprocess for the intra-subject.....	153
Figure 8-3: Spectra plot after the preprocessing of the PDS.....	154
Figure 8-4: Variance Comparison Plot of NIR spectra - PDS preprocess vs. Non-treated (simple mean-centered preprocess).....	155
Figure 8-5: Rp correlation coefficient, PLS with PDS preprocess .....	156
Figure 8-6: RMSEP (Root Mean Square Error Prediction), PLS with PDS preprocess .....	157
Figure 8-7: Absorbance against Wavelength after 2nd derivative with Savitsky-Golay smoothing and differentiation (Savgol).....	158
Figure 8-8: Variance Plot of 2nd Derivative with Savitsky-Golay smoothing and differentiation (Savgol) .....	159
Figure 8-9: Correlation coefficient of prediction (Rp) comparison; Rp_combine: Rp obtained by all predicted glucose levels and the corresponding finger-prick glucose levels.....	160
Figure 8-10: RMSEP (Root mean square error prediction) comparison; rmsep_combine: the rmsep between the predicted glucose levels and the finger-prick glucose levels. ....	161
Figure 9-1: R correlation coefficient of prediction, Rp; little finger Rp by using the calibrations of the thumb, index, middle and ring fingers, respectively. ....	172
Figure 9-2: Root mean square error prediction, rmsep; little finger rmsep by the calibrations of thumb, index, middle and ring fingers. ....	174
Figure 9-3: Rp of prediction from different calibrations sets: 1-4.....	175
Figure 9-4: rmsep of prediction from different sets of calibrations 1-4.....	176
Figure 10-1: Variance comparison between intra- and inter-subjects .....	182

Figure 10-2: Inter-subject: calibrated by index + middle + ring + little fingers to predict blood glucose level of thumbs. ....	183
Figure 10-3: Inter-subject: calibrated by thumb + middle + ring + little fingers to predict blood glucose level of index fingers. ....	184
Figure 10-4: Inter-subject: calibrated by thumb + index + ring + little fingers to predict the blood glucose level of middle fingers. ....	185
Figure 10-5: Inter-subject: calibrated by thumb + index + middle + little fingers to predict blood glucose level of ring fingers.....	186
Figure 10-6: Inter-subject: calibrated by thumb + index + middle + ring fingers to predict blood glucose level of little fingers.....	187
Figure 10-7: Rp of predicted blood glucose level from each finger by using the other four fingers as the calibration.....	188
Figure 10-8: RMSEP of predicted blood glucose level from each finger by using the other four fingers as the calibration.....	189
Figure 10-9: Intra-subject, calibrated by index + middle + ring + little fingers to predict blood glucose level of thumbs. ....	191
Figure 10-10: Intra-subject: calibrated by thumb + middle + ring + little fingers to predict blood glucose level of index fingers. ....	192
Figure 10-11: Intra-subject: calibrated by thumb + index + ring + little fingers to predict glucose level of middle fingers. ....	193
Figure 10-12: Intra-subject: calibrated by thumb + index + middle + little fingers to predict glucose level of ring fingers.....	194
Figure 10-13: Intra-subject: calibrated by thumb + index + middle + ring fingers to predict glucose level of little fingers. ....	195

## List of Tables

(In original colors)

Table 2-1: Summary and Comparison of the optical light for the non-invasive blood glucose application.....	29
Table 4-1: R correlation of coefficient and rmse (root mean square error) comparison; absorbance of Day 1 > 0.06 AU of absorbance of Day 2 ....	76
Table 5-1: Results of the regional hospital, R correlation coefficient of calibration/prediction (Rc/Rp) and root mean square error of calibration/prediction (rmsec/rmse) comparisons. No preprocess: simple mean-centered preprocess; Savgol preprocess: Savgol with simple mean-centered preprocess; pds preprocess: PDS with simple mean-centered preprocess; sorted: data arranged into ascending order .....	92
Table 6-1: R correlation coefficient of calibration/prediction (Rc/Rp) and root mean square error of calibration/prediction (rmsec/rmse) comparisons. No preprocess: simple mean-centered preprocess; Savgol preprocess: simple mean-centered and Savgol preprocesses; pds preprocess: simple mean-centered and PDS preprocesses; sorted: data arranged in ascending order .....	110
Table 9-1: Calibration-to-prediction arrangement where each column represents each finger and the calibration combination; 1 = thumb, 2 = index finger, 3 = middle finger, 4 = index finger, 5 = little finger .....	171
Table 10-1: Data arrangement of stage 4 clinical trial.....	203

# Chapter 1

## Introduction

### 1.1 Preface

The incidence of diabetes is increasing. Diabetes is an incurable disease with many associated complications. It is a disease in which blood glucose levels cannot be regulated normally, by the body alone. The possible treatment methods involve controlling blood glucose levels via dietary regulation, oral medication and/or insulin injection, all of which have adverse effects on daily living. The control of blood glucose levels relies on blood glucose measurement. Currently, diabetic patients are recommended to check their blood glucose levels frequently by using a finger prick glucose meter. This practice can help to closely monitor blood glucose levels. Thus, diabetic patients and their physicians can obtain a clear picture of blood glucose for therapy optimization. This is also an indicator for the insulin dosage adjustment amongst the diabetic patients who need daily insulin injections.

However, finger pricking for blood glucose is not easy for diabetics who need to check their glucose levels several times a day. This is a painful experience. This may also result in damage to the finger tissue in the long term. It also increases the risk of infection. The finger-prick glucose meter is only a discrete glucose measurement device. It is not practical for continuously monitoring blood glucose. Some incidences of hyperglycemia or hypoglycemia may not be recorded between

the measurements. Further, the resultant monitoring may not fully represent the blood glucose pattern.

Non-invasive, continuous blood glucose measurement normally does not require blood sampling. Thus, it can help to reduce a lot of the painful pricking experience, while obtaining a clearer blood glucose trend. Therapy can then be optimized on the basis of a continuous measurement of blood glucose. However, this device is still under development and validation, and a truly reliable, non-invasive blood glucose meter has, as yet, to be achieved.

## **1.2 Glucose measurements**

Blood glucose is controlled homeostatically; diabetes mellitus (DM) disrupts this mechanism and causes many complications (1), such as high blood pressure and high cholesterol, which may lead to heart disease and stroke (2). Blood glucose monitoring, therefore, is necessary to avoid many diabetic complications. Conventionally, blood glucose is monitored by pricking the finger to obtain the capillary blood sample (3). Diabetic patients are advised to check their blood glucose several times per day (4). Sometimes, they may feel that the frequent checking is too burdensome (4). A patient who has diabetes for 20 years, and checks his/her blood glucose three times daily, will prick his/her finger more than 21,900 times (5). The risk of being infected is therefore increased, as are the inconvenience and discomfort. A non-invasive approach for blood glucose measurement would be a

very good solution to stop the pain and reduce the risk of infection amongst diabetic patients.

### **1.2.1 Non-invasive briefing**

Non-invasive blood glucose measurement provides a technique for blood glucose measurement without pricking for a blood sample or body fluid in the tissue underneath the skin (6). The non-invasive concept was launched more than 20 years ago, but still no reliable system has been delivered. Many researchers have tried to produce a non-invasive blood glucose meter with variable results. The repeated testing had sometimes demonstrated improvement, while other groups showed poorer prediction rates. Non-invasive blood glucose measurement is possible by using near infrared (NIR) spectroscopy, or other optical approaches, but the method is still unreliable. Many problems remain unsolved, perhaps due to individual differences in physiology. Changes in metabolism/physiology in response to temperature and physical activity, as well as body temperature, may consequently affect the glucose level. Blood contains tiny quantities of glucose, but this quantity can vary materially depending on outlying components in the blood. Other blood components such as protein, triglycerides and red blood cells (RBC) may significantly interfere with glucose measurement. These dependent, physiological processes can make calibration difficult.

Error sources due to detector position, temperature and cardiac pulse effect, motion, mechanical pressure of the test device, hydration state, sweat, blood volume and hematocrit change (7) may introduce uncertainty into blood glucose measurement. Amongst many optical, non-invasive blood glucose methods,

researchers tend to use NIR as the method of choice due to its stable process, strong signal-to-noise (S/N) ratio under the room conditions and low interference by other biological components (8).

### **1.2.2 Non-invasive approach**

The non-invasive blood glucose meter is the preferred approach used to closely monitor the glucose levels of diabetic patients. NIR spectrometer was selected for the development of the non-invasive blood glucose measurement. The experiment and the clinical trials were divided into four stages. These were tests on glucose solutions for obtaining a basis of NIR spectra to glucose concentrations. Both transmittance and reflectance of NIR spectroscopic measurements were used for the clinical trials, in which volunteer diabetic and non-diabetic subjects joined the trials. The following shows the brief description of each stage.

### **1.2.3 Stage 1: Ground work among glucose solution**

Glucose concentration tests using NIR spectroscopy were performed. Several different tests were carried out in a closed chamber where the humidity and the temperature were controlled in a typical room environment. The tests were used to obtain the basis of different glucose concentration to NIR spectroscopic measurements. The effects from machine drift and time drift in the measurements were also investigated in this stage.

#### **1.2.4 Stage 2: Studies among diabetics**

Ninety-nine diabetic patients volunteered for this clinical trial. The transmittance NIR spectroscopic measurement was used. Fasting blood glucose levels were obtained and tested, from the arm, in the laboratory. The results were positive for the non-invasive blood glucose measurement for about 98% of the predicted glucose levels, located within clinically acceptable regions in the Clarke Grid Error plot (9). However, further improvement is needed for higher reliability.

#### **1.2.5 Stage 3: Short-term measurement among non-diabetics**

This stage used transmittance NIR spectroscopic measurement to obtain the data from non-diabetic subjects within four hours. Two finger-prick glucose levels and three NIR spectroscopic measurements were obtained in total, in which one set of finger-prick glucose levels and one set of spectral readings were from preprandial and one set of finger-prick glucose levels and two sets of spectral readings were from postprandial. The results from different spectral ranges were compared in different preprocesses. This showed that a larger spectral range could obtain higher predicted results. This also showed that NIR spectroscopic measurement was feasible for non-diabetics as well.

#### **1.2.6 Stage 4: Longitudinal measurement for diabetics**

This was the clinical trial on diabetic patients. It was designed and completed in three months using reflectance NIR spectroscopic measurements. Each patient visited 30 times during the trial. Partial Least Square (PLS) was the principal analysis tool used with preprocesses. The data were extracted for preprocess



comparison; specifically, for testing the sampling size ratio. The designed clinical trial was also used for the comparisons between glucose predictions from inter- and intra-subject, in which the physiological effect was evaluated. The results provided indications for the improvement of non-invasive blood glucose measurement approach.

### **1.3 Aims**

Currently, many researchers have focused on developing mathematical models for prediction. However, the results obtained have only little improvement on the current approach, and some were even poorer. Reliability is needed. The current researchers have used different methods for their investigations. Some results showed a positive improvement on NIR spectroscopic measurements, while many of them were poorer. Some scientists mentioned that intra-subject analysis was better than inter-subject analysis for non-invasive blood glucose measurement by NIR spectroscopy. However, there are no strong clinical data supporting these claims. This causes many researchers to continue to work on inter-subject analysis.

In addition, the sampling size for this application is varied. Sometimes, an inappropriate preprocess for calibration and prediction on PLS may be used. Other questions may be raised on the elimination of drift effects and physiological effect.

The aim of this thesis is to evaluate development of the non-invasive blood glucose measurement in intra- and inter-subjects, focusing on the following items:

- To evaluate the possibility of non-invasive blood glucose measurement by NIR;
- To evaluate the most suitable ways for non-invasive blood glucose measurement, clinically supported, and evaluate the ratio of the sampling size of the calibration to sampling size of the prediction and
- To evaluate the analysis between intra-subject and the inter-subject.

#### **1.4 Objectives**

- Propose a new method for comparison of non-invasive blood glucose measurement via NIR spectroscopy between inter- and intra-subjects;
- Compare intra-subject prediction and inter-subject prediction for NIR spectroscopic measurement among *in vivo* non-invasive blood glucose measurement;
- Evaluate the calibration to prediction sample data ratio;
- Compare the reflectance and transmittance approaches in human finger measurement;
- Evaluate whether partial least square (PLS) regression with preprocess is able to reduce machine drift and time drift and
- Evaluate both short- and long-terms NIR spectroscopy blood glucose measurement.

## **1.5 Research approach**

Four stages of the non-invasive glucose measurement were designed and tested. The first stage (Stage 1) was glucose solution measurement using NIR spectroscopy. In this stage, PLS and Beer's law approaches were applied and compared. Results showed that NIR could measure glucose concentration either by using PLS prediction or by using the Beer's law approach. However, machine drift and time drift existed for long-term measurement.

In the second study (Stage 2), NIR measurement was used for diabetic patients to analyze the NIR spectra with venous blood glucose under fasting conditions. Higher error and more interference were observed, although PLS was used for the analysis.

In the non-diabetic study (Stage 3), meal tolerance measurements (NIR and finger prick glucose levels) between fasting and post-prandial conditions were obtained. This showed relatively higher predictably than the previous study (Stage 2). Results initially demonstrated that reliability in short-term glucose measurement was more achievable.

The last clinical trial (Stage 4) was specifically designed for the comparison between intra- and inter-subjects' glucose predictions, which enabled the comparison between inter-subject data and that of the intra-subjects, with a limiting physiological influence. PLS with preprocess Savitsky-Golay smoothing and differentiation (Savgol) were the principal analytical tools for glucose prediction in this study. Reflectance NIR spectroscopic measurement, through a probe, was used as assistance.

During all the clinical trials, PLS, with two common preprocesses, piecewise direct standardization (PDS) and Savgol, were used for the prediction of blood glucose. The predictabilities were compared by using the R correlation of prediction ( $R_p$ ) and root mean square error of prediction (rmsep).

Calibration is the basis of prediction. The design and analysis of the last clinical trial had demonstrated, preliminarily, that the ratio of the sampling size with regards to the calibration of the sampling size for prediction is important. This result could help to enhance the prediction of the non-invasive blood glucose by NIR spectroscopy.

This thesis helps to standardize NIR spectroscopic measurement. The clinical trial was designed for both inter- and intra-subjects' analysis and comparisons. Using intra-subject analysis for non-invasive blood glucose measurement was recommended. Reflectance NIR spectroscopic measurement was more suitable than transmittance NIR spectroscopic measurement via fingertip glucose levels. Small NIR spectral variance might indicate the higher prediction, but it demonstrated that it might be interference by selecting an improper preprocess.

## **1.6 Thesis organization**

### Chapter 1: Introduction

This chapter briefly describes the aims and objectives of the thesis, as well as the contributions of this thesis. The necessity of blood glucose measurements to a diabetic patient and the need for a non-invasive blood glucose method and the uncertainty of its results were introduced. Thesis organization was also highlighted.

### Chapter 2: Literature Review

This chapter provides the background of the previous, relevant research in non-invasive blood glucose measurement. It briefly described diabetes and its complications, as well as the contraindications of frequent finger-prick glucose measurements and how they could affect daily life. It also reviewed the literature and compared different *in vivo* and *in vitro* glucose measurement methods, from traditional invasive glucose monitoring to non-invasive blood glucose methodology and also discussed their respective advantages and disadvantages. The different non-invasive methods were introduced, with reporting on the continuous measurement. Some preprocessing methods, PLS and Beer's Law, were discussed.

### Chapter 3: Methods

The thrust of this portion of the research was to design a blood glucose measurement approach. Analytical methods were designed and introduced in this chapter for non-invasive blood glucose calibration and prediction. The method of comparison on

predictability – Rp and rmsep was also included. The prediction procedures were reported as well.

#### Chapter 4: Stage 1: Ground Work among Glucose Solutions

Preliminary glucose solution concentration was tested by NIR spectroscopy. PLS and Beer's law were used for the analysis. Machine drift and time drift were evaluated in this chapter under PLS and Beer's Law, respectively. Results showed that PLS was able to correct the machine drift and time drift in this case.

#### Chapter 5: Stage 2: Studies among Diabetics

A clinical trial for random blood glucose measurements at a regional hospital was carried out. Both Type 1 and Type 2 diabetic patients were measured by transmittance NIR spectroscopy, and PLS was used in the analysis. A high variance of the spectroscopic signal and the predicted results were found, but over 80% of the predicted glucose levels were located within clinically acceptable regions (under the analysis of the Clarke Grid Error plot, Chapter 2, a description of this analysis was provided). Two different ranges of spectra were compared with full-ranged spectra for prediction analysis.

#### Chapter 6: Stage 3: Short-term Measurement among Non-diabetics

A short-term clinical trial held on healthy, non-diabetic subjects with a meal tolerance for non-invasive blood glucose measurements was demonstrated. Results

show a slight improvement in comparison with the previous stage, Stage 2. Two different ranges of spectra for calibration and prediction by PLS were compared with full-ranged spectra of the spectroscopy. The reference glucose levels were obtained by using a finger-prick glucose meter.

#### Chapter 7: Stage 4: Longitudinal Measurement for Diabetics

A clinical trial for the individual diabetic subject was covered. Five fingers from the left hand were measured, for each subject, during each visit. The design of the clinical trial provided for the ability to compare the data between the inter- and intra-subjects. Reflectance NIR spectroscopic measurement was used. Results showed further improvements among Stages 2, 3 and 4. Three spectral peaks have been revealed in the measurement.

#### Chapter 8: Evaluation of preprocesses

This chapter evaluated three preprocesses for PLS by comparing simple mean-centred preprocess (as basis), PDS and Savgol. Although results showed that higher spectral variance might lead to poor prediction, it might be a crucial difference. PDS could reduce the variance of the spectra, but the prediction was worse. Among these preprocesses, Savgol was the best for reflectance NIR spectroscopic measurements via fingertips.

## Chapter 9: Evaluation of the Effect of Sampling Size Ratio of Calibration to Prediction

With the special design implemented for the clinical trial (Stage 4), a preliminary effect of calibration sampling size to prediction sampling size ratio was reported for NIR non-invasive blood glucose measurement. Results showed that the sampling size of data for calibration to prediction should be at least 3:1. A larger calibration-to-prediction ratio might net a higher predictability. This evaluation was limited to 4:1, 3:1, 2:1 and 1:1 ratios.

## Chapter 10: Physiological Evaluation by Inter- and Intra-subjects

This chapter clinically demonstrated and evaluated the relationship between inter- and intra-subject NIR non-invasive blood glucose measurements. The demonstration was analyzed by using Savgol and PLS.  $R_p$  and  $rmsep$  were used for the predicted result comparisons. This chapter also showed that intra-subject data were recommended for further research in order to obtain a more accurate result.

## Chapter 11: Conclusions

Research questions and significant results were summarized in this chapter. Conclusions were reported as well.



## **Chapter 2**

### **Literature Review**

#### **2.1 Background**

Diabetes mellitus (DM) is a chronic and incurable disease caused by the malfunction of insulin production which affects the blood glucose level (1; 10; 11) in the body, normally leading to hyperglycemia. Prolonged hyperglycemia causes damage to nerves and blood vessels (1; 10; 11), which may cause many complications. Thus, the role of blood glucose monitoring and measurement becomes very important for diabetic therapies.

##### **2.1.1 Diabetes prevalence**

The number of diabetics is increasing. According to the World Health Organization (WHO), there were 171 million people with DM worldwide (12; 13). In the year 2030, the number of diabetics may reach to 366 million, of which 90 – 95% will suffer from Type 2 diabetes (13; 14). The highest prevalence was in the developing countries, India and China (20.8 million) in the year 2000 (13). It is predicted that the number of the diabetics will significantly increase to 42.3 million in China after 30 years (13).

##### **2.1.2 Diabetes classifications**

Diabetic Mellitus (DM) can be classified into three different types: Type 1, Type 2 and gestational type. Type 1 and Type 2 diabetes occur most frequently. The

following paragraphs briefly describe their causes, main complications and treatment and controlling method.

Type 1 diabetes(1; 10; 11; 15) is an autoimmune disease with pancreatic islet beta-cell destruction. It is an autoimmune disorder in which the body's own immune system attacks the beta cells in the Islets of Langerhans of the pancreas, destroying them or damaging them sufficiently to reduce insulin production. The autoimmune attack may be triggered by reaction to an infection. A subtype of Type 1 (identifiable by the presence of antibodies against beta cells) develops slowly and so is often confused with Type 2 DM. Also historically called insulin dependent diabetes, it is more commonly found in children and adolescents, and seldom occurs in adults.

Type 1 DM is treated with insulin injections, lifestyle adjustments and the careful monitoring of blood glucose levels (currently via finger prick blood sampling). Insulin injection is also available by an insulin pump, which allows the infusion of insulin 24 hours a day at pre-set levels and the ability to administer boluses of insulin as needed at meal times. This treatment must be continued indefinitely.

Type 2 DM is the most prevalent form of diabetes (1; 13), which results from insulin resistance with an insulin secretory defect. Unlike Type 1 DM, insulin is always present in blood and is sometimes increased. It is a long-term metabolic disorder that is primarily characterized by insulin resistance and consequent hyperglycemia. There is little tendency toward ketoacidosis in Type 2 diabetics (16). Complex and multi-factorial metabolic changes lead to damage and functional impairment of many organs, most importantly the cardiovascular system (2). This

leads to substantially increased morbidity and mortality in both Type 1 and Type 2 patients, but the two have quite different origins and treatments despite the similarity in complications, which are often clinically confused.

Genetic factors, usually polygenic, have been identified in a significant number of patients. Environmental factors, like obesity, lack of exercise and sedentary lifestyle can also lead to insulin resistance. Insulin resistance means that body cells do not respond appropriately when insulin is present.

Type 2 DM is initially treated by dieting and through weight loss in obese patients. This can restore insulin sensitivity, even when the weight loss is modest (17), e.g. around 5 kg. If it is needed, Type 2 DM can be treated with oral anti-diabetic drugs.

If this approach is unsuccessful, insulin therapy may be needed, usually as an adjunct to oral therapy, to maintain normal glucose levels. The term ‘non-insulin-dependent diabetes’ is no longer be used (11). The classification of diabetes is determined by the underlying cause of the diabetes, not the type of therapy. Many Type 2 diabetic patients will progress to require insulin for blood glucose control, but they are still classified as Type 2 diabetics.

Other specific types of diabetes are grouped with the various known etiologies of DM (18). For instance, gestational diabetes mellitus is the term used when an woman has developed diabetes during pregnancy (18).

### **2.1.3 Diabetes complications**

Diabetes is the leading cause of neuropathy in many countries. Neuropathy is the most common complication and greatest source of morbidity and mortality in diabetic patients. The main risk factor for diabetic neuropathy is hyperglycemia. According to the studies from the Diabetes Control and Complications Trial (DCCT) and United Kingdom Prospective Diabetes Study (UKPDS), the progression of neuropathy is dependent on the degree of glycemic control in both Type 1 and Type 2 diabetes (19). Control relies on glucose measurement, which is fundamental to the success of dietary and other therapies.

### **2.1.4 Diabetes management**

Diabetes management aims to minimize chronic diabetes complications and hyperglycemia/hypoglycemia. Poor control of diabetes can cause blindness, limb amputation, heart disease and kidney failure, while adequate diabetic control may lead to lower risk of these complications (14; 20).

As diabetes can lead to many other complications, it is critical to maintain blood glucose levels as close to normal as possible, and diet is the leading factor in this blood glucose control. Thus, regular blood testing is essential for the monitoring of blood glucose and to reduce the chance of long-term side effects from the disease.

Chronic high blood glucose can cause serious diabetic complications, which may be fatal (21). Therefore, it is important that diabetic patients check their blood glucose levels regularly, either daily or every few days, to monitor their diabetic

management. Some patients should check on a more regular, daily, basis due to insulin therapy.

Diabetes can be identified by using the Fasting Plasma Glucose (FPG) Test (22): a fasting blood glucose level between 100 and 125 mg/dl (5.6 and 6.9 mmol/l) can indicate a pre-diabetic state (5). A person with a fasting blood glucose level of 126 mg/dl (7 mmol/l) or higher has diabetes (5). Blood glucose equal to or greater than 200 mg/dL (11.1 mmol/l) at any time of the day, regardless of dietary pattern, is an indicator of diabetes (5).

## **2.2 Blood glucose monitoring**

There are three main types of blood glucose measurement: invasive, semi-invasive and non-invasive. For invasive sampling, finger-prick glucose meters are common and can provide reliable glucose readings. Another alternative glucose monitoring type, called semi-invasive, has also attracted the attention of many scientists. This semi-invasive device relies on the measurement of interstitial fluid or transdermal fluid (23), which gives delayed or different glucose interpretations (24), compared to capillary blood glucose levels. A non-invasive approach is the painless method for blood glucose measurement. However, no non-invasive blood glucose meter currently in use has provided consistently reliable results, due to many interfering non-specific physiological signals during the measurement (especially for long term measurement). Thus, diabetic patients still need to rely on the painful finger-prick sampling for daily glucose measurement. These three main, different types of blood

glucose measurements are discussed in the following sections, with the focus on the ability of non-invasive techniques.

### **2.2.1 Invasive**

Diabetic patients should monitor their blood glucose at least once every day and are advised to record their glucose levels three times a day (5). Finger prick blood glucose metering is the current measurement device for the self-monitoring of blood glucose (SMBG). The various invasive blood glucose monitoring devices are virtually the same. A small blood droplet is obtained by pricking the finger using a lancet (a sterile pointed needle). The blood droplet is usually put onto the end of the test strip while the other end of the test strip is inserted into the glucose meter. This test strip contains various chemicals in the test pad, which change colour in response to the glucose content in the blood (25). These colour changes are then converted into a reading (25). The results displayed on the glucose meter are expressed in either mg/dL (milligrams per decilitre) or mmol/L (millimoles per litre) of blood.

Finger-prick meters do not continuously monitor blood glucose and therefore cannot present a precise glucose trend. In addition, since blood samples are needed for the glucose measurement, this repeated sampling causes pain and damage to the skin tissue, which may raise the chance of infection.

Another invasive approach is the blood plasma or serum test in the laboratory by using biochemical analyzers. This traditional test is the most reliable blood glucose measurement. Patients usually need to have 8-10 hours of fasting prior to the blood test (26). However, it is not applicable for daily monitoring/measurement.

### **2.2.2 Semi-invasive**

Semi-invasive measurements are not as painful as the traditional finger prick devices. Basically, they are mini-invasive devices, which use a tiny sharp pin or laser pin or electrical charge to obtain the body fluid (interstitial/transdermal fluid) from the fingers or other parts of the body for glucose measurement. The measurements are established via the chemical reactions between the sensors and the body fluid. Well-known, semi-invasive blood glucose monitoring devices are GlucoWatch (27-29) and Continuous Glucose Monitoring System (CGMS) (30-33). They are the only two interstitial glucose monitoring devices (using reverse iontophoresis, and an electrochemical-enzymatic sensor) approved by U.S. Food and Drug Administration (FDA) (34-37). GlucoWatch generates an electrical charge to extract interstitial fluid from the subdermal compartment of the skin surface to determine glucose measurement (38). However, skin irritation with this device happens (39). CGMS needs to implant its sensor into the abdominal skin to extract interstitial fluid over a 72-hour monitoring period (30; 40; 41). Both these devices may be described as bloodless, but both are also invasive.

However, interstitial fluid measurement techniques cannot truly represent the blood glucose level since they only reflect the glucose level of the body fluid in the measuring area (24), which can be affected by sweat (39). GlucoWatch does not provide real-time glucose measurement, it obtains a 10-minute delayed glucose level; and in one hour, it can only obtain three readings, which may also cause a 'skipped reading' due to sweat or a significant inconsistency between two readings (39). Both devices need two hours' warming up and finger prick calibrations before

each use. Gebhart et al. (23) conducted clinical trials on the transdermal glucose measurement compared to capillary glucose measurements and found that a lag time of 15 minutes occurs during the rapid glucose change, while Kulcu et al.(24) obtained  $17.2 \pm 7.2$  minutes lag on their research. The delayed reading may cause extreme danger to the diabetic patient if hypoglycemia occurs.

In summary, interstitial fluid is the alternative sampling choice for the capillary blood samples. The measurement claims to be less painful. However, the lag time of the interstitial fluid from the blood samples could lead to a fatal risk if hypoglycemia develops. Thus, a non-invasive glucose monitoring device will be a great choice for diabetic patients for the real-time glucose monitoring.

### **2.2.3 Non-invasive**

Non-invasive blood glucose measurement mainly uses optical light as the medium, such as near infrared, mid infrared, fluorescence, photoacoustic, optical coherence tomography, polarization changes or Raman spectroscopy to determine blood glucose. However, a non-invasive blood glucose meter is not yet ready for diabetic patients to use because 'noise' may cause many unrepeatable and unreliable measurements. These various technologies are discussed in the following section.

## **2.3 Non-invasive blood glucose monitoring technologies**

As mentioned, non-invasive blood glucose measurement has attracted much attention using optical methods. These techniques are reported as shown below:



### **2.3.1 Fluorescence**

Fluorescence can be used to measure blood glucose on the principle that when light is emitted from a laser or an incandescent light to a position on the body, a relatively longer wavelength of light is emitted from the body (42). Visible or ultra-violet (UV) lights are mainly used, but UV and visible light in the surrounding environment may affect the signals and must be screened out from the fluorescence. Sierra et al. (43) developed a glucose test by using wavelengths in the UV region through a biochemical analyzer using glucose oxidase. Ballerstadt and Schultz (44) demonstrated glucose measurement by using wavelengths of 490nm and 520nm. This *in vitro* study was the preliminary for the sensor implantation into the skin for sub-dermal tissue measurement of glucose. The results showed a positive sign for the application of fluorescent light. Some scientists applied this technology by using longer wavelengths of 675nm and 720nm, respectively. However, this application was not used for the non-invasive application; it was successfully applied to semi-invasive (*in vitro*) glucose measurement techniques.

### **2.3.2 Photoacoustic**

Photoacoustic (PA) spectroscopy (45) utilizes an optical beam to heat the sample rapidly. This produces an acoustic pressure wave which can be measured by microphone or more sensitive piezoelectric detector, i.e., laser excitation of a sample is used to generate an acoustic response and a spectrum as the laser is tuned (46). The sensitivity of the PA technique is higher than the conventional spectrometer, but it may be subject to more interference from the environment (47). An *in vitro* (glucose solutions) and an *in vivo* (nine volunteers performed Oral Glucose

Tolerance Tests, called OGTT, via PA measured from the fingers) PA, non-invasive blood glucose experiment performed in 1995 using laser diodes (48) showed a positive result and obtained a good R correlation between the predicted results and the reference values.

On the other hand, Mackenzie et al. (49) reported unrepeatable results from their series of PA experiments of glucose level acquisitions, which included both *in vitro* and *in vivo* trials. They demonstrated that PA signals were changed with glucose concentrations in both *in vitro* and *in vivo*. They pointed out that the structure and composition of human tissue and the complicated PA signal generation process could affect measurements and cause insensitivity. They also commented that PA measurement still could not provide repeatable results due to physiological effects which were not limited to tissue scattering noise, but many other body substances as well.

A model of using pig blood by applying Nd:YAG (neodymium-doped yttrium aluminium garnet; Nd:Y<sub>3</sub>Al<sub>5</sub>O<sub>12</sub>) laser on wavelengths of 1064 and 532nm showed that PA could measure blood glucose levels (50). The results could be affected by many parameters, such as the variations of the red blood cells. In addition, the highly scattering effect of skin tissues changed the optical energy distribution, which might affect the PA detection (50).

Zhao and Myllyla (51) found that PA could be affected by the physiology and the composition of the skin tissue which could cause optical scattering (51). Thus, PA is not the best choice for non-invasive blood glucose determination due to the scattering effects.

### 2.3.3 Optical coherence tomography

Optical coherence tomography (OCT) (52) works on the measurement of coherently backscattered light to provide images of tissues (52; 53), i.e., the light is projected onto the tissue and then reflected from different layers of the tissue. The image resolutions are about 1-15 $\mu$ m (53). Esenaliev et al. (54) performed their initial trials on hairless Yucatan micropigs and New Zealand rabbits by using OCT. They demonstrated that the glucose levels were correlated to the OCT scattering coefficient. After one year, they reported their pilot study in human subjects by using OCT with a wavelength 1300nm (55). Fifteen healthy volunteers were investigated in 18 OGTT clinical experiments. OCT images were taken from the left forearm while venous blood samples were taken from the right arm. The results reflected the glucose from the skin depth of 200 - 600 $\mu$ m, in which the glucose levels were correlated to the OCT signals. However, the results can only reflect the OGTT test or clamping test in about three hours. This showed that glucose levels were correlated to the OCT in a short period of time, in which the R correlations could approach to 0.8 and 0.95. Although the results gave a positive sign of using OCT, there were several limitations, including a temperature effect on OCT (56). In addition, it was also found that the highly inhomogeneous skin and tissue gave varying density and refractive index which significantly influenced the OCT (56). Kinnunen et al. (57) reported *in vitro* experiments of glucose monitoring by using OCT. The experiments measured the glucose-induced changes in artificial intra-lipid and in mouse skin samples. The results of the intra-lipid samples established that glucose concentrations were correlated to the OCT signal. However, the experiments on the

mouse skin demonstrated poor correlations in most cases. They also indicated that many other osmolytes of extracellular fluid, such as potassium chloride and urea might affect the refractive index and thus interfere with glucose measurement using this technique.

#### **2.3.4 Polarization changes**

Glucose concentration can be measured via polarization changes (PC) since glucose is a good optical rotator (58). The concentration of the optical solute is related to the rotation of the polarization. In a non-invasive approach, the signal should go through the body tissue without depolarizing the beam. However, it is nearly impossible to pass through the thick tissue since the skin possesses high scattering coefficients. The signal magnitude is very small and is easily influenced by the surrounding environment. The angle of rotation for 1 cm of tissue would be  $<0.00004^\circ$  for 1 mg/dl in glucose concentration (59). Cote et al. (60) showed, by using a Helium Neon Laser at wavelength of 632nm, that polarization could predict D-glucose solutions with less than 5% error ( $R^2 = 0.997$ ). This could prove that glucose is a good rotator of polarization. However, when the experiment was conducted using an excised human eye, the results were poor since there were many obstacles in the excised eye, such as the slightly cloudy eye and the mechanical strain, which reduced the transparency of the eye. This shows that many parameters can depolarize signals, leading to poor polarization measurement.

Cote and Vikin (61), and Ansari et al. (62) tested their methods by using turbid media and aqueous humor of the eye, respectively. Both groups reported that the glucose concentration could be measured accurately *in vitro*. However, this was

only a model test and they had neglected the physiological effects *in vivo*. Other groups (60; 63) demonstrated their new dual-wavelength polarimetry measurement method for the aqueous humor of the eye by using both a red 635nm laser and a green 532nm laser. They showed that the method could successfully measure the glucose concentration and also compensate the birefringence noise due to the motion artifact of the cornea. The polarization change seems to apply only in the aqueous humor measurement. However, tear secretion may affect the result, and eye tissue glucose may not be representative of blood glucose.

### **2.3.5 Raman spectroscopy**

Raman spectra are measured with laser lines from scattered light which can be influenced by the oscillation and rotation of the scatter (64-66). This laser light is used to induce emissions from transitions near the level excited (67). Its disadvantages are that it is highly absorbing, there is a low signal-to-noise (S/N) ratio and it requires a long acquisition time. Raman is useful for identification of symmetrical dipole molecular vibrations (68), the more rigid bonds like C=C stretching. Berger et al. (69) performed a whole blood experiment by using Raman spectroscopy with a diode laser at 830nm. They demonstrated that Raman spectra were correlated with glucose concentrations in whole blood samples. Another Raman *in vitro* experiment was shown by using Bovine Plasma/serum (70; 71). The result of the Root Mean Square Error Prediction (RMSEP) was about 5.12mM. Lambert et al. (72) applied the Raman technique (laser diode of 785nm) to show a good correlation with glucose in a rabbit aqueous humor model which was built with several blood components. However, this was the controlled experiment, in which no

physiology took place, i.e., *in vitro*. Enejder et al. (73) reported their Raman *in vivo* test by using a wavelength of 830nm. The results showed a good correlation between the Raman signal and the glucose level, but only over two to three hours of glucose measurement. As a caveat to this approach, it has been noted that using a laser diode on humans can burn the skin.

### **2.3.6 Mid-infrared**

The wavelength of 2500 – 25000nm is defined as mid-infrared (MIR). MIR exhibits fundamental vibration absorption bands in response to glucose. MIR is widely used in biochemical measurements for many compounds (74). Kim et al. (75) used MIR to determine the glucose levels in whole blood samples with good accuracy. Further, Martin et al. (76) used MIR to measure glucose in serum, in which urea and albumin were added as interference. The predicted results showed a linear relation with the reference values, and the error at  $1035\text{cm}^{-1}$  frequency was at 1.1 mmol/l.

It has been claimed that MIR could provide non-invasive blood glucose measurements. Heise and Marbach (77) used MIR successfully on whole blood while Malchoff et al. (78) demonstrated positive results on their novel MIR, non-invasive blood glucose monitor over a period of about four hours. They measured the tympanic membrane and used serum glucose as a reference, with an R correlation of 0.94. Heise and Marbach (79) demonstrated the clinical trials by FT-IR spectrometers to obtain the spectra from human lips in 4.5 – 9 hours; finger-prick glucose levels were used as references, but the correlation was not reliable. Although some positive results were shown with MIR, some scientists (e.g., Heise (80; 81)) prefer NIR for non-invasive blood glucose measurement.

### **2.3.7 Near infrared**

Near Infrared (NIR) is located in the wavelength region of 730nm to 2500nm (8). Glucose generates one of the weakest NIR absorption signals per concentration unit of the body's major components (8). NIR measurement can explore tissue between 1 and 100mm with a general decrease in penetration depth as the wavelength value is increased (8). Most biological substances and impurities in the various bioprocesses absorb and fluoresce between 190 and 650nm(8). A high Signal-to-Noise (S/N) ratio minimizes NIR from the interference of the florescent light. It is a highly sensitive wavelength range and is also sensitive to not only body temperature but any temperature (82).

NIR spectroscopy employs the same principles as Infrared (IR) spectroscopy. NIR spectra are made up of broad bands corresponding to overlapping peaks, the overtones (first, second, third and combination overtones), formed by the molecular fundamental vibrations (83). NIR spectra are less distinctive than IR spectra. All four major ingredients - water, carbohydrates, proteins and fats are assessed with vibration spectroscopy. In IR C-H, O-H, N-H, C-O and C=O stretching bands dominate the spectra, whereas only the very enharmonic vibrations (i.e., bonds including the light hydrogen atoms such as C-H, O-H, N-H) give intensive bands in NIR (83; 84). Thus, IR and NIR overtones principally happen in the vibrations of side groups.

Heise (85), the pioneer of the non-invasive blood glucose techniques, has tried on many aspects of NIR applied to non-invasive blood glucose measurements. However, he has also pointed out many shortcomings of the non-invasive approach

due to physiological differences and the relatively small fraction of the glucose in blood. Maruo et al. (86-88) used NIR diffuse-reflectance spectroscopy through fibre optics on the forearms of diabetic patients. The results showed a positive correlation between predicted values and the reference glucose levels. Meanwhile, many *in vitro* (whole blood or plasma glucose) tests by NIR showed reliable results (89-93). Riley and Crider (94) analyzed glucose *in vitro* by NIR and reported that NIR could be measured at concentrations as low as 0.3 to 0.6 mmol/l in animal cell/culture media. Thus, the use of the NIR may be the most suitable for non-invasive blood glucose measurement through skin tissue.

### 2.3.8 Summaries of the non-invasive approach for glucose measurement

The advantages and the disadvantages of the non-invasive approach are summarized in the following table.

**Table 2-1: Summary and comparison of the optical light for the non-invasive blood glucose application.**

Media	Advantages	Disadvantages	Comments
PA	<ul style="list-style-type: none"> <li>• Greater sensitivity</li> </ul>	<ul style="list-style-type: none"> <li>• Sensitive to environment</li> <li>• Using laser which can burn skin</li> <li>• High signal noise from skin tissue (high scattering)</li> </ul>	<ul style="list-style-type: none"> <li>• Interference due to skin cannot be avoided</li> <li>• Causes mismatching of refractive index</li> </ul>
PC	<ul style="list-style-type: none"> <li>• Glucose – a good optical rotator</li> </ul>	<ul style="list-style-type: none"> <li>• Low S/N ratio</li> <li>• Hard to penetrate the skin</li> </ul>	<ul style="list-style-type: none"> <li>• Rotation is too small with skin tissue</li> </ul>



Media	Advantages	Disadvantage	Comments
NIR	<ul style="list-style-type: none"> <li>• High S/N ratio</li> <li>• Sensitive</li> <li>• Low Absorbance in skin tissue</li> <li>• Large sample size – inhomogeneous samples</li> <li>• Nondestructive</li> </ul>	<ul style="list-style-type: none"> <li>• Temperature sensitive</li> <li>• High scattering in skin</li> </ul>	<ul style="list-style-type: none"> <li>• Most scientists carry out their research by using NIR</li> </ul>
OCT	<ul style="list-style-type: none"> <li>• Limit the sampling depth – avoid the unwanted signal</li> </ul>	<ul style="list-style-type: none"> <li>• Temperature sensitive</li> <li>• High optical inhomogeneity of skin effect</li> <li>• High optical motion artifacts, affected by the muscle motion.</li> </ul>	<ul style="list-style-type: none"> <li>• OCT signals only detect relative changes in the scattering properties; causes mismatching of refractive index</li> </ul>
Mid-IR	<ul style="list-style-type: none"> <li>• Good for <i>in vitro</i> glucose measurement</li> </ul>	<ul style="list-style-type: none"> <li>• Strong water absorption</li> </ul>	<ul style="list-style-type: none"> <li>• No correlation for the <i>in vivo</i> glucose test has been found</li> </ul>
Fluorescence	<ul style="list-style-type: none"> <li>• Good for the biochemical analyzer</li> </ul>	<ul style="list-style-type: none"> <li>• Highly influenced by surrounding environment (UV / visual light)</li> </ul>	<ul style="list-style-type: none"> <li>• UV or visible light will cause trouble when using the short wavelength</li> </ul>

## 2.4 Blood Glucose

Blood carries a range of nutrients and helps to remove the waste from the body.

Glucose is one of the most important nutrients which supplies energy to the body. It can be found in various kinds of food and mainly exists in carbohydrate form.

### **2.4.1 Dietary carbohydrates**

Carbohydrates are a nutritional source which supplies energy. They are mainly ingested as complex polymers, particularly starch (95). During digestion, the complex polymers are broken into smaller polymers in the small intestine. The smaller carbohydrate molecules (such as glucose) then pass through the intestinal wall and are transported to the tissues and the liver (96). Along with fatty acids, amino acids and glycogen, glucose is metabolized to provide energy, or it is stored, depending upon the needs of the body (97). Thus, the lack of or excess of glucose is harmful. Glucose contains the NIR sensitive groups  $-CH_2$ ,  $-CH$  and  $-OH$ .

### **2.4.2 Mechanism of blood glucose regulation**

Blood glucose is monitored by the pancreas (58). It is negative-feedback regulated in order to keep the body in homeostasis (58). When the glucose level drops, through uptake into tissue to meet the body's energy demands, the pancreas releases glucagon, a hormone which targets cells in the liver (98). These cells then convert glycogen into glucose (98). The glucose is then released into the bloodstream and increases blood glucose levels.

Once blood glucose rises, another hormone, called insulin, is released from pancreatic islet cells. Insulin then stimulates the liver to convert more glucose into glycogen (98) and blood glucose levels decrease.

### 2.4.3 Glucose

$C_6H_{12}O_6$  is the molecular formulation for glucose. Glucose can exist in difference forms in humans, such as D-Glucose which exists in isomeric forms of Alpha and Beta types (99) (Figure 2-1). Different isomers of glucose can inter-convert (58).

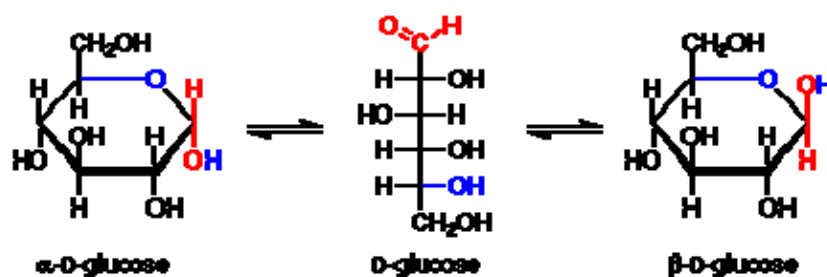


Figure 2-1: D-Glucose Transformation (100)

The isomers of glucose shown above can exist in both open-chain (acyclic) and ring (cyclic) forms. The  $CH_2$ ,  $CH$  and  $OH$  side group can be stimulated by NIR spectroscopy causing vibrations in carbon bonds, and a subsequent release of energy, to form overtones. NIR absorptions occur principally at four band overtones (83; 101) which could indicate the existence and concentration of the above mentioned side groups. These overtone groups are as shown below:

1. Combination band region is from 1950nm to 2500nm
2. First overtone is from 1475nm to 2050nm
3. Second overtone is from 1050nm to 1650nm
4. Third overtone is from 700nm to 1150nm

## **2.5 Skin tissue and finger structure**

Finger skin is relatively thin, and is filled with capillaries (102). This highly vascularized feature may therefore provide a suitable place for the finger-prick glucose measurement. Measurement of glucose for the other parts of the body always has a lag time problem relative to the glucose levels of the fingers, e.g., blood glucose level from an arm is behind the glucose level in a finger (103). The use of the finger for measurement may avoid the physiological influences and the time lag/lead conflicts between fingers and other parts of the body when the finger-prick glucose measurement is used for the calibration tool.

### **2.5.1 Finger**

Human fingers mainly consist of tissue, bone and nail. The rigid nail can protect the finger and also prevent deformation when touching an object (104). The rigid properties may provide a suitable measuring situation for the non-invasive glucose measurement as relatively small deformation occurs, which may affect the NIR signal (105).

### **2.5.2 Human tissue**

Human skin tissue is made up of multiple layers (Figure 2-2). Normally the skin thickness is about 3 – 4mm (106). The outermost layer is the epidermis, deeper is dermis layer and the layer closest to the bone is the subcutaneous layer. The epidermis is the hardest layer, with the smallest elasticity and is about 0.5mm - 1mm thick (104; 107). The dermis is a softer layer with more elasticity, and is about 1 to 3mm thick(104). Numerous protrusions at the boundary between the epidermis and

dermis secure the two layers. The subcutaneous layer, which fills the space between the dermis and bone, is mainly composed of fat and functions as a cushion when a shock load is applied to the finger (104). Fat can interfere with glucose measurement using NIR and therefore the subcutaneous area should be avoided. Some capillaries are located in the dermis layer, thus the optimal depth for glucose measurement may be targeted to 2 to 4 mm under the skin's surface.

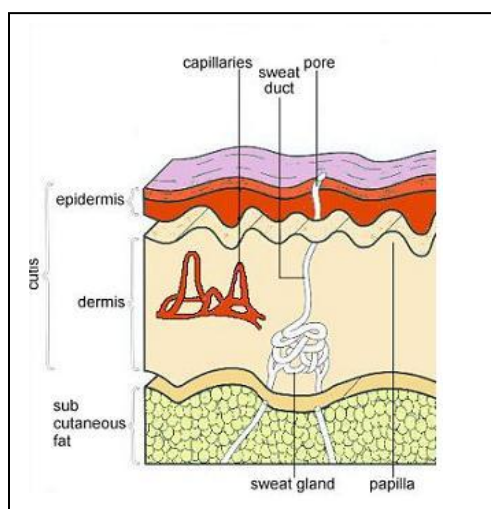


**Figure 2-2: Skin and tissue cross-sectional structure (108)**

## **2.6 *In Vitro* clinical trials**

Scientists normally will test the NIR glucose concentration *in vitro* for preliminary analysis before *in vivo* measurements are made. Pure compositions of carbohydrates with side groups (-CH, -OH) can be tested by NIR spectra for their ability to form overtones (109; 110). Various chemical components such as lipid, protein and amino acids can then be added to the glucose to determine the degree of interference. Thus,

glucose was the only changing variable in the mixture. Therefore, results usually showed positive.

Artificial body tissue, known as tissue phantoms (mostly involving intra-lipid (111; 112)) had also been used experimentally. Pig skin had been used with blood added (54) and also an artificial combination of water, soybean oil, lecithin, albumin, urea and glucose (111) had been tested. Results showed that the first overtone, between 1500 and 1840nm, and the second and combination overtones obtained a higher standard prediction error when compared to the whole spectral signal. The correlation was  $>0.7$  between the true/reference glucose concentration and the predicted glucose concentration.

Amerov et al. (113) mixed glucose with urea, triacetin, hemoglobin(Hb), bovine serum albumin (BSA), cholesterol and water at 37°C. They showed that the predicted glucose concentration correlated very well with the reference glucose concentration when interference occurred. The results of standard errors of calibration and prediction were 1.27mmol/l and 1.34mmol/l, respectively, over a glucose concentration range of 1.9 to 19mmol/l. The experiment was conducted at an average, normal human body temperature, 37°C. *In vitro*, the results obtained via NIR are usually positive but the experimental conditions are not as complex as the *in vivo* physiology. The advantage of the *in vitro* experiment is that all parameters can be controlled, so that the glucose concentration is the only changing variable.

## **2.7 *In Vivo* clinical trials**

*In vivo* is related to living beings, including human subjects. They may not be diabetic patients. The test can be either by the Oral Glucose Tolerance Test (OGTT) or meal tolerance test. However, there are many parameters which can affect *in vivo* tests for blood glucose, such as temperature, physiological differences, contact areas, contact points, degree of pressure, tissue deformation and the location of the blood sampling. Human tissues contain many components which can interfere with the accuracy of *in vivo* glucose measurements (114). Many scientists have conducted different skin/tissue experiments to determine the optimal characteristics of skin/tissue for NIR glucose measurement. Olesberg et al. (115) used NIR spectroscopy at wavelengths of 2000 – 2500nm on rat skin. Over seven hours, NIR was continuously applied to the same area of the skin while blood glucose was increased above 30mmol/l through a venous infusion of glucose. However, the results were not very encouraging since the root mean square error of prediction (rmsep) was 5.5 mmol/l. Although rat skin might not accurately resemble human skin, this experiment demonstrated that numerous interfering factors might compromise results *in vivo*.

### **2.7.1 Oral glucose tolerance test**

NIR, with an Oral Glucose Tolerance Test (OGTT), has been usually tested on normal, non-diabetic subjects. These subjects drink a sugar solution with a known concentration of glucose at two to three hour intervals in order to vary their blood glucose level, after they had fasted for eight to ten hours. Glucose levels are usually within the normal range, i.e., 3.9mM to 11.1mM. Malin et al. (116) tested non-

invasive blood glucose measurement using NIR spectroscopy following OGTT. Only three subjects out of seven showed promising results. They pointed out that the results could be affected by skin temperature and skin-contact positions. Danzer et al. (117) extended NIR measurement to diabetic patients following OGTT, used a wavelength range of 820 to 1320nm and reported encouraging results for short-term prediction, although long-term prediction was less reliable. The long-term unreliability might be due to the physiological differences amongst subjects and time drift factors.

Similar findings were reported by Blank et al. (118) using NIR spectroscopy with a wavelength range from 1050 – 2450nm on three non-diabetic subjects given five OGTTs at two- to three-day intervals, over a period of two weeks. Their data showed that OGTT experiments might not provide good results for long term prediction using NIR.

Maruo et al. (86; 87) used a novel fibre optical probe and spectrometer with a cut-off at 2100nm to measure blood glucose following OGTT. The contact interface between the probe and the contact point of the forearm of the six subjects was temperature-controlled. They found that the regression coefficient vectors had a positive peak at around 1600nm (the absorbance band of glucose) in both *in vitro* and *in vivo* experiments. They also showed that a fibre optical probe could reduce ‘noise’ and optimize the signal. However, it was uncertain whether the blood glucose readings were affected by the heat convection during the temperature control.



## **2.8 Other considerations**

Beside of the above-mentioned factors *in vivo* and *in vitro*, there are many other factors which need to be considered when dealing with NIR blood glucose measurement. These include the following items:

### **2.8.1 Machine drift and time drift consideration**

The ‘machine drift’ and ‘time drift’ effects can influence results when an experiment takes place over a longer time. The problem may come from the machine or from the environment. Blank et al. (119) conducted their clinical trials to test the ‘time drift’ effect. They determined blood glucose using NIR spectra in the wavelength range 1050 – 2450nm, *in vivo*, from samples collected from the arms of 138 subjects over more than 24 weeks. The results showed that accurate glucose prediction was applicable for long-term application by using NIR. However, many data points were omitted from the analysis as outliers, which raised a question whether long-term, non-invasive blood glucose measurements could be really achieved. Liu et al. (120) used the wavelength region from 1100 – 1800 nm to measure the palm of the hand through diffuse reflectance, both *in vitro* and *in vivo*. For the *in vivo* experiment, they investigated two subjects for three hours, one with OGTT and another with no water and glucose. Thirty sets of spectra were obtained from each subject. The results of the subjects who followed OGTT showed a higher accuracy in predictions than the subject not given glucose and water.

## 2.8.2 Temperature consideration

Temperature is one of the key effects on NIR glucose measurement. Many researchers have found that temperature variations at the tissue surface could significantly affect NIR readings. According to Tarumi et al. (121), the effect of temperature on NIR absorbance was largely relative to glucose concentration. Many researchers had investigated the effects of temperature on NIR *in vitro* (82; 121; 122) and demonstrated that temperature changes could cause significant spectral shifts. Burmeister and Arnold (110) reported that the effect of temperature on spectral shift could be reduced by minimizing the temperature variation on the measurement interface.

The effect of temperature is significant in non-invasive blood glucose measurement. As such, some scientists have focused their efforts *in vivo* in experiments where the temperature was controlled at a fixed point or where variations were compensated. Kawano et al. (123) developed a calibration equation for the temperature compensation from an NIR spectrometer by using multiple linear regression (MLR) and showed very good glucose prediction at a temperature range from 21 to 31°C. However, Abe et al. (124) attempted to apply this technique using a NIR spectrophotometer with wavelength range of 1100 to 2500nm with variable outcomes. They concluded that calibration for temperature compensation might not always be predictable by simple MLR. This is because the body surface temperature can affect the NIR approach; scientists had tried to investigate the influence of body skin/tissue temperature to the NIR measurement. Yeh et al. (125) studied non-invasive blood glucose measurement by modulating the temperature of the

contacting disc of the subjects between 22 and 38°C. He also paired up with Khalil et al. (126) to investigate the interrelationship between different skin temperatures. The reduced scattering coefficient of human forearm skin was linearly dependent on temperature within a subject. In the modulating temperature, the prediction could reach to  $R_p = 0.73$ (125). It also concluded that temperature change could mimic the effect of change in glucose concentration (126), with a larger absorption coefficient at 38°C than at 22°C.

### **2.8.3 Contact interface consideration**

Consistency of the NIR measurement location may help to reduce physiological and physical variations amongst different parts of the body. Different forces, or even the same force applied on the contacting surface, may also affect the spectral measurement signal due to the various tissue-deforming reactions, since the tension of the skin may change from time to time. This depends on the reaction of the body and the external stimulation and may lead to an uneven optical measurement. Various tissue properties may cause different spectral shifts and scattering effects. As mentioned in Section 2.5, more rigid parts of the body can reduce the deformation effect.

By using a contact measurement method, S/N ratio is relatively increased since noises from the surrounding environment cannot directly affect light transmission, and the specular effect may be minimized. Chen et al. (105) demonstrated their experiments on the human palm by using wavelengths in the range 1100-1700nm, following OGTT. They suggested that the optimal contact state was by pressing the skin to about 0.5mm with the measuring time at one-thirtieth of

a second. This was because the probe touched the skin at about 0.5mm depth, where the spectral signal was more stable after touching for 30 seconds, after reaching the palm.. This demonstrated that measurement in the same anatomical position could standardize non-invasive glucose analysis.

#### **2.8.4 Location of the body**

Time lag/lead between glucose measurements of several body parts is another consideration. McGarraugh et al. (127) studied the influence of different body locations on glucose measurement. They compared the glucose levels between fingers and arms from thirty subjects in two six-hour sessions and found that there was a 5-20 minute time lag from the arm glucose value as compared to finger glucose value.

Other locations such as tongue, oral mucosa, palms and eyes had been tested. Burmeister and Arnold (128) tried to evaluate the most suitable body sites for the non-invasive measurement of blood glucose by NIR spectroscopy with a wavelength range from 1.52 to 1.82nm. They prepared different thicknesses of water and bovine fat tissue for simulating different body sites such as webbing tissue (between thumb and forefinger), tongue, upper lip, lower lip, nasal septum and cheek. Results showed that the best NIR measurement site was on the tongue since there was relatively less fat interference. Burmeister et al. (129) carried out further testing on five human subjects with Type 1 diabetes. NIR spectroscopy with cutoff wavelength 1900nm was used for the transmittance measurement for the tongue, with variable results. Although the tongue contains less fatty tissue, saliva and salivary components may

influence measurements, and they may also be affected by the composition of food taken as a meal before the measurement.

Fingers are the most convenient location for glucose measurement. The palm is a location near to the finger, but may be subject to the 'time-drift' effect, although Bina et al. (130) found that many of the blood glucose measurements between the palm and fingertip were similar. Therefore the 'time-drift' effect between palm and finger for glucose levels might be minimal.

The arm is also an easy location for glucose measurement, but a time lag will be present relative to finger-prick measurements, if used as a calibration. The skin on the arm is relatively thicker and may contain a relatively larger percentage of fat, which is one of the major interference factors in NIR measurement (128).

Oral mucosa seems a little easier than the tongue with regards to obtaining a signal, but the moisture of the lips and the breathing action may affect the results since NIR is highly affected by water. Marbach et al. (131) demonstrated the NIR measurement on the human inner lip. The mean square prediction error by cross-validation was 2.5 to 3.1mmol/l . However, there was a 10 minute time lag from the capillary blood glucose of the fingers and the results were poorly reproducible.

Eyes are more difficult for glucose measurement by NIR. A laser cannot be used, and tears may alter the results. Eyeball movement can also affect measurements. In addition, glucose in the eye does not accurately reflect blood glucose levels; it is an alternative glucose indicator. Schrader et al. (132) investigated glucose measurement in the human eye using NIR and reported that

predictions were unreliable since they were affected by eye flickering and also by the low reflectivity of the eye lens of the subject.

## **2.9 Calibration and prediction**

Researchers tend to rely on partial least square (PLS) regression for the experiments and clinical trials analysis. Most scientists have used PLS regression for non-invasive analysis, because PLS could provide stable predictors for the unknown variables (133). The data (i.e., spectra: spectra 1 and spectra 2, and finger-prick glucose readings: FP1 and FP2), obtained normally, were divided into two sets ('spectra 1 and FP1' and 'spectra 2 & FP2'). One set of the data was used for calibration, in which PLS was used to maximize the correlation between calibration value (spectra 1) and the true/reference value (FP1). From that, it was possible to obtain the model from the calibration. The other data set (spectra 2) was then paired to the calibration model by PLS for the predicted value, where FP2 was used for validation.

Many researchers had successfully demonstrated non-invasive blood glucose measurements using artificial phantoms (111; 134). These *in vitro* experiments mainly contained glucose variables with other materials as interference (e.g., protein, lipid) to the glucose measurement. *In vivo*, experiments always take place as clinical trials in humans. Finger-prick glucose levels (maybe plasma or serum) act as reference values. A clinical trial can last between several hours to a few months. Most long-term clinical trials had shown poor prediction and reliability, generally

due to changing characteristics of tissues, such as proteins and fat, in different body tissue compartments. Thus, physiological variations introduce the majority of confounding factors in blood glucose measurement *in vivo*.

## **2.10 Analytical method**

The following section presents fundamental aspects of NIR spectroscopic analysis, including absorbance, transmittance/reflectance, Beer's law and the Clarke Grid Error plot. As mentioned in Sub-section 2.4.3 and Section 2.9, NIR spectroscopic analysis is measured by molecular vibrations which cause overtones and is mainly analyzed by using multivariate calibration techniques, such as partial least square, PLS.

### **2.10.1 Transmittance and reflectance**

Glucose concentrations are measured through NIR chemometric technology. There are two common NIR measurement methods: reflectance and transmittance. Reflectance is the use of bounce-back light for analysis while transmittance measures light passing through the sample. Both techniques have advantages and disadvantages. In transmittance, the light may not have sufficient power to pass through the sample, while in reflectance, where the light is partially bounced back, larger interference through diffusive reflection may occur.

The transmittance approach was recommended by Jeon et al. (135) for non-invasive blood glucose measurement. Comparing transmittance and reflectance, it

was found that transmittance provided less error, while reflectance was mainly due to the non-specific effects of scattered light.

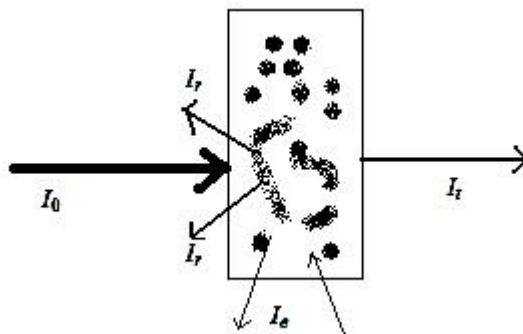


**Figure 2-3: Light intensity passing through a sample;  $I_0$ : incident light,  $I_r$ : reflected light,  $I_t$ : transmitted light,  $I_e$ : light emitted and received to and from other source.**

Transmittance (T) (136) is the ratio of transmitted light and the incident light in a specific wavelength.

$$T \equiv \frac{I_t}{I_0} \tag{2.1}$$

where

$I_t$  = transmitted light of a sample

$I_0$  = incident light

The transmittance is usually represented as a percentage shown below.

$$T \equiv \frac{I_t}{I_0} \times 100\% \tag{2.2}$$

Reflectance(R) (136) is the ratio of reflected light and the incident light.



$$R \equiv \frac{I_r}{I_0} \times 100\% \quad (2.3)$$

where  $I_r$  = reflected light of a sample

$I_0$  = incident light

### 2.10.2 Absorbance

The absorbance (136) is given in terms of the transmittance  $T$ ,

$$A_t \equiv -\log T \quad (2.4)$$

$$A_t \equiv \log \left( \frac{1}{T} \right) \quad (2.5)$$

Thus, the absorbance is expressed as below:

$$A \equiv \log \left( \frac{I_0}{I} \right) = (\ln 10) c \varepsilon l \quad (2.6)$$

where  $I$  is the intensity,  $c$  is the molar concentration,  $\varepsilon$  is the molar absorptivity (in  $\text{cm}^{-1} \text{M}^{-1}$ ) and  $l$  is the path length. This Equation (2.6) sometimes is known as Beer's Law.

### 2.10.3 Beer-Lambert law

The Beer-Lambert Law, also known as Beer's Law is an empirical relationship that relates the absorption of light to the properties of the material through which the light is traveling. Equation (2.6) in Section 2.10.2 can be derived as below:

$$A = \alpha lc \quad (2.7)$$

$$\frac{I_1}{I_0} = 10^{-\alpha lc} \quad (2.8)$$

$$A = -\log_{10} \frac{I_1}{I_0} \quad (2.9)$$

$$\alpha = \frac{4\pi k}{\lambda} \quad (2.10)$$

where

- A is absorbance
- $I_0$  is the intensity of the incident light
- $I_1$  is the intensity after passing through the material
- $l$  is the distance that the light travels through the material (the path length)
- $c$  is the concentration of absorbing species in the material
- $\alpha$  is the *absorption coefficient* or the molar absorptivity of the absorber
- $\lambda$  is the wavelength of the light
- $k$  is the extinction coefficient

The law states that there is a logarithmic dependence between “the transmittance of light through a substance” and “the concentration of the substance,” and also between the “transmittance” and “the length of material that the light travels through” as shown in Figure 2-4. Thus when  $l$  and  $\alpha$  are known, the concentration of a substance can be deduced from the quantity of light transmitted.

The value of the absorption coefficient  $\alpha$  varies between different absorbing materials and also with wavelength for a particular material. It is usually determined through experiment and applying Beer's Law.

In spectroscopy and spectrophotometry, the law is always defined in terms of common logarithms and powers of 10, as mentioned before.

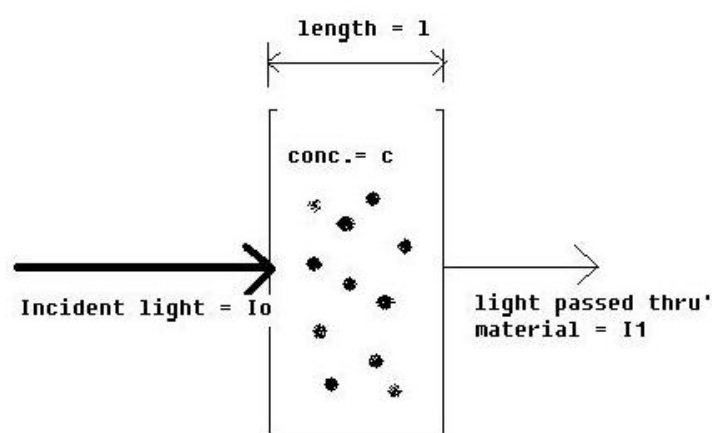


**Figure 2-4: Light passing material with path length = l**

For glucose measurement by spectroscopy, the absorbance takes place for the spectral measurement. The predictable analysis always relies on the following partial least square regression.

#### **2.10.4 Partial least squares regression (PLS Regression)**

Non-invasive blood glucose meter studies have been conducted for more than 20 years. Most scientists now use Near Infrared (NIR) as the medium for non-invasive blood glucose measurement. However, there are problems of low S/N levels when NIR is used to penetrate through human skin and tissue to the blood vessels or

capillaries. This is due to the relatively small glucose amount in blood and in tissue components. Various techniques have been applied to optimize the signal to obtain the best correlation and prediction. The most common and powerful process is by using partial least square (PLS) regression (133; 137-140) with a preprocessing technique.

PLS is a well-established tool in chemometric analysis. Recently, many signal interpretation processes have utilized PLS as the analytical tool, especially for the bio-signal and bio-medical signal. Furthermore, many researchers employ it as the preferred non-invasive prediction tool. The PLS introduced here focuses on utilization for the non-invasive blood glucose prediction.

The non-invasive glucose measurements are generally associated with physiological interferences, resulting in many unwanted noises, which cause inaccurate results. PLS has the ability to maximize the spectral signals by its generated latent variables while minimizing less important variables and eliminating them from analysis (141).

PLS regression is applied to the linear model, thus:

Let  $Y=(n \times m)$  response matrix

$X= (n \times p)$  predictor matrix

$B = (p \times m)$  regression coefficient matrix

$E =$  noise with  $(n \times m)$  matrix

For the linear regression model,

$$Y = XB + E \quad (2.11)$$

Then, let  $T = XW$

where  $W =$  weight matrix

$$Y = TQ + E \quad (2.12)$$

where  $Q =$  loadings of  $T$

Thus,

$$Y = XWQ + E \quad (2.13)$$

where  $B = WQ$

### **2.10.5 Nonlinear iterative partial least square (NIPALS) and SIMPLS**

There are different methods for PLS prediction. The following introduces the two most common PLS construction methods. NIPALS (140; 142), nonlinear iterative partial least squares is the standard algorithm of the computing PLS regression. The major disadvantage of the NIPALS over SIMPLS, an alternative approach to PLS regression (143), is that it is computationally inefficient (144); their results are similar. Thus, SIMPLS takes the advantage over PLS application.

### **2.10.6 Clarke grid error plot**

The Clarke Grid Error (CGE) plot is the most common analysis for blood glucose measurement (9). The figure of a CGE plot is shown in Figure 2-5. Most blood glucose-related measurements and research have utilized CGE for the comparison tool. The advantage of CGE, as stated by Clarke et al. (9), is that it can more accurately represent the actual situation of the blood glucose measurement. Five

different zones are represented with different measurement information in CGE.

They are as shown below:

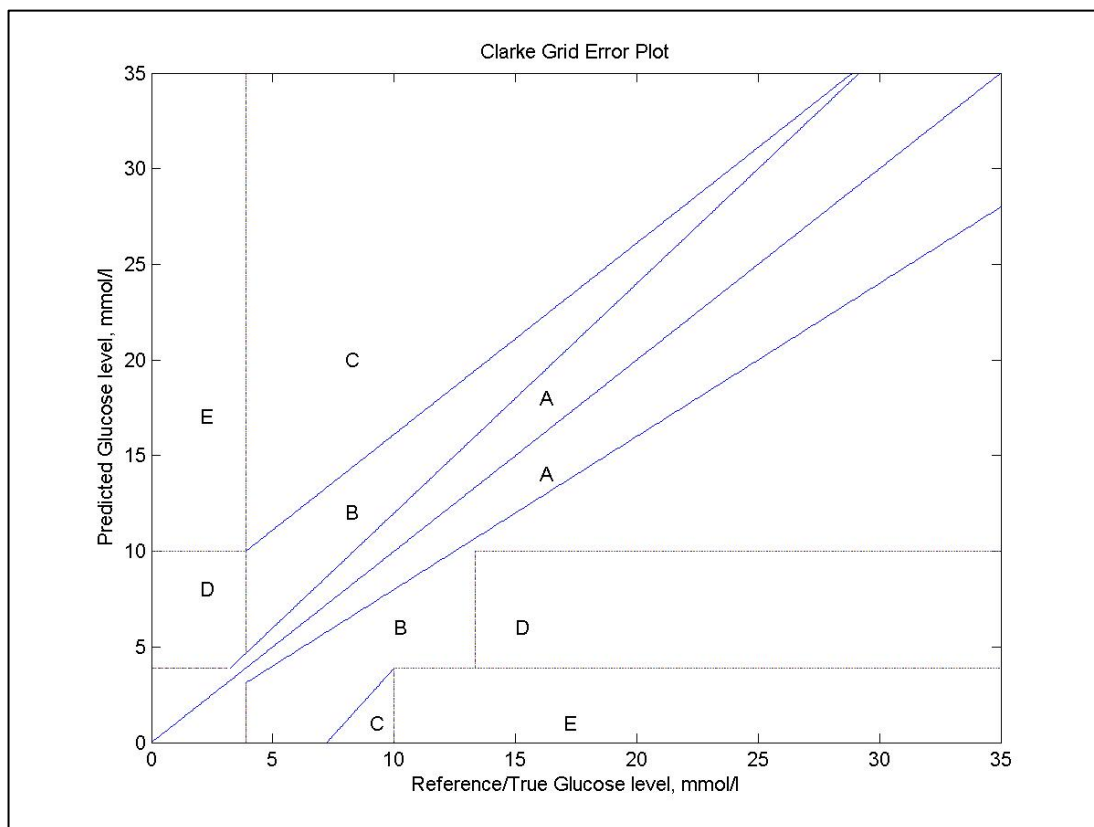


**Figure 2-5: Clarke Grid Error plot**

Zone A: The measured/predicted blood glucose is within 20% deviation of true blood glucose (or both measured blood glucose and true blood glucose). Both are around a boundary value of 70 mg/dL (3.9mmol).

Zone B: Deviation from true blood glucose is greater than 20% but no treatment, or only minor treatment, is necessary.

Zone C: Over-correction of acceptable blood glucose levels; treatment might cause the actual blood glucose to fall below <70mg/dl (3.9mmol/l) or rise above 180mg/dl.

Zone D: Region of ‘dangerous failure to detect and treat’ blood glucose errors.

Zone E: An erroneous treatment, contrary to the treatment required.

Amongst the five regions, both A and B are called clinically acceptable; zones C, D, E are dangerous as they may introduce clinically significant errors.

## **2.11 Conclusions**

Many different technologies have been applied to non-invasive blood glucose monitoring. NIR is one possible approach, and has been demonstrated in many *in vitro* studies. However, application of NIR has been provided relatively poor result *in vivo* due to confounding factors such as temperature, physiological effects and the interfering influences of protein, cholesterol and fat in the blood.

NIR usually detected a significant amount of noise during *in vivo* experiments. Scientists claimed that many of these noises are due to the physiological differences between subjects and, as such, have recommended focusing on intra-subject investigations. For intra-subject clinical trials, errors are thought to be due to the temperature, as well as time drift effect, blood and other physiological differences. However, there is still no evidence showing that the prediction of the intra-subject (within subject) provides more accurate results than the prediction of inter-subject (between subjects). Thus, many groups still perform inter-subject trials.

In addition, there are no proven data on the ratio of calibration to prediction in NIR, non-invasive blood glucose measurement. Many scientists still arbitrarily

draw a ratio of the calibration set to the prediction set, but the number of calibrations required for the prediction is still not yet standardized. The precise use of calibrations with regard to the prediction ratio may help to optimize data from clinical trials.

The analysis by PLS regression may help to improve the accuracy of the prediction. The OGTT test usually seemed to provide positive results for NIR, non-invasive blood glucose measurement. The OGTT acts to rapidly vary the blood glucose level, while other variable may remain unchanged, or the change is relatively small. This shows that NIR has the potential to measure short-term changes in blood glucose.

Besides the time drift and physiological effects, many unknown factors have rendered the non-invasive measurements unreliable. The Food and Drug Administration (FDA) and other authorities have not yet approved any non-invasive blood glucose measurement devices, and diabetics still need to rely on the painful finger-prick glucose meters.



## **Chapter 3**

### **Methods**

The development of a non-invasive blood glucose monitor was divided into four stages. The first stage was used to check the relationship of the glucose solutions to the NIR spectra. The second stage comprised the pilot studies on volunteer diabetic patients who had been fasting for 10-12 hours. The third stage was the clinical trial on healthy subjects. The trial was mainly used to check meal tolerance effects on the non-invasive blood glucose prediction. The last stage was designed for the physiological comparisons of the diabetic patients for three months, over 30 visits.

#### **3.1 Preprocess**

Two common preprocesses, piecewise direct standardization (PDS) and the Savitsky-Golay smoothing and differentiation (Savgol), were selected for the comparison. A simple mean-centred preprocess was also added to these two preprocesses for PLS analysis. This allowed for the selection of a suitable preprocess for boosting the positive results of the non-invasive, NIR spectroscopic measurement.

##### **3.1.1 The Savitsky-Golay smoothing and differentiation (Savgol)**

Savgol (145) is a differential filter for many applications, such as spectrum filtering (146; 147). It includes differentiation and curve smoothing and also helps to reduce

the variance of spectra. The NIR spectra obtained were taken for a second derivative of the Savgol by using the PLS Tool\_Box 3.5 (from Eigenvector Research, Inc.) under the environment of Matlab. These Savgol preprocessed signals then were divided into two groups, for calibration, prediction and validation as shown in Figure 3-1.

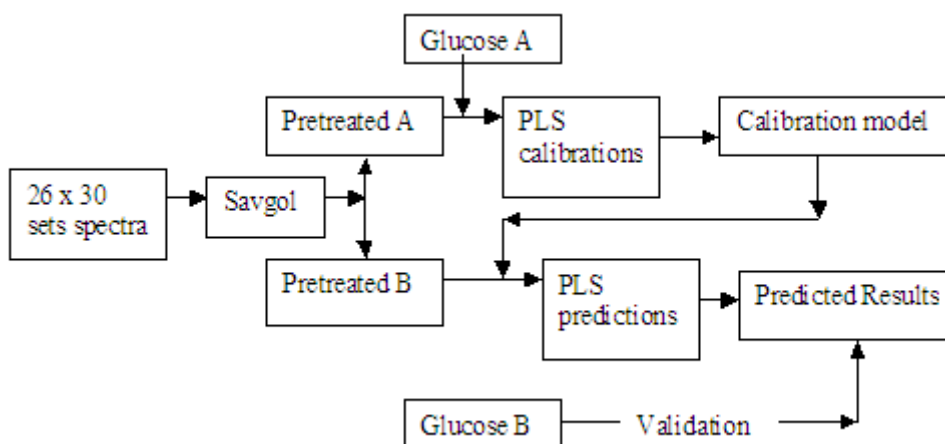


**Figure 3-1: Block Diagram – PLS prediction with Savgol preprocess**

After the Savgol preprocess, the pretreated data were then separated into two groups: Pretreated A and Pretreated B. The Pretreated A group and the corresponding finger-prick glucose level, Glucose A, were applied for the PLS calibration to obtain the calibration model. The Pretreated B and the calibration model were inputted for the PLS prediction. The predicted results were then obtained and validated using the corresponding finger-prick glucose level, Glucose B.

For the glucose prediction with simple mean centre preprocess (SMCP), a similar prediction approach was applied with SMCP block replacement of the Savgol

block. The spectra obtained from the NIR spectrometer were separated into two groups of spectra for calibration and prediction.

### 3.1.2 Piecewise direct standardization (PDS)

PDS (148) is another signal filter which helps to reduce the variance of the spectra. Spectra were divided into two groups; one for PDS preprocessing and calibration with the corresponding glucose levels, and another for the prediction and validation, as shown in Figure 3-2. Spectra A and glucose data A (same as Glucose A stated in Figure 3-1) ( were preprocessed by PDS. The results of the preprocessed A were then used for the PLS calibrations to form the calibration model. Spectra B were also preprocessed by PDS and inputted to the calibration model for PLS predictions and validations. The predicted values were then validated by the corresponding glucose data B (same as Glucose B stated in Figure 3-1).

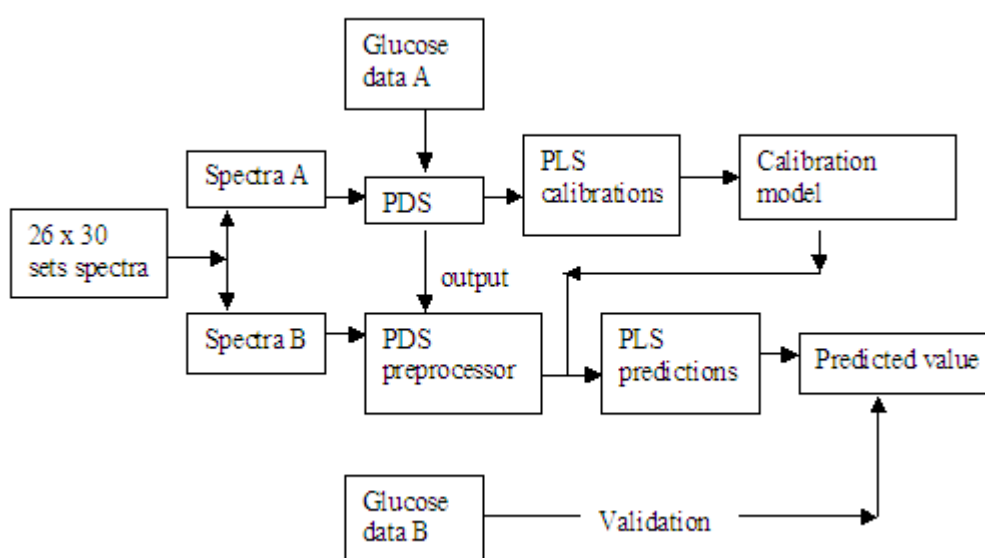


**Figure 3-2: PDS preprocessing for PLS application**

### 3.1.3 Simple mean centred preprocess

Simple mean-centred preprocess is a basic preprocess for PLS. It helps to arrange the large amount of data for PLS. In this method, data are arranged and returned to the mean with zero columns, as shown in the following matrix. All the data were applied to simple mean-centred process to centralize the data for the following two preprocesses. This prediction process basically is same as the prediction process with Savgol, but the data sets are preprocessed by the simple mean-centred method.

$$X = \begin{bmatrix} x_{11} & x_{12} & . & . & x_{1n} \\ x_{21} & . & . & . & . \\ . & . & . & . & . \\ . & . & . & . & . \\ x_{m1} & . & . & . & x_{mn} \end{bmatrix} \quad (3.1)$$

$$\bar{X} = \text{mean} [X]$$

$$= [\bar{x}_1 \quad \bar{x}_2 \quad . \quad . \quad \bar{x}_n] \quad (3.2)$$

$$X_c = \begin{bmatrix} x_{11} - \bar{x}_1 & x_{12} - \bar{x}_2 & . & . & x_{1n} - \bar{x}_n \\ x_{21} - \bar{x}_1 & . & . & . & . \\ . & . & . & . & . \\ . & . & . & . & . \\ x_{m1} - \bar{x}_1 & . & . & . & x_{mn} - \bar{x}_n \end{bmatrix} \quad (3.3)$$

### 3.2 Data analysis and presentation

The NIR signal and the glucose level were mainly analyzed by using the Clarke Grid Error plot, as mentioned in Chapter 2. Bar charts were used for the comparison of the predictability, plotted by Excel and Matlab. All predictions were programmed using Matlab 6.5 and PLS Tool\_Box 3.5 from Eigenvector Research, Inc.

#### 3.2.1 PLS

Partial least squares regression (PLS regression) (133) was applied to the spectra for the calibration and prediction of the glucose level after preprocessing with simple mean-centre data arrangement and/or the preprocesses (Savgol and PDS, respectively). The prediction was obtained by the linear relationship method. Thus the following equation is applied:

$$gc = MX_c + e_1 \quad (3.4)$$

where

$gc$  = Glucose levels used for calibrations

$X_c$  = NIR spectra used for calibrations

$M$  = the models constructed by  $gc$  and  $Xc$

$e1$  = error of the calibrations

One portion of the data of the spectra and corresponding glucose levels were used to build a model  $M$ ; the other portion of data was for the predictions. After calibration by PLS, model  $M$  was obtained. The remaining spectra were then fitted into the model, as shown below, and predicted by PLS.

$$gp = MXp + e2 \quad (3.5)$$

where

$M$  = the model obtained from the calibration

$Xp$  = the remaining NIR spectra for the predictions

$gp$  = the predicted results due to  $M$  and  $Xp$ .

$e2$  = error of the predictions

The results were scatter plotted with the Clarke Grid Error plot. The predictabilities were then calculated in the following section.

### **3.3 Predictability**

The predictabilities of the NIR spectra were compared through the R correlation coefficient of prediction ( $R_p$ ) and the root mean square error of prediction (rmsep). The data were scatter plotted and put onto the Clarke Grid Error plot to show the prediction distributions of the non-invasive, NIR spectroscopic blood glucose prediction against the reference glucose level.

### 3.3.1 Rp correlation

The Rp correlation of prediction was used for comparing the correlation between the predicted value and the true/reference value. The value normally is between magnitudes of 0 to 1. Zero shows no correlation, one is 100% (maximum) correlation.

$$R_p \text{ or } R_c = \frac{n \sum x_i y_i - \sum x_i \sum y_i}{\sqrt{n \sum x_i^2 - (\sum x_i)^2} \sqrt{n \sum y_i^2 - (\sum y_i)^2}} \quad (3.6)$$

where

$x_i$  = reference value

$y_i$  = predicted value

$i = 1, 2, \dots, n$

### 3.3.2 Root mean square error of prediction

Error of the prediction was determined using root mean square error of prediction (rmsep). The higher value of the rmsep, the greater the error is.

$$\begin{aligned} \text{rmsep or rmsec} &= \sqrt{\frac{(x_1 - y_1)^2 + (x_2 - y_2)^2 + \dots + (x_n - y_n)^2}{n}} \\ &= \sqrt{\frac{\sum (x_i - y_i)^2}{n}} \end{aligned} \quad (3.7)$$

where

$x_i$  = reference value

$y_i$  = predicted value

$i = 1, 2, \dots, n$



## **Chapter 4**

### **Stage 1: Ground Work among Glucose Solutions**

#### **4.1 Glucose solutions test**

Glucose is the energy source for the human body. It circulates to every part of the human body. Near Infrared (NIR) spectroscopy is able to measure glucose concentration. This experiment was used to link the optical NIR to glucose concentration. The experiment was under an open environment situation as the first step of a non-invasive blood glucose experiment.

##### **4.1.1 Objectives**

- To find out the relationship between the NIR spectra and the glucose concentrations;
- To evaluate the repeatability of the NIR measurement in glucose concentrations over long a period of time and
- To study the time drift and the machine drift effect for glucose measurement in the long term.

##### **4.1.2 Apparatus and equipment**

The major pieces of equipment in the experiment were the tungsten halogen light (NIR light source) and the NIR spectrometer. The NIR light went through the samples and reflected back from the white reference (a white plate, for details refer

to the Appendix A.5), the sensors of the spectrometer then picked up the light for transferring to spectrum.

#### **4.1.2.1 Light source**

The tungsten halogen lamp (covers wavelength ranging from 300nm ~2500nm) is the most typical NIR light generator because it generates continuous NIR spectral light and is relatively cost effective. The spectrometer used for the experiment was Control Development's TH/DR (refer to the Appendix A.2 for details), which was a 35 Watt Tungsten Halogen light with a gold reflector in a cast aluminum housing. The light source can generate a collimated light beam about two inches in diameter.

#### **4.1.2.2 Spectrometer**

Control Development's NIR spectrometer of NIR-128L-1.7-USB, with the wavelength range of 905 – 1701nm, a three-meter fibre optic was attached and the optical stand was used. These devices were connected for the NIR measurement as shown in Figure 4-1 and Appendix A.1. This system was selected due to its low cost and its wide range of coverage.

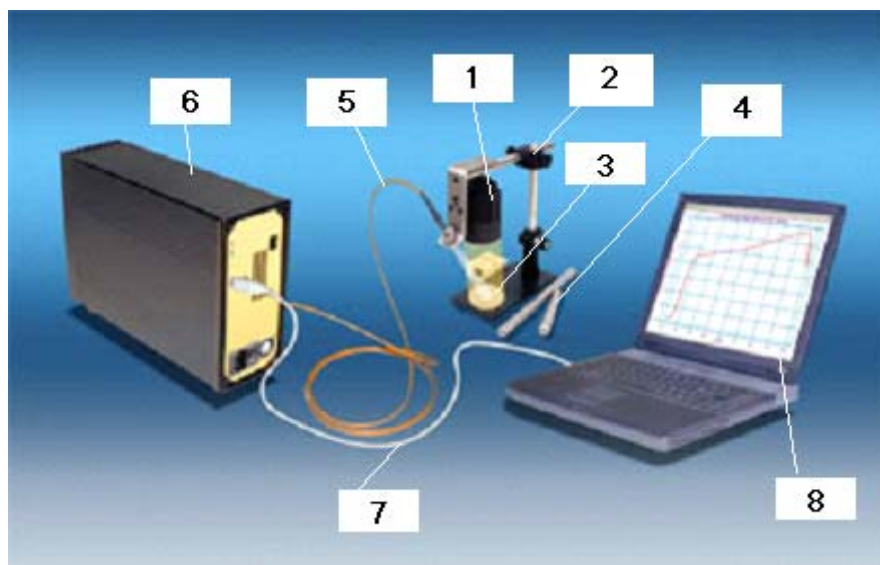


**Figure 4-1: Control Development's NIR spectroscopy of NIR-128L-1.7-USB; 1: tungsten halogen light; 2: optical light stand; 3: optical white plate; 4: optical extension rods; 5: optical fibre; 6: USB cable; 7: spectrometer; 8: spectral reading program with computer**

### **4.1.3 Materials/samples**

D-Glucose dissolved in deionized water (refer to Appendix A.10) was used in the experiment for its major contribution to energy production in humans. Five sets of different glucose concentrations were prepared on each day of the experiment, under controlled room conditions.

A thermo-resistant petri dish made of Polystyrene(PS) was used as the container because of its high temperature resistance and good optical clarity (refer to Appendix A.7).

#### 4.1.4 Procedures

The experiment proceeded under controlled room conditions. Five different glucose concentrations were prepared with the same volume of 20ml for each experiment. The average of the NIR spectra had been recorded from 64 readings per sample. The experiment had been repeated on three different days – under the same room conditions, temperature and relative humidity were maintained at 24 – 25°C and 60-65%, respectively. For a detailed experimental procedure, refer to Appendix B.1.

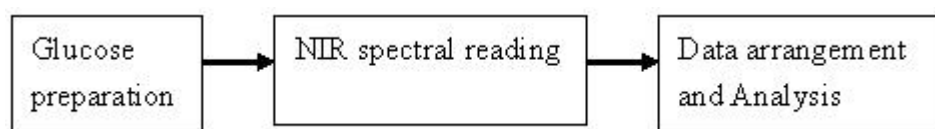


**Figure 4-2: Block Diagram – Glucose concentration analysis**

#### 4.1.5 Characteristics

Temperature variations during the experiment, under the same room conditions, were about 1-2°C. The relative humidity was about +/-5% difference. The glucose solution was sealed and kept for one hour under the measurement environment after the measurement conditions were stabilized.

Calibration against the background and the reference (under tungsten halogen light) was carried before each glucose measurement. This calibration action could help to compensate the background noise since the light and the receiver lens/head were exposed under the room's environment.

Each spectrum was obtained from the average of the 64 data readings for reducing the error generations. The experiments were carried out four times, on three different days, in order to check the effect of machine drift and time drift. The transmittance NIR spectroscopic measurement was used in these experiments.

#### 4.1.6 Analytical Techniques

The repeated tests helped to verify the reliability of the NIR spectrometer. According to Beer's Law, the absorbance is related to the concentration. Thus, based on Beer's Law, a single wavelength was selected for the glucose concentration evaluation. In addition, a simple scatter graph was plotted where the absorbance against the corresponding glucose concentration was shown.

Another technique of partial least square (PLS) prediction was also applied for the analysis. One group of data from two different experiments was used for calibrations, another one was for prediction and validation purposes. The procedure of PLS prediction and validation is shown in the following block diagram.

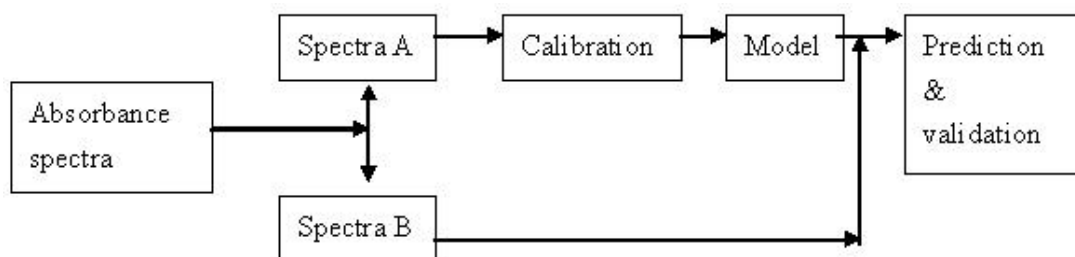


**Figure 4-3: Block Diagram - PLS prediction process of glucose solution concentration**

As mentioned, the spectra obtained were separated into two groups. One group (Spectra A) was used for calibration with the corresponding glucose concentrations and formed the calibration model (Model) shown on equations 4.1 and 4.2.

$$g_1 = M_1 X_1 + e_1 \quad (4.1)$$

where  $X_1 = \text{Spectra A,}$

$e_1 = \text{error 1,}$

$g_1 = \text{corresponding glucose concentrations,}$

$M_1 = \text{calibration model built}$

Then, Spectra B were substituted to  $M_1$  by PLS.

$$g = M_1 X_2 + e_2 \quad (4.2)$$

where  $X_2 = \text{Spectra B}$

$e_2 = \text{error 2;}$

$g = \text{predicted glucose concentrations;}$

The predicted glucose concentrations  $g$  were then validated with  $g_2$ , where  $g_2$  was the glucose concentration corresponding to Spectra B.

## **4.2 Results**

Glucose concentrations can be determined by using NIR spectroscopy, as the absorbance of the NIR is related to the concentration, as stated by Beer's Law. This experiment was to evaluate the relationship between glucose concentration and NIR spectra under NIR spectrometer. The analysis was performed using Beer's Law and PLS prediction, repetitively under two situations: a duration of two months between two experiments and a duration of one hour between two experiments.

### **4.2.1 Glucose concentration measurement**

The known concentrations of solutions were measured by NIR spectrometer in a room with a temperature range of 24 - 25°C and a relative humidity of 55%- 60%. The spectra were then plotted as shown in Figure 4-4.

Four sets of glucose solution measurements, each set with five concentrations (0mmol/l, 125mmol/l, 250mmol/l, 500mmol/l and 1000mmol/l), were measured on three separate days by NIR spectroscopy. The results showed that pure water provided a higher absorbance spectrum. Lower absorbance spectra represented higher glucose concentrations. The local highest peaks represented overtones of the spectra, in which these overtones were due to the excitation of -CH, CH<sub>2</sub> and -OH(83).

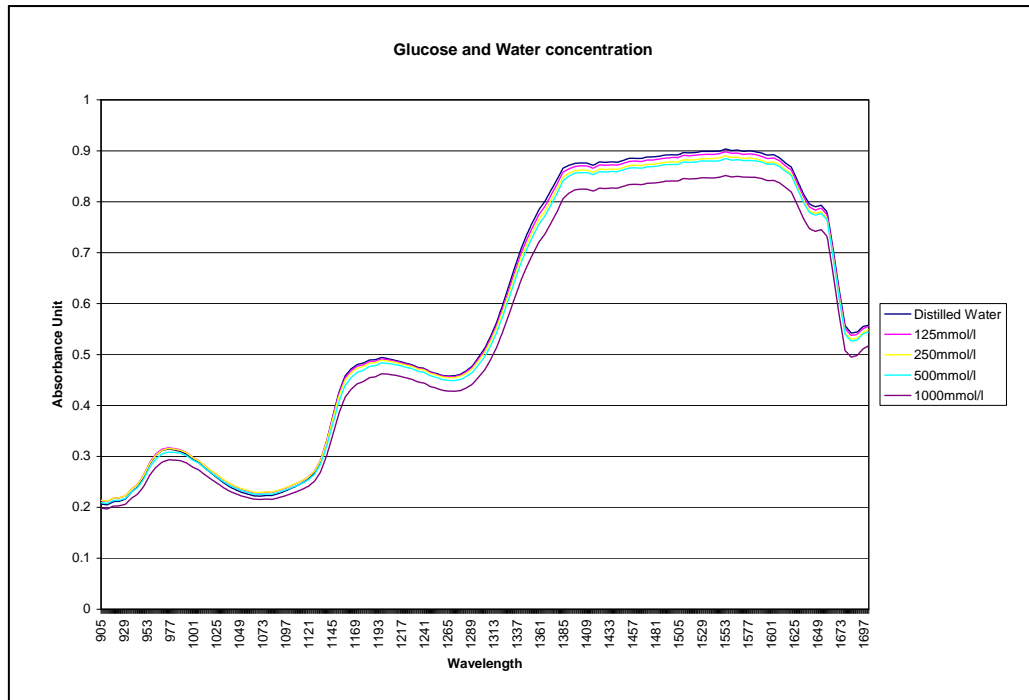


**Figure 4-4: NIR spectra – Glucose Solutions, Absorbance against wavelength (nm), Day 1, under room condition**

Figure 4-4 showed that the spectra gradually increased with three ranges in the local highest absorbance units (AU), called overtones, which were located between 905 and 1120nm, from 1150 to 1200nm and from 1400 to 1600nm, respectively. From around 1400 to 1600nm, there was a flattening of lines showing that the region had been reached saturation (149). Thus, the region could not form clear overtones. However, the absorbance of the spectra could be still distinguished.

#### **4.2.2 Glucose solutions measurement on the same day**

Different batches of glucose solutions were measured within one hour by NIR spectroscopy. These measurements were used to check the reliability of the NIR measurement within a short period of time, while trying to avoid machine drift and



time drift. The glucose concentration was first plotted against the NIR absorbance spectra. Comparison between predictions by PLS is shown in Figure 4-5.

#### 4.2.2.1 Single wavelength absorbance vs glucose concentration

Inverse linearity was observed with absorbance spectra at wavelength 1180nm, where the lower absorbance indicated a higher glucose concentration. The best fitted lines, shown in Figure 4-5, can be represented by the following linear equations, respectively.

Fit 3a:

$$y = -5.19e^{-5}x + 0.47 \quad (4.3)$$

(R = 0.91 and RMSE = 0.0108AU, 207mmol/l)

Fit 3b:

$$y = -4.84 e^{-5}x + 0.46 \quad (4.4)$$

(R = 0.87 and RMSE = 0.0098AU, 204mmol/l)

where

y = absorbance units;

x = glucose concentrations

R = R correlation coefficient;

rmsep = root mean square error

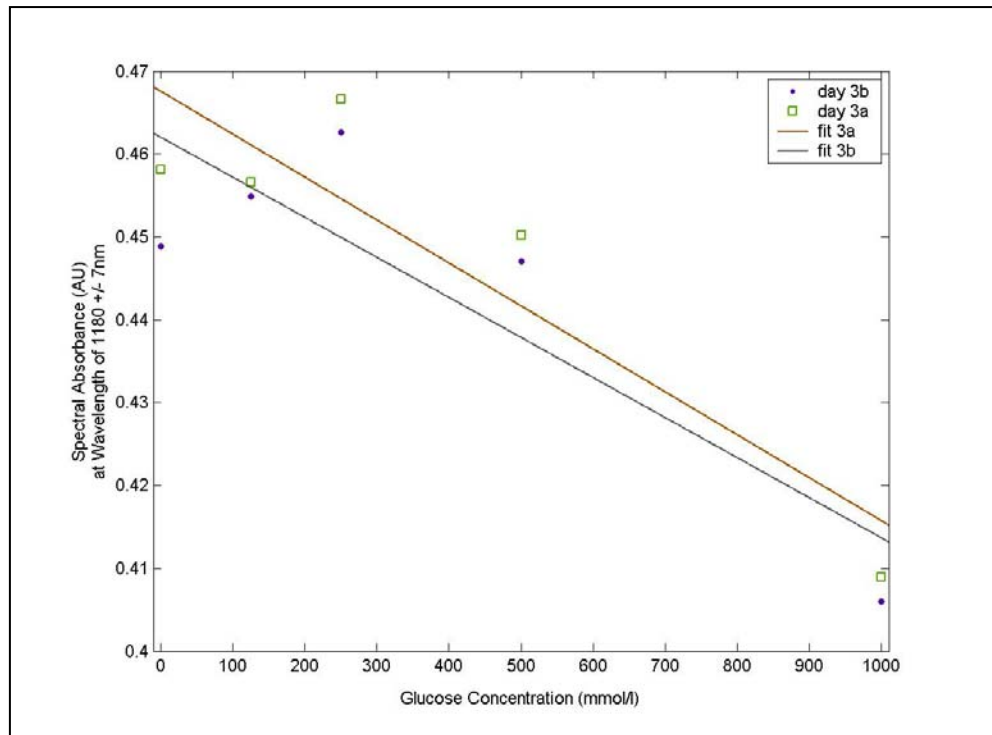


**Figure 4-5: Absorbance at 1180nm against glucose concentration, separated experiment in one hour; fit of Day 3a is close to fit of Day 3b.**

Figure 4-5 showed that the fit of 3a and 3b were close to each other. This showed that the results of the two experiments were nearly repeated. This also demonstrated that glucose concentrations could be measured via transmittance NIR spectroscopy, where the absorbance (AU) is related to the glucose concentrations.

#### 4.2.2.2 Glucose concentration predictions by PLS

PLS is another prediction technique mainly used for spectroscopic application. The spectral results were analyzed by PLS. The known glucose concentrations were calibrated with the measured spectra from Day 3a to form a model and then the measured spectra of Day 3b (after one hour) were predicted through PLS. Figure 4-6 shows the scatter plot of the calibration results and the prediction results of the glucose concentration within one hour.

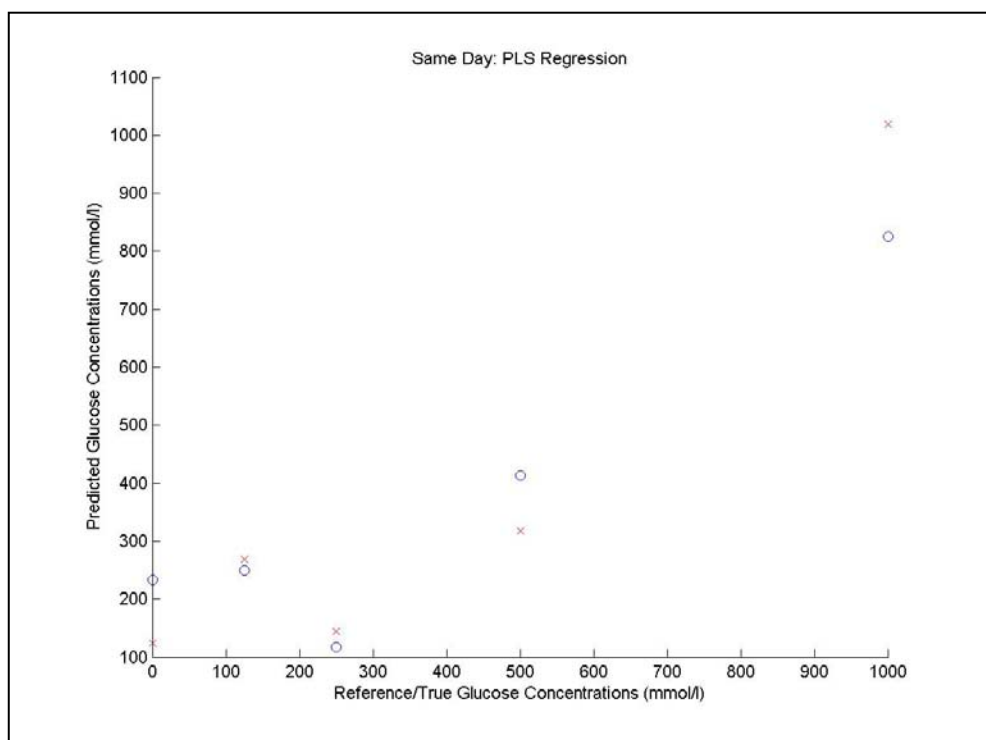


**Figure 4-6: PLS prediction scatter plot, separated experiment in the same day within one hour; cross (x) = calibration; hollow (o) = prediction**

These results showed the R correlation coefficient of the prediction ( $R_p$ ) = 0.92 and root mean square error (rmse) = 158mmol/l. The relationship between spectral signals (or the absorbance unit under Tungsten halogen at 1180nm

wavelength) and the glucose concentration was linear. The major predicted error occurred in the low glucose range.

### **4.2.3 Glucose solution measurements on different days**

The experiments were conducted on different days and were used to analyze machine drift and time drift effects over a two-month period. Different batches of known glucose solutions were measured on different days by the same NIR spectrometer. The glucose concentration was plotted against NIR absorbance for the evaluation. It was also analyzed by PLS.

#### **4.2.3.1 Single wavelength absorbance versus glucose concentration on separate days**

Absorbance of the single wavelength at 1180nm was plotted against the corresponding glucose concentration, as shown in Figure 4-7. The results showed that the data of Day 1 are about 0.06 AU (potentially a very significant error) higher than the data of Day 2. Their fitting equations are shown below:

Fit 1:

$$y = -3.32e^{-5}x + 0.47 \quad (4.5)$$

(R = 0.99 and RMSE = 0.0020AU, 60mmol/l)

Fit 2:

$$y = -3.23 e^{-5}x + 0.41 \quad (4.6)$$

(R = 0.91 and RMSE = 0.0052AU, 163mmol/l)

where

y = absorbance units;

x = glucose concentrations

R = R correlation coefficient;

RMSE = root mean square error

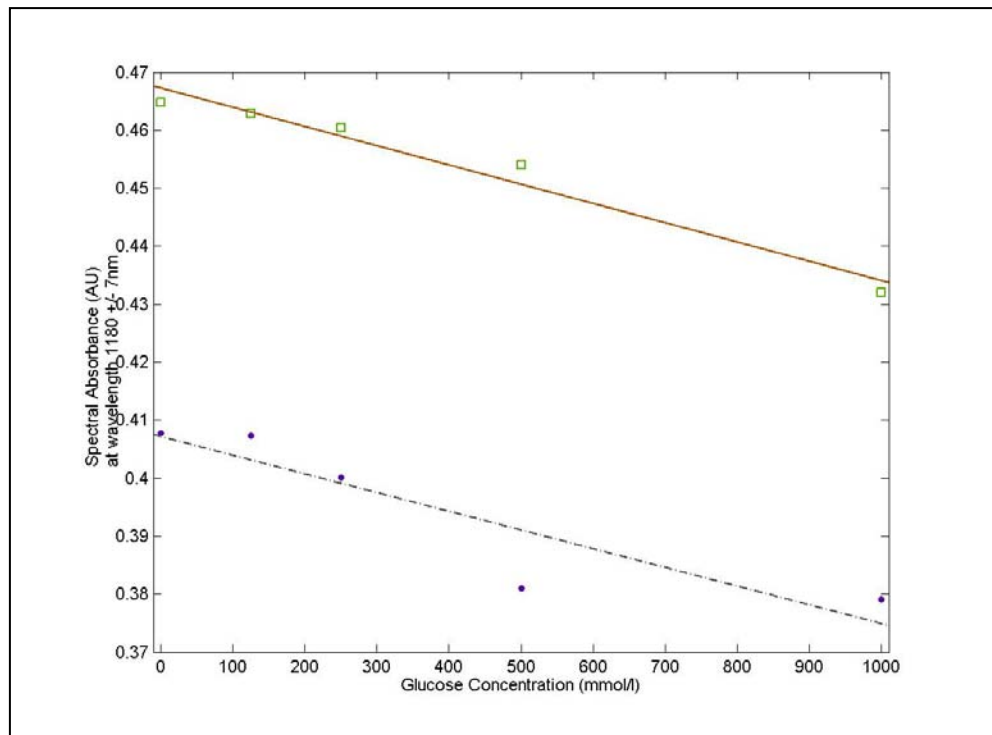


**Figure 4-7: Absorbance at 1180nm against glucose concentration, two experiments with a two-month separation.**

Two fits of large separation were shown in Figure 4-7. The results showed that machines drift and time drift occurred in the measurements after a two-month time separation. NIR spectroscopy could measure the glucose concentrations by using absorbance (AU) against the glucose concentrations. For the long term, there was an absorbance difference due to the machine drift and time drift.

#### 4.2.3.2 Spectra prediction versus glucose concentration by PLS on separate days

Preprocess of Piecewise Direct Standardization (PDS) was used to regulate the spectral drifts from different days. These preprocessed data were then calibrated and predicted by PLS regression. The results were then scatter plotted, as shown in Figure 4-8. These scatter plots from different days were close to each other.

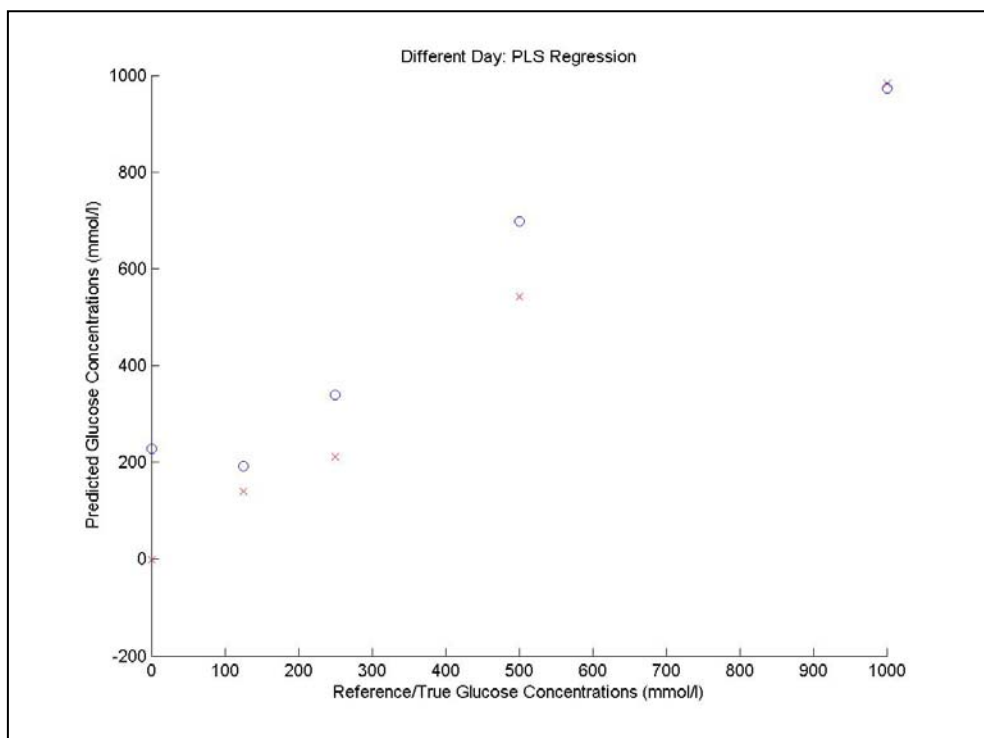


**Figure 4-8: PLS prediction scattered plot, separated experiment in different days in two month – cross (x) = calibration; hollow (o) = prediction**

The results showed that  $R_p = 0.97$  and  $rmsep = 144\text{mmol/l}$ . A major error also occurred in the low glucose concentration region, particularly for the pure water measurement. Table 4-1 shows the summary of R and rmse ( $R_p$  and  $rmsep$ ) by absorbance and PLS spectral analysis, respectively.

**Table 4-1: R correlation of coefficient and rmse (root mean square error) comparison; absorbance of Day 1 > 0.06 AU of absorbance of Day 2**

Analysis \ Day	Same Day (Day 3a, Day 3b)		Different Days (Day 1, Day 2)	
	R	RMSE	R	RMSE
<b>Absorbance</b>	0.91 (Day 3a)	207 mmol/l	0.99 (Day 1)	60 mmol/l (Day 1)
	0.87 (Day 3b)	204 mmol/l	0.91 (Day 2)	163 mmol/l (Day 2)
<b>PLS (prediction)</b>	$R_p = 0.92$	$rmsep = 158\text{mmol/l}$	$R_p = 0.97$	$rmsep = 144\text{mmol/l}$

On the row of the absorbance comparison, there are four batches of samples. For the Different Day analysis, there was a 0.06 AU difference between Day 1 and Day 2, as shown in Figure 4-7. This result showed that the effect of machine drift and time drift occurred. This made the error approximately 2000mmol/l occurrence between the two different measurements. However, these machine drift / time drift instances might be eliminated by using PLS, which demonstrated the calibration on Day 1 and made a prediction from the Day 2's data. The analysis showed promising results with  $R = 0.97$  and  $rmse = 144\text{mmol/l}$ .

### 4.3 Discussion

The spectra of Figure 4-4 showed that the absorbance rates were clearly distinguished among the spectra. This distinguished absorbencies were located approximately on the first and second overtone of the NIR spectrum, which showed elemental excitation (150).

The region (at wavelength of 1400 to 1600nm) showed a flattened line, instead of a bell shape, which indicated that this region was saturated for the spectroscopic measurement, although absorbance spectra could still be distinguished.

The wavelength 1180nm was chosen for the analysis, as it showed the most clearly distinguished absorbance and was also located in the region of second overtones (150). According to Beer's Law, as stated in Chapter 2, concentration is proportional to the absorbance unit under the same absorption coefficient and path length. Thus, as different concentrations reacted to different absorbance, different points of absorbance could react with different glucose concentrations and could be distinguished.

The results in Figure 4-5 showed that the higher glucose concentration, the lower the absorbance, which seemed to contradict Beer's Law. This was because the overtone occurred might be due to the -OH excitation. Therefore, higher -OH concentration could provide higher absorbance. Water contains a large amount of -OH. When glucose was added, the concentration of -OH would be relatively reduced, and absorbance therefore reduced.



### 4.3.1 NIR absorbance and PLS

There were four experiments on three separate days. The results in Figure 4-5 showed that the two fitting lines were close to each other. The absorbance and the glucose concentration were linearly correlated. This showed that the results of the two experiments were similar and reproducible. NIR spectroscopy was able to measure glucose concentration, even when partly saturated in a range of spectral regions. The high R correlation coefficient 0.9 showed that the glucose concentration was highly correlated to the NIR absorbance.

PLS provides another prediction technique for the glucose concentrations by using NIR spectroscopy. Figure 4-6 showed the predicted result from PLS. R correlation of prediction ( $R_p$ ) was equal to 0.92, but the poorest prediction was located in pure water region. PLS prediction provided partly poorer results when compared with the direct absorbance to the glucose concentration analysis. However, the prediction made through PLS was still better than just using the absorbance unit. Although glucose concentration is proportional to the NIR absorbance of a single wavelength, the rate of error may be higher when only a single wavelength is used. Alternatively, PLS was applied by using the whole range of the spectra for the prediction. The error may be relatively small since using the whole range spectra may cause to average the error.

In addition, results might not be reproducible under a single wavelength measurement after two months. This was due to machine drift and time drift. Even though there was only one variable – glucose, the machine might face micro-

deviation among the different inner parts which accumulated over a period of time. The results state in Figure 4-5 and Figure 4-7 were based on the same experimental setup and under the same room conditions. However, there was 0.06 AU difference. According to the fitted lines, 0.06AU represents 2000mmol/l. This showed that the absorbance difference between two experiments, after long time division, could introduce a very large error due to machine drift and time drift.

The machine drift and the time drift can be reduced or eliminated by using analytical techniques such as PLS with PDS preprocess. Therefore, Figure 4-8 showed that the glucose concentration prediction provided lesser or no machine drift and no time drift effect. Poor prediction occurred in the low glucose concentration region. The errors of the prediction were mainly due to the deviation of the glucose solution preparation and the difficulty of distinguishing low glucose concentration from a relatively large amount of 20ml water. Temperature was kept constant, with about  $\pm 1^{\circ}\text{C}$  variation during the experiment.

Temperature was monitored during the experiment since it could affect the NIR absorbance measurement. According to Arimoto et al. (151), their results from glucose solutions with different temperature settings showed that a deviation shift of the spectra occurred. The shift varied with different concentrations in different temperature ranges. Therefore, the experiment was carried out under consistent conditions in order to reduce the effects of the temperature variation.

For comparison of the predictability between the absorbance unit and the PLS prediction, as shown in Table 4-1, the overall results showed that PLS was another technique for NIR spectroscopic measurement of glucose. It could also

eliminate/minimize the effect of the machine drift and the time drift. This also demonstrated that PLS was suitable for complex signal analysis.

### **4.3.2 Overtones**

Referring to “Introduction to NIR Technology of Analytical Spectral Devices, Inc.(ASD)” (83), the -OH stretch first overtone is at 1450/1490nm, -CH stretch second overtone is at 1200nm and -CH<sub>2</sub> third overtone is at 930nm. In this experiment, the peaks occurred at about 950nm, 1200nm and 1400-1650nm (although it reached saturation), respectively. NIR absorbance was due to hydrogen excitation. According to Mark (152), hydrogen was a key element of all organic materials which absorb in the NIR region. This limited the spectroscopic active vibrations to those of -CH, -OH and -NH side groups. Both ASD and these experiments obtained similar peaks. This clearly showed that NIR might not be affected by the surrounding background, except for temperature variations (121). Thus, an experiment under a conditional temperature environment was recommended for glucose concentration measurement.

In these experiments, glucose concentrations were distinguished through absorbance. Glucose absorbance mainly occurs and is distinguished in overtone regions, which could represent different side groups of -OH and -CH, as mentioned by Chen et al. (153) and Amerov et al. (113), for their NIR prediction.

Absorbance of a single wavelength is applicable to glucose concentration measurement. However, for complicated measurements which involve different substances or time frames, it leads to indistinguishable results. In these glucose

concentration measurements, a longer time division (two months) between two identical experiments introduced a relatively large error of 0.06 AU difference. Thus, a longer range of spectra is applicable for complex situations. These series glucose concentration tests also demonstrated that PLS analysis was suitable for NIR spectroscopic measurements for glucose concentrations.

### **4.3.3 Error and noise**

There were possible measurement errors, or noise, of the glucose solution. The experiment was carried out under the exposure to the surrounding environment. The results might not be affected by the surrounding florescent light which exists at 190nm to 650nm, while NIR is ranged from 730nm to 2500nm. The indium gallium arsenide (InGaAs) detector (NIR detector could only sense within the NIR region) of the spectrometer was not affected by the surrounding visible light. However, NIR might have derived from other NIR environmental sources, such as temperature variations, if some of the other equipment present generated an NIR wavelength range.

In addition, the resolution of the spectrometer is 6.22nm, thus, the specificity of the absorbance at 1180nm could be  $1180 \pm 6.22$ nm. The results might not really represent the absorbance of the exact corresponding wavelength. However, NIR overtones always overlap to multiple wavelengths or a certain range of the spectrum (83). The separation of each measurement pixel forms the spectrum by interpolation. This indicates that the resolution might not provide a significant effect to the absorbance. Unless there was a particular wavelength that had fallen in

between two pixels, an error might occur. However, as NIR overtones always cover multiple wavelengths, the resolution of the absorbance was enough to cover the measurement.

Nevertheless, the measurement area in the experiment was relatively large within the petri dish, and it might affect the results, particularly on the low glucose concentration. The glucose particles might not be equally distributed among the large area. The error could be relatively large due to the external environment and the glucose preparation error, particularly in low glucose concentration areas.

NIR spectroscopy is able to measure glucose concentrations. However, blood glucose measurement is more complicated. For non-invasive blood glucose measurement, many interfering signals such as proteins, red blood cells and lipids exist. The concentration of glucose in the blood is relatively low compared with these nutrients. Thus, non-invasive blood glucose measurements made through NIR is a challenging technique. Nevertheless, NIR is one of the weakest signals in human tissues, so it is possible to carry on as a medium for non-invasive blood glucose measurements *in vivo*.

## **4.4 Conclusions**

From the experiment, results showed that the higher the glucose concentration, the lower the spectral absorbance was in the spectrum. However, NIR spectroscopic measurements deviated due to machine drift and time drift after two months. This caused errors in the NIR spectroscopic measurements. These drifts could be reduced or eliminated by the PLS technique.

NIR spectroscopic measurement under PLS analysis showed promising results on the glucose solution test in both short- and long-term experiments. Thus, the result was positive with regards to using NIR measurement in diabetic patients. This will be considered in the following chapter.

## Chapter 5

### Stage 2: Studies among Diabetics

#### 5.1 Clinical research on diabetic patients

This stage of the study was carried out in a regional hospital. A total of 99 patients were recruited for the two-month long clinical trial. The diabetic patients were subjected, as usual, to regular body checking and blood glucose measurements. After that, they were measured by NIR spectroscopy via the transmittance approach.

##### 5.1.1 Objectives

- To determine the relationship between the NIR spectra and blood glucose levels from diabetic patients;
- To evaluate the feasibility of the NIR spectroscopic measurement for *in vivo* glucose measurement and
- To find a suitable method for the NIR spectroscopic measurement *in vivo*.

##### 5.1.2 Apparatus and equipment

The same spectrometer and tungsten halogen light mentioned in Section 3.1 were used for the studies. The patients' index fingers were put in contact with the lens while the halogen light was indirectly shone on the fingers via the white plate. Refer to Appendices A.1-A.5 for the specification of the equipment used.

### **5.1.3 Subjects**

Diabetic patients fasted for 10-12 hours before the blood extraction and the NIR measurement. Their age range was 29 – 84 years, mean age was 57.65 and the standard deviation was 11.16. Four subjects were diagnosed with Type 1 diabetes and 95 had Type 2 diabetes.

### **5.1.4 Procedures**

Blood was taken from the arm of each patient by a registered nurse in the hospital as part of his/her regular check-up; afterwards, the finger surface temperature and the NIR spectroscopic measurement procedures were performed. The time between the NIR measurement and the blood sampling was about 10-15 minutes. The whole process, from blood sampling to the completion of NIR measurement, took about 20 minutes. The blood glucose levels were then tested by the hospital. For detail of the procedures, refer to the Appendix B.2.

### **5.1.5 Characteristics**

All ninety-nine Chinese subjects fasted for 10-12 hours before the blood sampling and the NIR measurement. This action could help to reduce meal interference in the blood, providing a more accurate reading. Spectrometer self-calibration against the background of the room condition had been done before the measurement of each subject. Finger surface temperature was recorded. Subjects had touched the optical lens with their fingers for the measurement.

The NIR light was directly shone on the white plate (as shown in Appendix A.5). The light reflected from the white plate penetrated the finger and then passed



through the fibre optic to reach the spectrometer. The spectra were then recorded by a computer connected to the spectrometer. Figure 5-1 shows the measurement process in a block diagram.



**Figure 5-1: NIR spectroscopy measurement process**

### 5.1.6 Analytical techniques

An average spectrum was obtained from 64 spectral readings in each subject. Two-thirds of the spectra and the corresponding glucose levels were calibrated by PLS to form a calibration model for the prediction. Figure 5-2 shows the block diagram of the prediction analysis. Ninety-nine sets of spectra and corresponding glucose values were divided into 66 sets and 33 sets. The 66 sets were calibrated by PLS to form a calibration model. The remaining 33 sets were then applied to the model and analyzed by PLS to find the predicted results and to work on variation.

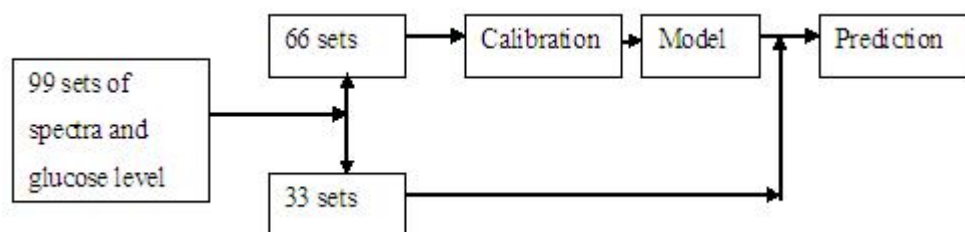


**Figure 5-2: Block Diagram – PLS prediction of the blood glucose levels from diabetic patient at a regional hospital**

The R correlation coefficient of the prediction ( $R_p$ ) and the root mean square error of the prediction (rmsep) were used to represent the predictability of the prediction results.

## **5.2 Results**

The following sections report the results from the clinical study from the regional hospital. Ninety-nine diabetic subjects were involved. Transmittance NIR spectroscopic measurement had been carried out after venous blood sampling on the morning after fasting for 10-12 hours. The NIR absorbance spectrum, surface temperature from the index finger and blood sampling were all taken from the same side as mentioned in Appendix B.2.

The following results were obtained by using PLS prediction to the corresponding blood glucose levels. The analysis mainly included preprocesses of PDS and Savgol, and the simple mean-centred process described in Chapter 3. The spectra were divided into two wavelength ranges (905 – 1380nm and 1381 – 1701nm) and one full range (905 – 1701nm) for prediction. The data were also arranged into ascending glucose levels, respectively. There were two prediction arrangements, one from the ascended data and the other from the original data.

### **5.2.1 Spectra**

Figure 5-3 shows the absorbance spectra obtained by using NIR spectroscopy. All the spectra contained similar patterns with various absorbencies. There were two overtones which appeared on wavelengths 980nm and 1200nm, respectively, of

which the latter showed a higher absorbance. On 1300nm, the absorbance began to increase until reaching 1380nm. The absorbance then dropped linearly and generated many tiny ripples. This showed that many noises appeared in this region. Furthermore, there should have been an overtone instead of a linear decay. Thus, the region may be explored for further analysis and discussion.

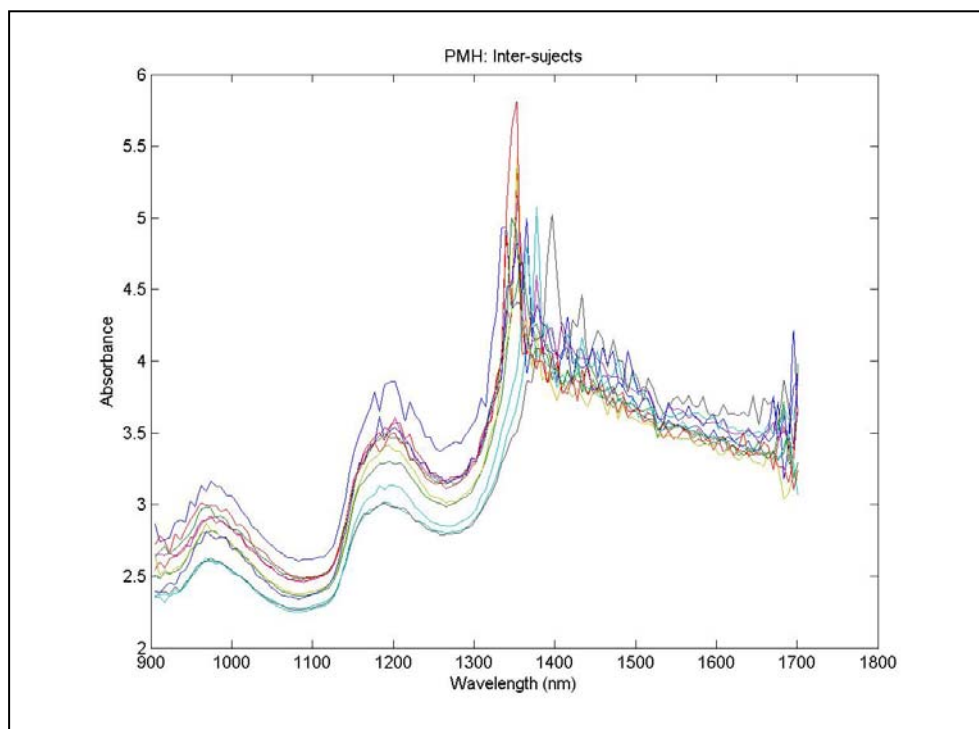


**Figure 5-3: NIR spectra – ten diabetic subjects, absorbance against wavelength (nm); highly noises at 1381-1701nm caused by finger blocking the light transmission**

On the other hand, the spectra in Figure 5-3 also showed a high variance. This might be caused by physiological differences among different patients and environmental influences. The two overtones found were similar to the spectra of the glucose solutions stated in Chapter 4: they were also at the approximate wavelengths of 980nm and 1200nm. However, the spectral ranges from wavelength 1381 –

1701nm showed that decay had occurred with high, frequent ripples. This indicates that NIR light might not have enough power to penetrate the fingers in this region. The light might be blocked by the fingers so as to cause noise in the form of ripples.

### 5.2.2 Prediction

The PLS predicted results from the spectra of the regional hospital were scatter plotted on a Clarke Grid Error plot (9), as shown in Figure 5-4.  $R_p$  and  $rmsep$  represent the R correlation coefficient of the prediction and the root mean square error of prediction, respectively.

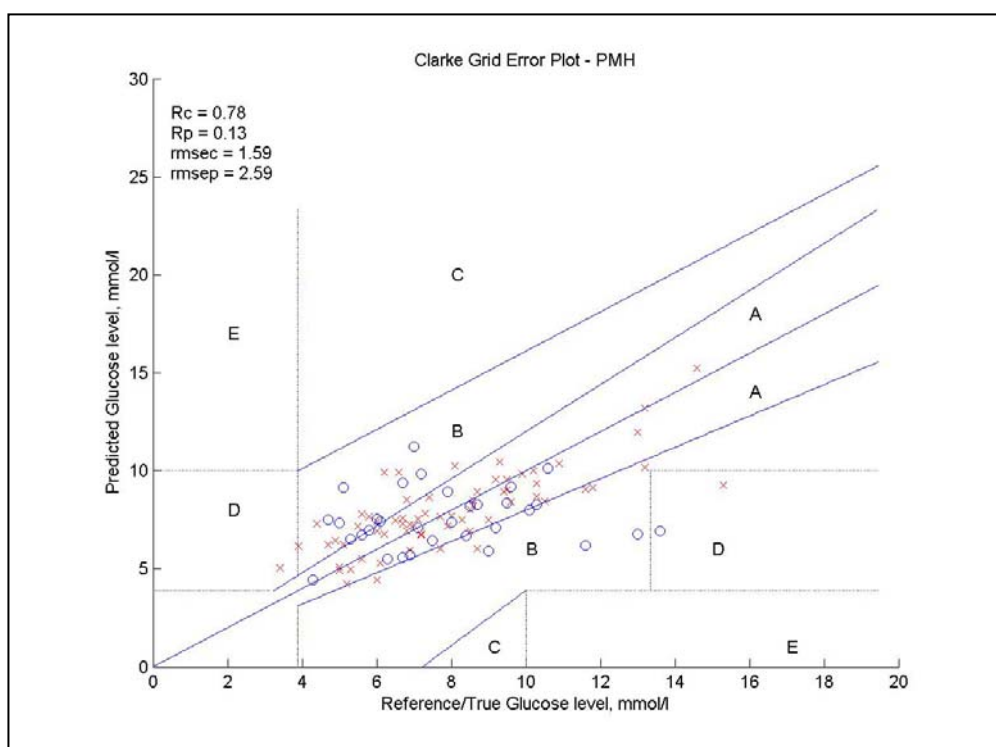


**Figure 5-4: Predicted against Actual Blood Glucose Level: (x) calibration, (o) prediction; data was arranged to an ascending order and preprocessed by simple mean-centred preprocess.**

The results in Figure 5-4 showed the scatter plot from the prediction of the glucose levels by using the full range (905 – 1701nm) of spectra.  $R_p$  was 0.13 and  $rmsec$  was 2.59mmol/l. The overall temperature variance was 6.67°C, and the mean temperature was 30.16°C. Although  $R_p$  and  $rmsec$  were poor, almost 98% of the predicted glucose levels were located inside clinically acceptable regions, A and B. Only one predicted point was located in region D, the “dangerous failure to detect and treat blood glucose errors” according to the Clarke Grid Error plot (9).

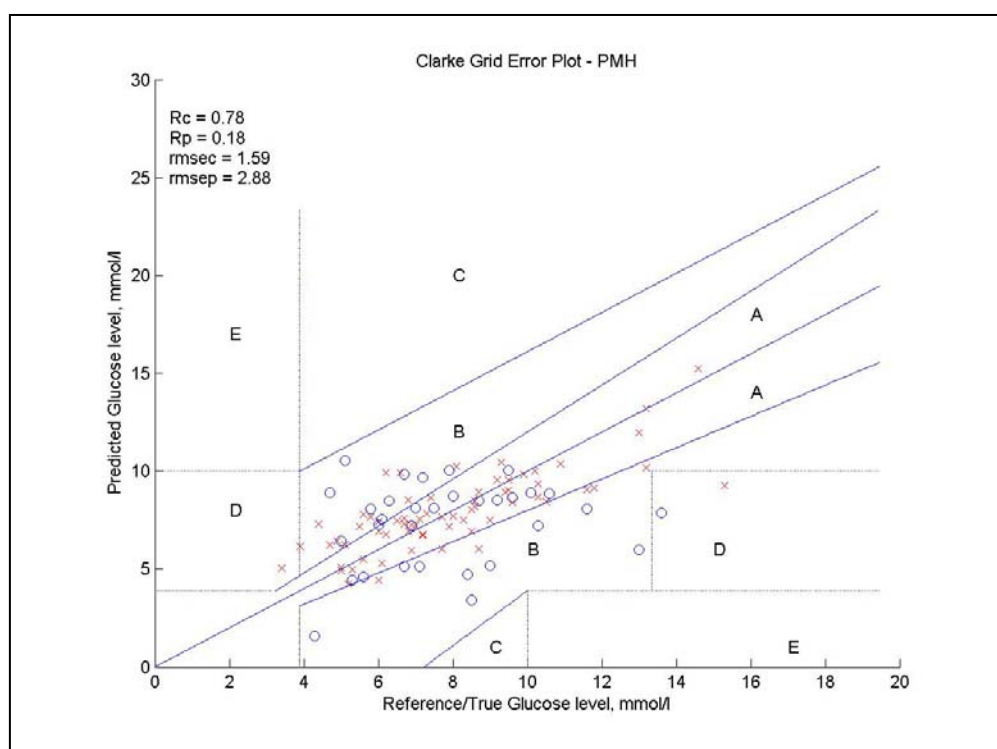


**Figure 5-5: Predicted against Actual Blood Glucose Level: (x) calibration, (o) prediction; data was arranged to ascending order and preprocessed by simple mean-centered preprocess and PDS preprocess.**

The results shown in Figure 5-5 showed another scatter plot from the prediction of the glucose levels by using the full range (905 – 1701nm) of spectra

without arranging in ascending order. The PDS preprocess had been applied before PLS prediction. The results of  $R_p$  were shown to be slightly better than those in Figure 5-4, but the rmsep was still poor. Its  $R_p$  and rmsep are 0.18 and 2.88mmol/l, respectively. Almost all of the predictions were located inside the regions A and B of the Clarke Grid Error plot.

### 5.2.3 Comparisons

**Table 5-1: Results of the regional hospital, R correlation coefficient of calibration/prediction (Rc/Rp) and root mean square error of calibration/prediction (rmsec/rmse) comparisons. No preprocess: simple mean-centred preprocess; Savgol preprocess: Savgol with simple mean-centred preprocess; pds preprocess: PDS with simple mean-centred preprocess; sorted: data arranged into ascending order**

Selected Ranges	905-1701nm	905-1701nm, sorted	905-1380nm	905-1380nm, sorted	1381-1701nm	1381-1701nm, sorted
No preprocessed						
Rc	0.77	0.78	0.63	0.67	0.66	0.7
Rp	-0.07	0.13	0.1	0.1	-0.07	-0.11
rmsec (mmol/l)	1.77	1.59	2.16	1.88	2.1	1.81
rmsep (mmol/l)	3.66	2.59	2.73	2.43	3.59	3.37
Savgol preprocessed						
Rc	0.69	0.67	0.5	0.53	0.58	0.72
Rp	-0.29	-0.51	-0.15	-0.15	-0.22	-0.57
rmsec (mmol/l)	2.01	1.89	2.41	2.15	2.25	1.77
rmsep (mmol/l)	3.93	3.4	3.17	2.58	3.47	4.1
pds preprocessed						
Rc	0.77	0.78	0.63	0.67	0.66	0.7
Rp	-0.04	0.18	-0.12	0.02	0.01	-0.24
rmsec (mmol/l)	1.77	1.59	2.16	1.88	2.1	1.81
rmsep (mmol/l)	2.77	2.88	2.68	2.86	2.5	5.17

Table 5-1 showed the summaries of the predictions from PLS with Savgol and PDS preprocesses. The preprocess Savgol is a well proven filtering technique, which has been in use since 1964, and PDS is another well-known filter for spectroscopic application. Two preprocesses and a simple mean-centred preprocess were compared for their ability to assist the prediction of PLS. All the  $R_p$ ,  $R_c$ ,  $rmsep$  and  $rmsec$  from different arrangements were used as indicators for the comparison. The highest  $R_p$  was 0.18, which was from the PLS prediction of “sorted data and PDS preprocess,” while the corresponding  $rmsep$  was 2.88mmol/l. The lowest  $rmsep$  was 2.43mmol/l, which was located at “sorted data of 905 to 1380nm.” This demonstrated that the arrangement of the data set for PLS affected the prediction results.

### **5.3 Discussion**

The summarized results in Table 5-1 showed that non-invasive blood glucose prediction *in vivo* was not as good as the prediction in the glucose solutions. This implied that NIR prediction for blood glucose *in vivo* was not as easy as *in vitro*. Many uncertain parameters exist within *in vivo* measurements, especially the changing and unpredictable metabolic rate and other physiology. During the glucose solution tests, glucose concentration was the only interactive substance for NIR spectroscopy. This might have led to an error based on machine drift and time drift, the preparation of glucose solutions and a temperature factor. Therefore, NIR spectroscopic measurement for glucose concentration was easy to obtain. Although



PLS with preprocessing technique could have reduced the above-mentioned drifts, the physiological effect was an unpredictable factor existing *in vivo*.

The results obtained from PLS with Savgol showed the poorest results. PLS with PDS provided the best  $R_p$ . The PLS without preprocess showed the lowest rmsep. This showed that Savgol might not be suitable for this application. The predicted results were not reliable, probably due to the physiological effect from the different diabetic patients over the two-month clinical trial. However, most of the predicted glucose levels were located inside the regions, A and B, in which the glucose levels represented clinically acceptable values, as shown in Figures 5-4 and 5-5.

This indicated that non-invasive blood glucose measurement was possible, *in vivo*. The *in vivo* NIR measurement could not solely rely on a partial range of spectra or from a specific absorbance of a single wavelength. A wider range of spectra is recommended since measurement noise can be averaged in a wider spectral signal. The wider the spectral range of the measurement in NIR spectra, the more the noise may be dampened. This is because when NIR reacts with blood glucose, the wider range of obtained spectra provides more information. This helps to increase the signal-to-noise (S/N) level. In contrast, when the blood glucose measurement relied on one wavelength or shorter spectra range, the noise would be relatively increased, unless there was no physiological effect or no metabolic change *in vivo*. Single wavelength measurement was not able to establish *in vivo* blood glucose measurement among the range of 905 to 1701nm. Although using a single wavelength for glucose solution measurement was successful in this study, it reacted

with a single variable, glucose concentration. In addition, non-invasive blood glucose measurement for *in vivo* contains many changing variables. Single wavelength measurement by NIR may only detect a small portion of the necessary signal, which may be due to OH- or CH- of glucose, protein and/or fat, not just from glucose. Thus, a wide range of NIR spectroscopy is suggested.

### **5.3.1 Simple mean-centred preprocess**

In the results of the “no pretreated,” the data of two full range “905-1701nm” and “905-1701nm, sorted” showed that both Rcs were close to each other. However, the predicted results Rp showed that “905-1701, sorted” provided more accurate results. When compared to the rmsec (root mean square error of calibration), the result was also similar, but the rmsep provided a greater difference; rmsep of the sorted spectra was 41% poorer. This indicated that good calibration might not imply good prediction. The accuracy of the predicted results depended on the choices of the data arranged and suitable preprocess for PLS prediction. The selected partial range of spectra might have caused an increase of noise level, which affected the prediction since a particular range might have generated a relatively large noise at the moment. Clearly, the main influence was due to the physiological effect which caused larger spectra variation.

In the region of 905-1380nm, both sorted and unsorted data gave similar results. However, in the range of 1381 – 1701nm, their results were poorer, especially for Rps, where negative correlations between predicted glucose levels and true/reference glucose levels were shown. This might be caused by the insufficient information in this region or by relatively large noise sources, in which the signals

were blocked by the fingers. Thus, highly rippled noise existed, as shown in Figure 5-4.

### **5.3.2 Savgol Preprocess**

Savgol is well known as a low-pass filter or as a background noise filter (154). During the preprocess of Savgol from these clinical data, all the spectra had been taken for second derivative and smoothing. One-third of the Savgol-treated spectra were used by PLS for calibration in order to generate the calibration model. The rest of the Savgol-treated data were then analyzed by PLS to obtain the predicted glucose levels.

However, poor results were acquired. All the  $R_p$  showed negative correlation. This might be caused by many factors. One possible factor was that the Savgol filter might not be useful in a highly noisy signal, particularly in the region of 1381 to 1701nm. According to Bromba and Ziegler (154), Savgol could be optimal for a spectrometric signal of a signal form that was nearly equal to a polynomial shape. They also mentioned that Savgol might not be suitable for the non-polynomial application where a higher signal distortion might occur. This observation of the advantage and the disadvantage of the smoothing and differentiation filter was confirmed by Savitzky and Golay (145). This led to the possibility that Savgol might wrongly interpret the glucose level signal as a noise signal. When compared with the rmsep, the best two were in the range of “905 – 1380nm,” since the spectra were close to the polynomial shape. The poorest two rmsep were located at “1381-1701nm, sorted.” Results showed that spectra portions in this range contained the highest noise since the NIR could not penetrate through the finger to reach the

detector, which meant that S/N ratio was very low. The second poorest rmsep was at “901-1701nm.” The poor prediction might have happened on the highly noisy signal of “1381-1701nm.” This also showed that not every preprocess was suitable for *in vivo*, NIR spectroscopic prediction, since partial spectra were approximately equal to polynomial curves.

### **5.3.3 PDS preprocess**

PDS is a common preprocess for NIR spectral application. The calibration spectra and the corresponding finger prick glucose readings had firstly been pretreated by simple mean-centred preprocess and the PDS preprocess. These preprocessed spectra and their corresponding finger prick readings were then applied to PLS and formed into a calibration model. The rest of the pretreated spectra were then fitted into the calibration model and analyzed by PLS to obtain the predicted glucose levels.

The best  $R_p$  was PLS analyzed data of “905-1701nm, sorted,” but the rmsep was not the best. The results demonstrated that PDS might improve the  $R_p$  values, while it might not provide a great help for rmsep values.

PDS was tasked to reduce the variation of the spectral data. Compared to the calibration values shown in Table 5-1, the results of PDS and the non-pretreated data showed the same calibration results. This demonstrated that the predictability of PLS with PDS provided no significant improvement. The use of PDS in NIR spectral application *in vivo* is still in question since the results were not promising. Thus, the selection of preprocess is important. However, it could show some correlation between NIR and blood glucose level.

Moreover, there were many noise sources, such as the physiological effect amongst different subjects and the time lag effect of the venous blood of the forearm and the NIR measurement of the fingertip. The incomplete signal in the range of 1381 to 1701nm also caused another prediction error. All of the noise could generate a certain error which PDS might not be powerful enough to deal with.

#### **5.3.4 Calibration and noise**

In comparison with the previous spectra from Stage 1: glucose solution test, the absorbance variance of the *in vivo* study shown in Figure 5-1 was relatively large. This indicated that the noise or the uncertain effects for the *in vivo* experiment were relatively large.

The practice on Stage 2 might not cover every range of the data. Sometimes, the glucose level or the spectra might exceed the range of the calibrations set or create bias on some ranges of measurement. For example, the calibration was set from 5-10mmol/l, but the prediction or the reference/true value might be higher or lower than 10 and 5mmol/l, respectively. The result might lead to a higher chance of poor predictions, as the calibration might not be well established.

According to Table 5-1, the results showed that PDS and Savgol might not have been useful in this prediction regardless of their good calibration. For the Savgol, the case was even poorer. On the other hand, it also demonstrated that the higher the variation of the absorbance spectra, the poorer the prediction. However, it may not be applicable for the signal after preprocessing. In order to reduce the highly various spectra, a shorter duration clinical trial was introduced, where a lower physiological effect was targeted.

## **5.4 Conclusions**

NIR Blood glucose measurement seemed partly achievable in this stage. However, high physiological noise affected the predicted results. The use of preprocess might not have provided help regarding PLS for glucose prediction. The time lag influence between the glucose level from the venous arm and the finger prick sampling might have also affected the prediction. The results demonstrated that blood glucose in diabetic patients was measurable using NIR, but required some further fine-tuning.

Due to the many uncertainties from the physiological effect among different diabetic patients and the two-month clinical trial, a short-term clinical trial might be helpful to reduce the physiological effect, in which consecutive measurements should be carried out.

## **Chapter 6**

### **Stage 3: Short-term Measurement among Non-Diabetics**

#### **6.1 Non-diabetic subjects**

In this stage, thirty-six healthy subjects were recruited from the staff and students of Hong Kong Polytechnic University. The spectrometer was modified with the intention of minimizing the effects from the external environment. All subjects were requested to fast overnight (8-10 hours). The clinical trial required about four hours in order to evaluate the preprandial and postprandial measurements on the day.

##### **6.1.1 Objectives**

- To evaluate NIR measurement amongst non-diabetic subjects with a meal tolerance;
- To evaluate the possibility of using NIR glucose measurement in non-diabetic subjects;
- To evaluate any improvement of the non-invasive blood glucose measurement by using a modified spectrometer;
- To further study the physiological effect of non-invasive blood glucose measurements in the short-term and
- To further evaluate a suitable spectral ranges for PLS application.

### **6.1.2 Apparatus and equipment**

The same spectroscopic set used in Chapter 4 was modified. The tungsten halogen light exposed to the surrounding environment had been covered by a semi-closed stainless steel case in order to reduce the effect from the external environment. The NIR spectra and the finger-prick glucose level were recorded for the analysis. An AccuChek Active Finger Prick meter was used to obtain the reference glucose level (refer to Appendix A for the details equipment specifications).

### **6.1.3 Subjects**

Thirty-six healthy subjects voluntarily joined the clinical trial and had been fasting overnight before the first NIR and the first finger-prick glucose measurement in the morning. The subject group comprised eight males and 28 females, all of whom were non-diabetic.

### **6.1.4 Procedures**

Finger pricks and NIR measurements were performed at the preprandial (fasting stage) and again at the postprandial (after having breakfast) stage. The whole procedure for data capture (including NIR spectra, finger surface temperature and finger-prick glucose levels) took approximately 3-5 minutes, per patient. Each subject was provided with the same breakfast in the same quantity after the preprandial measurement. A sucrose candy had also been provided for each subject 15 – 30 minutes before the postprandial measurements. This helped to increase their respective glucose level, thus the glucose levels would be varied. Detailed procedures are shown in Appendix B.3.



### **6.1.5 Characteristics**

This clinical trial was designed to test the characteristics of the NIR glucose levels in both preprandial and postprandial readings for the modified spectrometer. Transmittance NIR spectroscopic measurement was applied. This trial also evaluated the NIR glucose measurement over a short period of time, which might reduce the effects of physiology. Fasting glucose levels and the corresponding spectral signals were measured by using a finger-prick meter (as reference/true value) and NIR spectrometer, respectively after 8 - 10 hours of fasting. The postprandial glucose and NIR measurements were performed after their breakfast. The spectrometer was also calibrated against the environmental background before the measurement of each subject. Extra spectra (each from 64 spectral readings) were measured in the postprandial situation due to some unstable signals which occurred during the measurement.

### **6.1.6 Analytical techniques**

The same prediction techniques discussed in Chapter 5 were applied, in which PLS was the major procedure in place for the analysis. The spectra had been separated into two groups for the calibration and the prediction. In addition, the predictability was presented by the R correlation coefficient of prediction ( $R_p$ ) and the root mean square error of prediction (rmsep).

The overtone regions and the whole range of the spectral signals were preprocessed and analyzed for comparison. The preprocesses included PDS (Piecewise Direct Standardization)(148) and Savgol (Savitzky-Golay smoothing and differentiation)(145; 146) for the comparison with a simple mean-centred preprocess.

As with the previous chapter, Chapter 5, one part of the analysis also involved the arrangement of ascendant data (finger-prick glucose levels).

## **6.2 Results**

All thirty-six healthy subjects had fasted for 8 – 10 hours, overnight. NIR spectra, the corresponding finger prick blood glucose levels and the surface temperature of the index fingers had been recorded before and after breakfast, within one hour. The entire clinical trial lasted less than four hours.

The results were represented by using different spectra ranges, which were presented as in Chapter 5. Meal tolerance tests were conducted with NIR and finger-prick glucose measurements under PLS analysis.

### **6.2.1 Spectra**

Figure 6-1 shows a spectral plot of absorbance against wavelength. The spectra were similar to those shown in Figure 5-1, the previous diabetic studies in Stage 2. These absorbance spectra were relatively close to each other and showed a relatively smaller variation in this clinical trial. Overtones also occurred on 980nm and 1200nm. Many ripples appeared in the wavelength region of 1381nm to 1701nm, which had no overtone occurrence. This indicated that high occurrences of noise were detected in this region. This would lead to the assumption that the finger had blocked the transmissions of the NIR light, even when the high powered tungsten light (35W) was used.

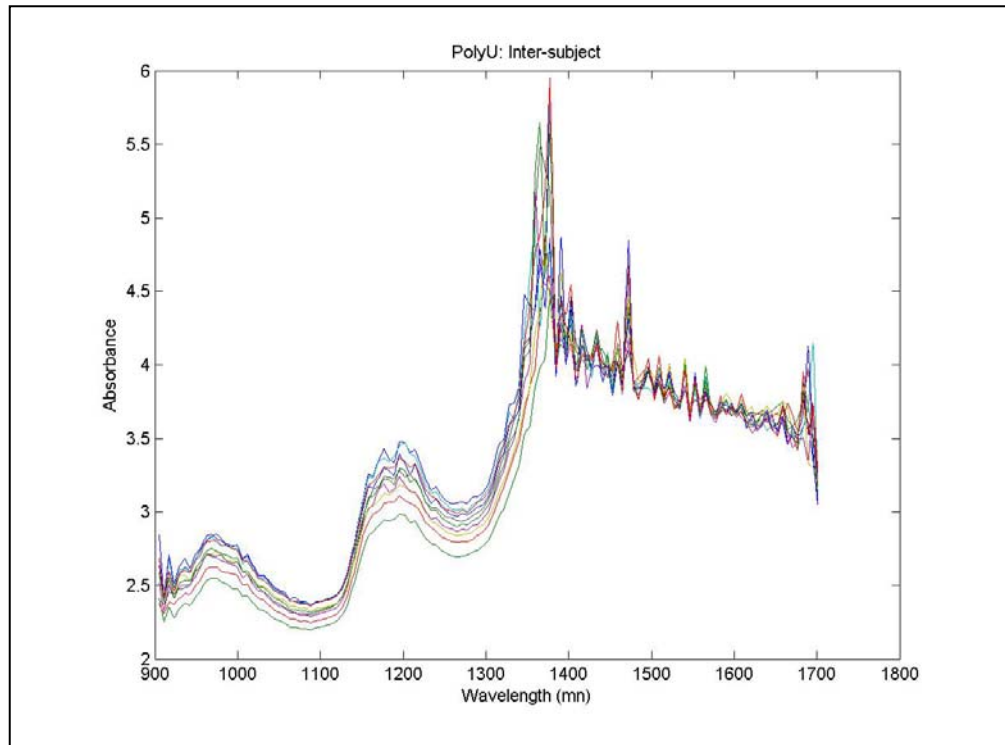


**Figure 6-1: Absorbance against wavelength (Stage 3); high noises at 1381-1701nm caused by finger blocking the light transmission**

### 6.2.2 Predictions

A total of 108 sets of spectra were obtained. Thirty-six sets of spectra were obtained before breakfast. Seventy-two sets of spectra (where one additional set of spectra was obtained from each subject in postprandial measurement) were obtained after breakfast. PLS was applied for the prediction (each third of the data of the spectra and the corresponding glucose readings were used for prediction, while the remaining sets of data were used for calibration). Results are presented in the scatter plot shown in Figures 6-3 to 6-5, which were arranged by simple mean-centred preprocess and predicted by PLS. In the results, the predicted values tended to be unevenly distributed, where more data sets appeared in the low glucose level region,

while the calibration plots were relatively more consistent. The detailed results are discussed in the following sections.

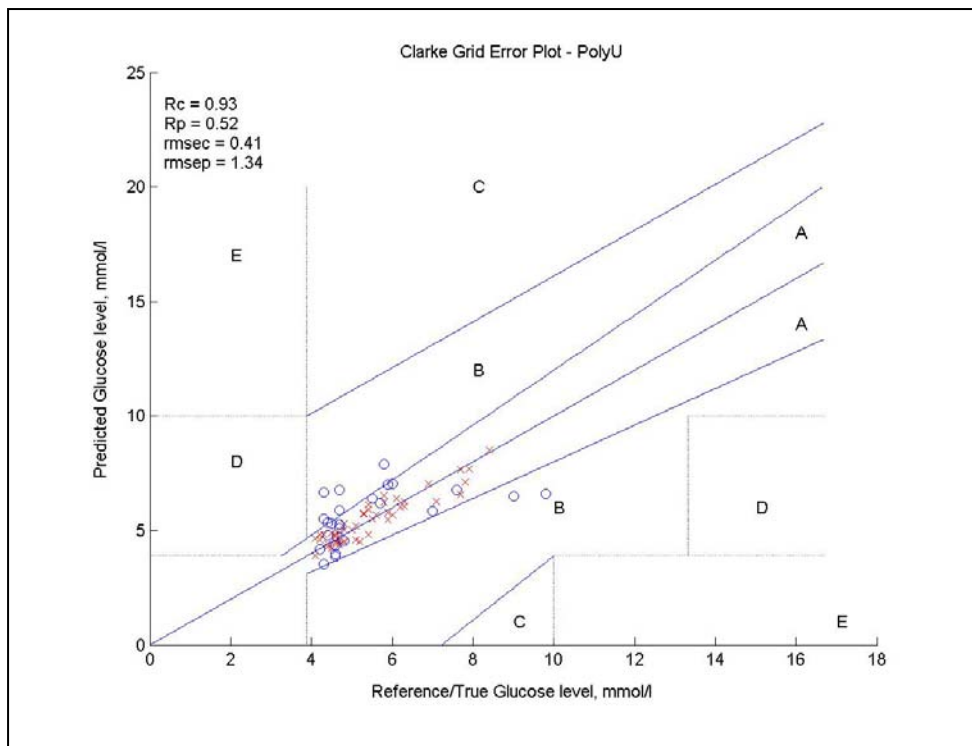


**Figure 6-2: Scatter plot of predicted glucose level against Finger Prick blood glucose level, where is treated by simple mean centred preprocess; full wavelength range was used, (x) calibration, (o) prediction.**

Figure 6-2 showed that both the calibrations and predictions were located within the clinically acceptable regions, A and B. The R correlation coefficient of the calibration ( $R_c$ ) was 0.93 and the root mean square error of calibrations ( $rmsec$ ) was 0.41mmol/l. The R correlation coefficient of the prediction ( $R_p$ ) was 0.52, which was about three-times higher than the predictability level from Stage 2, from the regional hospital. The root mean square error of prediction ( $rmsep$ ) was 1.34mmol/l, which was about 50% lower than the result from Stage 2. Both the  $R_p$

and rmsep of this stage showed significant improvement when compared with the diabetic clinical trial of Stage 2.

Most of the prediction spots fell in Region A, where errors were within 20% deviation. Regions A and B were clinically acceptable regions as stated by the Clarke Grid Error plot. This demonstrated that NIR spectra and the blood glucose levels of non-diabetics were correlated after applying PLS for the prediction.

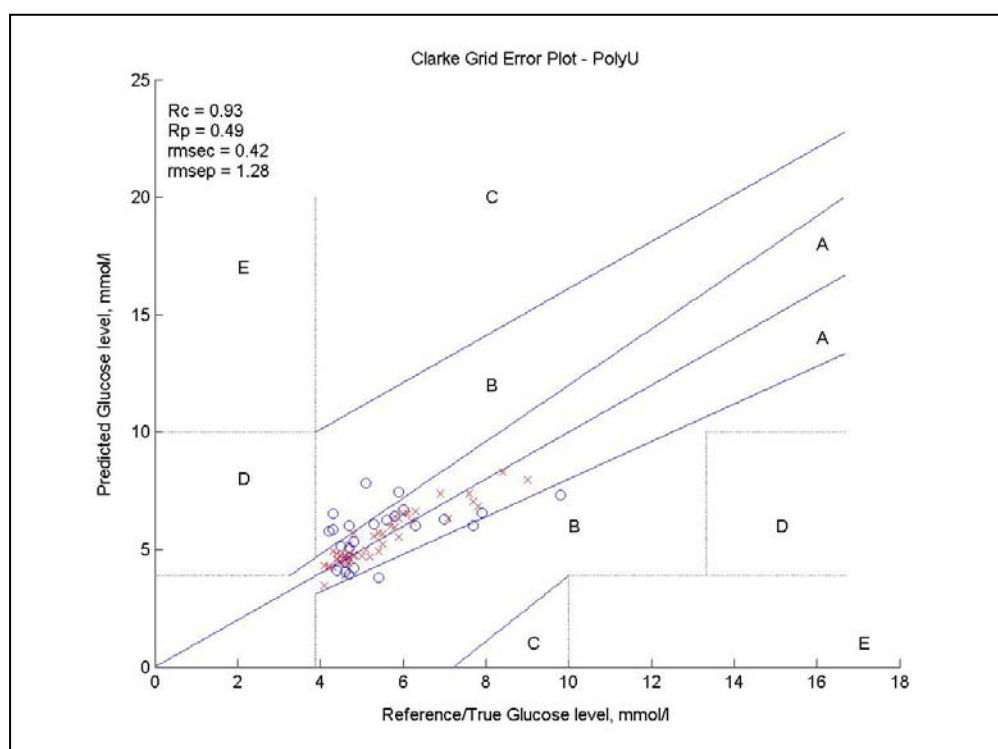


**Figure 6-3: Scatter plot of predicted glucose level against finger-prick blood glucose levels where glucose level had been sorted in ascending order and treated by simple mean-centred preprocess, full wavelength range was used, (x) calibration, (o) prediction.**

Figure 6-3 showed the scatter plot of using ascending glucose levels and was treated by simple mean-centred preprocess before engaging PLS prediction. The prediction results showed that  $R_p$  was 0.49, which was lower than the  $R_p$  stated in Figure 6-2, but the  $rmsep$  was 1.28mmol/l, which was relatively lower than the  $rmsep$  of Figure 6-3. Most of the predicted glucose levels and the calibration readings occurred at about 5mmol/l of the reference glucose level/finger-prick glucose reading. This might have caused a bias data distribution in the prediction.

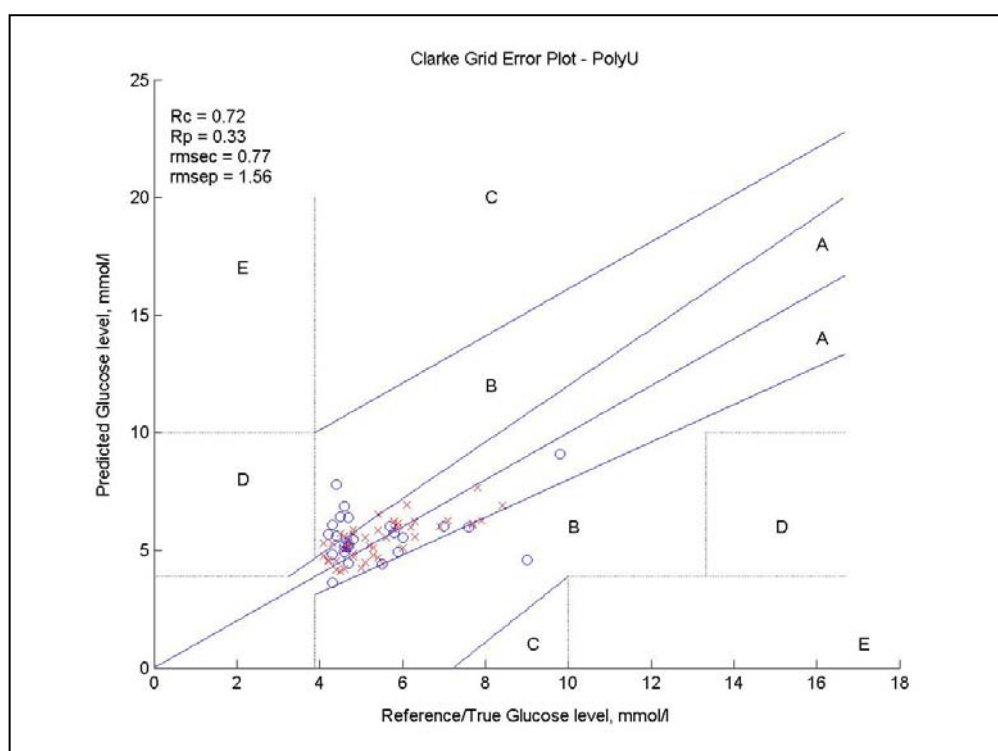


**Figure 6-4: Scatter plot of predicted against finger prick blood glucose level, where spectra of full wavelength range were treated by simple mean-centred preprocess and Savgol preprocess; non-arranged data, (x) calibration, (o) prediction.**

The predictions made by using the simple mean-centred and Savgol preprocesses for the non-arranged data obtained poorer  $R_p$  and  $rmsep$ , as shown in

Figure 6-4. The cause of the error was mainly located in the lower portion of the data/prediction at about reference glucose level 5mmol/l. Rp was 0.33 and the rmsep was 1.56 mmol/l. Half of the predicted glucose levels were located in Region B.

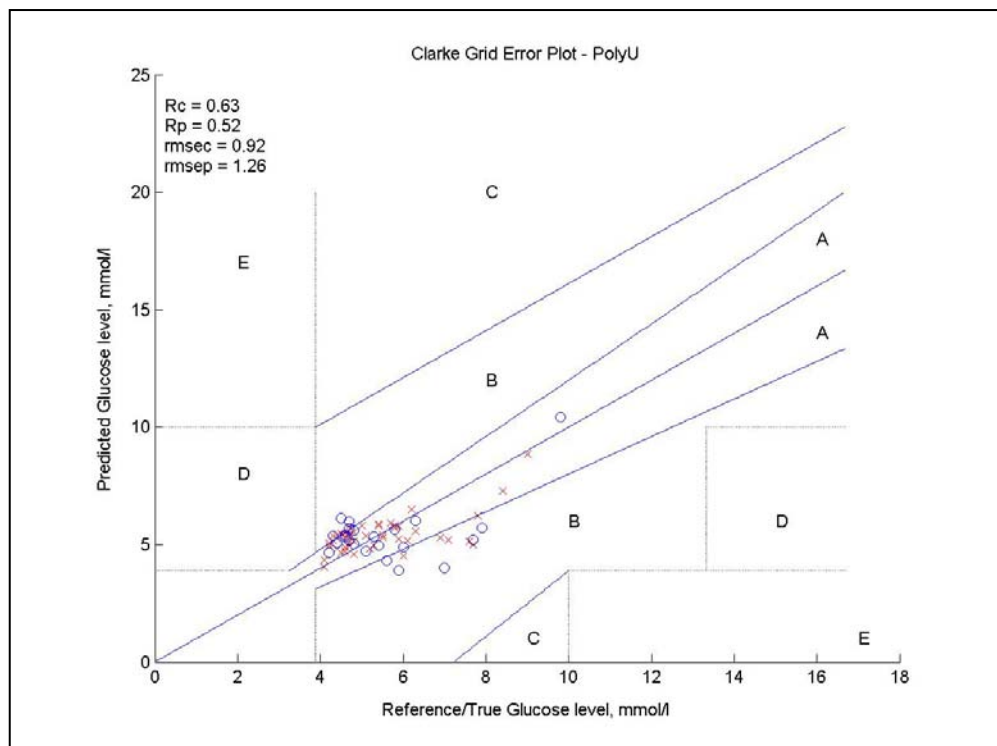


**Figure 6-5: Scatter plot of the prediction against the finger-prick blood glucose level with a simple mean-centred preprocess and Savgol preprocess; glucose level had been sorted in ascending order, using wavelength 905 to 1380 nm, (x) calibration, (o) prediction.**

Figure 6-5 showed the predictions from the regional wavelength of 905 to 1380nm. The predictability of Rc and Rp were quite similar, with only a 0.11 difference, while Rc was 0.63 and Rp was 0.52. The rmsep was 1.26 mmol/l. All the predicted points were located inside the clinically acceptable Regions, A and B. The results indicated that Savgol may be suitable for this regional application. As with

the previous figure, Figure 6-4, the data were close to each other at a glucose level around 5mmol/l.

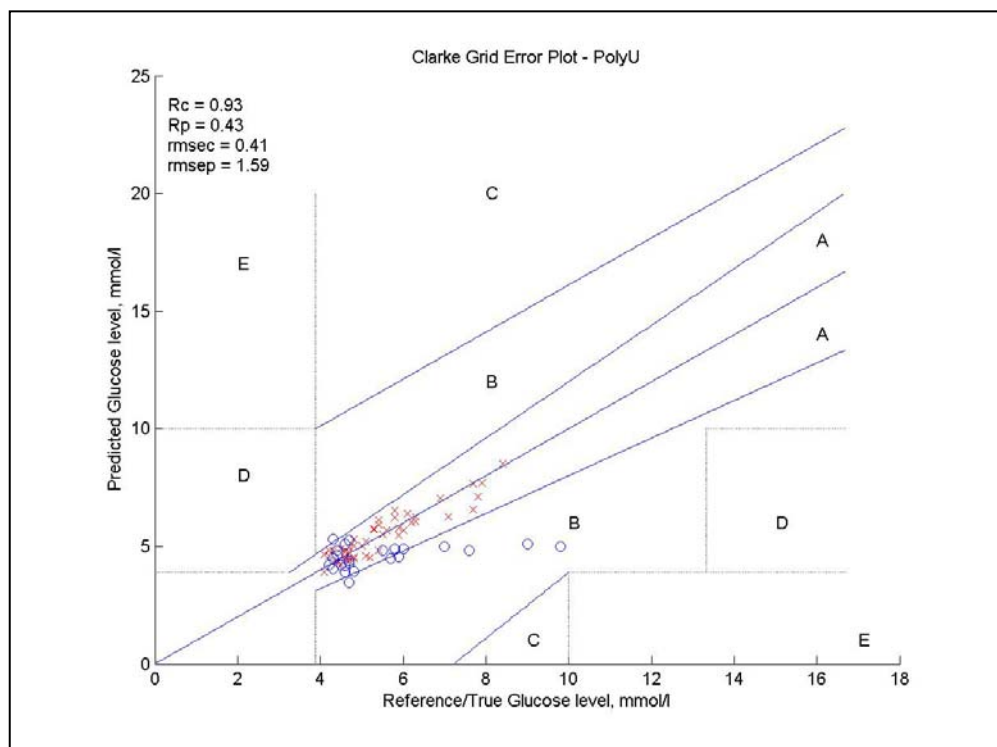


**Figure 6-6: Scatter plot of predicted against finger-prick blood glucose level with simple mean-centred preprocess and PDS preprocess, for full wavelength and non-arranged data, (x) calibration, (o) prediction.**

The results of Figure 6-6 showed that the scatter plot had been preprocessed by simple mean-centre and PDS preprocesses before PLS analysis. The Rc was high at 0.93, but the Rp was not proportional, which provided a relatively poorer prediction. The predicted glucose levels were concentrated to the low glucose level with the poorest prediction amongst reference glucose range 7 – 10mmol/l. Most of the glucose levels were at about 5mmol/l reference/true value. However, those predicted points were also located inside Regions A and B. They were also clinically acceptable predicted results.



### 6.2.3 Comparisons

**Table 6-1: R correlation coefficient of calibration/prediction (Rc/Rp) and root mean square error of calibration/prediction (rmsec/rmse) comparisons. No preprocess: simple mean-centred preprocess; Savgol preprocess: simple mean-centred and Savgol preprocesses; pds preprocess: simple mean-centred and PDS preprocesses; sorted: data arranged in ascending order**

Selected Ranges	905-1701nm	905-1701nm, sorted	905-1380nm	905-1380nm, sorted	1381-1701nm	1381-1701nm, sorted
<u>No preprocess</u>						
Rc	0.93	0.93	0.85	0.8	0.91	0.92
Rp	<b>0.52</b>	0.49	0.48	0.47	0.46	0.46
Rmsec (mmol/l)	0.41	0.42	0.57	0.7	0.45	0.46
Rmse (mmol/l)	<b>1.34</b>	1.28	1.34	1.39	1.5	1.6
<u>Savgol preprocess</u>						
Rc	0.72	0.78	0.59	0.63	0.66	0.78
Rp	<b>0.33</b>	0.26	<b>0.39</b>	<b>0.52</b>	0.31	0.32
Rmsec (mmol/l)	0.77	0.74	0.89	0.92	0.82	0.73
Rmse (mmol/l)	<b>1.56</b>	1.84	<b>1.53</b>	<b>1.26</b>	1.51	1.73
<u>Pds preprocess</u>						
Rc	0.93	0.93	0.85	0.8	0.91	0.92
Rp	<b>0.43</b>	0.19	0	0.24	0.28	0.01
Rmsec (mmol/l)	0.41	0.42	0.57	0.7	0.45	0.46
Rmse (mmol/l)	<b>1.59</b>	1.69	1.74	1.46	1.88	1.93

According to Table 6-1, the best prediction was obtained by using the full spectral range of 905 – 1701nm, which was pretreated by a simple mean-centred preprocess. The spectral range of 905 – 1380nm, which was pretreated by simple mean-centred and savgol preprocesses, provided an  $R_p$  of 0.52 as well. Both case analyses obtained an rmsep of 1.34 and 1.26mmol/l, respectively. This indicated that Savgol may have provided the most suitable prediction preprocess for spectral the range of ‘905 – 1380nm’ because they obtained the highest predictability upon different spectral ranges.

By comparing the overall prediction, it seemed that the simple mean-centred preprocess would provide, on average, better predictions, while Savgol would be the second best, on average. The poorest prediction was obtained with PDS, where it showed the best prediction at spectral range ‘905-1701nm’ with  $R_p = 0.43$ , rmsep = 1.59mmol/l.

## **6.3 Discussion**

The results showed that the study of non-diabetics provided a positive sign for non-invasive blood glucose prediction and also demonstrated an improvement when compared with the previous study. The following subsections will provide further discussion regarding this clinical trial.

### **6.3.1 Spectra**

The spectra shown in Figure 6-1 also contained the same problem as the previous studies; at about the spectral wavelength range of 1381 to 1701nm, no overtones

occurred, but defections happened. This was because in using the “transmittance” spectroscopic measurement technique, the light was blocked by the finger in the region of 1381 – 1701nm. As a result, higher noise occurred. Thus, blood glucose prediction provided a greater range of error. This indicated that there were probably an insufficient number of photons passing through the fingers for measurement by the detector. According to Hampton et al. (155), they studied the penetration depth for the optical probe by using NIR spectroscopy ranging from 700 to 1100nm on fish skin. They found that the probe light could penetrate the fish tissue for up to 130mm thickness; while for the longer wavelength, the penetration was relatively small (8). This might explain why the clinical trials, using the transmittance method, could not provide the proper signal at a range of 1381 to 1701nm. Although Jeon et al. (135) in their study mentioned that the transmittance method was more effective for the NIR non-invasive blood glucose measurement, their study was based on *in vitro* experiments. Many restrictions from the human body might limit their recommendation, such as the poor penetration power through human tissue over a longer NIR wavelength.

The spectra in this chapter have a relatively lower variation when compared with the previous diabetic study of Stage 2. High variation may lead to difficulties for blood glucose prediction. The spectral variation might indicate that higher noise level or uncertainty of signals might be obtained in addition to the necessary signals. This might be due to time drift, machine drift and physiological differences in a long-term clinical measurement.

### 6.3.2 Simple mean-centred preprocess

The predictions used a simple mean-centred preprocess and PLS showed the best predictability among the full wavelength range spectra, as shown in Table 6-1. The predicted results demonstrated relatively better predictions against the previous diabetic prediction of Stage 2. These two studies showed that ‘time and machine drifts’ and ‘physiological difference’ could affect *in vivo* blood glucose prediction. However, as mentioned in Chapter 4, the glucose solution experiment in Stage 1 showed that machine drift and time drift could be reduced by using PLS with preprocess. Thus, the error might be due to physiological differences over a long period of time and due to insufficient information from the spectra beyond 1380nm, in this case. On the other hand, there was no significant difference for the NIR spectra after the tungsten halogen light was semi-covered. This also indicated that there was no influence from the surrounding environment where the NIR frequency did not exist.

Figure 6-3 showed that the error was mainly located at about reference glucose level 5mmol/l. The calibrated and predicted glucose levels mostly were located at the reference glucose level, 5mmol/l. This unbalanced calibration probably provided incomplete information for the calibration model. The bias may have happened in about this range. The prediction may then be relatively worse and subsequently resulted in a biased prediction.

The results also indicated that the best predictions were from the full spectral range of 905 – 1701nm for comparisons with all simple mean-centred preprocessed signals. The range of 905 – 1380nm was the second best prediction. The poorest

prediction was located in region of 1381 - 1701nm. This further explained that the region of 1381 – 1701nm may have contained insufficient glucose information (and with high level of noise occurring), in which the fingers had blocked the NIR light.

The NIR spectroscopic measurements contained many non-specific signals which affected the glucose prediction, and the narrower wavelength range might have contained bias for the glucose signals. Some of the signals might have appeared outside the selected wavelength region, thus the full wavelength range for the glucose predictions provided better and more stable prediction results when compared to a single specific wavelength. Thus, the wider wavelength range of the spectra would be recommended for PLS analysis under NIR spectroscopic measurement.

### **6.3.3 Savgol preprocess**

Preprocessing which used Savitsky-Golay smoothing and differentiation (Savgol),  $R_p$  and  $rmsep$  showed the second poorest prediction rate in the range of 905-1701nm. This might have been due to insufficient information and relatively high noise in 1381-1701nm. The best two predictions were located at both the sorted and unsorted spectral range of 905 – 1380nm. This showed similar results when compared with the previous diabetic study in Stage 2. This was because the spectral region of 905 – 1380nm was the polynomial spectra equivalent. Thus, they were suitable to having used the Savgol application, which had been proven by Bromba and Ziegler (154). They stated that the Savgol could be optimized in the polynomial spectra.

For the comparison with the same wavelength range, '905 – 1380nm, sorted' showed the best prediction, in terms of both  $R_p$  and  $rmsep$ , was 0.52 and 1.26 mmol/l, respectively. Savgol in this case provided a relatively large effect in the polynomial spectra. This further confirmed that the Savgol preprocess was suitable for the polynomial spectra, i.e., located at '905-1380nm'.

In Figures 6-4 and 6-5, the plots showed that there was a lack of data for the calibration in the glucose levels of 6- 10mmol/l, which may have resulted in poor prediction. This indicated that the sampling range may not have been enough for glucose predictions; either that, or that the data obtained were too narrowly distributed, and that they were biased into falling into particular glucose regions. The calibration and the prediction did not have enough data in some glucose levels, thus the predicted glucose level might not have been based on a well-defined calibration model.

#### **6.3.4 PDS preprocess**

In this case, the calibration provided a comparatively good result because of the preprocessing of the PDS, but the prediction was not as good as the  $R_p$  and  $rmsep$  of the 'no preprocessed' shown in Figure 6-6 and Table 6-1. PDS helped to reduce the variations of the spectra, but the calibration results showed no improvement when compared with the 'no preprocess.' On the other hand, the prediction ( $R_p$  and  $rmsep$ ) of the 'no preprocess' showed better results. This showed that PDS might not be suitable for NIR spectral measurement.

Although better calibrations may result in better predictions, the spectra for prediction may not be well fitted for the calibration model after being calibrated by

PDS. Besides, the predictions with PDS showed relatively poor  $R_p$  and  $rmsep$  in the range of '905 – 1701nm'. This demonstrated that the selection of a suitable preprocess was important for the prediction. Thus, many researchers have focused on the improvement of preprocessing techniques for non-invasive blood glucose measurement and prediction.

Furthermore, the range of '905 – 1701nm' showed relatively better prediction when compared with the other two ranges of '905 – 1380nm' and '1381 – 1701nm'. This also demonstrated that the full wavelength range for the NIR spectroscopic measurement would be recommended.

### **6.3.5 Prediction amongst inter- and intra-subject**

This clinical trial contained both inter-subject and intra-subject data. For inter-subject data, the data included 34 subjects. For intra-subject data, the data included two readings before and after breakfast, respectively. Preprandial and postprandial NIR spectroscopic signals of each subject were obtained. The study was also designed to find the significant effect among physiological difference.

The prediction of the diabetic study in Stage 2 provided the total inter-subject results, while the prediction of this clinical trial showed only partial inter-subject and partial intra-subject involvement. Results showed that the intra-subject data involved in the prediction could improve the prediction. This demonstrated that the influence of physiological differences affected the NIR measurement. The prediction might not be affected by physiological differences between subjects only. The physiological differences may have varied over time, within a subject. This made it difficult to properly select a suitable clinical trial, by intra-subject or by inter-subject. Many

researchers have tended to carry on with the intra-subject prediction when they found difficulty in their inter-subject analysis (22). Thus, many researchers still continue this vein of the inter-subject study (78).

This study demonstrated that the intra-subject prediction could provide a better result than the inter-subject analysis. This also showed that shorter time duration in between NIR measurements lead to a better result, whereas the physiological difference was relatively small when compared with the spectra of Stage 2.

### **6.3.6 Physiology against time**

The physiological influence from the human body was one of the key effects in relation to non-invasive blood glucose measurement.

Time factors have led to uncertain physiology, which could affect the prediction. The longer time span between each measurement, the more uncertainties due to the physiology occur; thus, the poorer the calibration and the prediction obtained. This is because of the higher chance of the reaction of the human body to both internal and external environmental changes. Therefore, the study of healthy subjects might have provided better predictions due to the shorter time span and relatively fewer physiological uncertainties.

The influence of the temperature was another consideration of the physiology. It seems that the surface temperature of the measurement may have also affected the NIR spectral signals. According to Cui et al. (156), temperature was one of the most significant influences on the NIR measurement. Their results



demonstrated that temperature could significantly influence the NIR measurement of glucose solutions (122; 156).

*In vivo*, Yeh et al. (125) demonstrated non-invasive prediction by regulating the contacting surface temperature. However, this action not only manipulated the temperature, it also affected the body's reaction and the physiology of the human body, such as blood flow rate and diameter of blood vessels. This could generate an argument for the measurement of the NIR signal, which was affected by the thermal source (via heat convection) or the human body. The NIR signal obtained, via temperature regulation, may only reflect the manipulated glucose levels.

Furthermore, the results of this clinical trial also showed that the larger variation caused larger error for PLS predictions. The large variation might have been due to the physiological influences, including temperature. Thus, NIR measurement also needed to be improved by reducing the variation during the measurements.

For the comparison between Stage 2 and Stage 3, the study of Stage 2 lasted about two months while the study of Stage 3 was over after about four hours. Longer time measurement might have led to a higher chance of physiological uncertainty, which caused significant impacts to the prediction.

### **6.3.7 Transmittance and reflectance NIR measurement**

The two clinical trials demonstrated that the measurement made through the transmittance method might have blocked the NIR light in the region of 1381nm and beyond. However, the narrower range of the spectra used, the poorer the prediction

may be. Thus, a wider range of the spectra is recommended for the prediction. This indicates that another measurement approach should be used.

The NIR measurement for the human body used a contact approach via the reflectance method. A reflection probe connected to fibre optics and the spectrometer was chosen. The reflection probe contacted the part to be measured in order to generate a relatively smaller noise. The contact area was relatively small as compared with the transmittance approaches of Stage 1 – 3. Thus, the reflected light was relatively less scattered. The non-contact measurement technique could have increased the light scattering area and the specular effect of the light. According to Maruo et al. (86-88), they demonstrated the use of an optical probe as the contact interface to obtain the spectra and provide more accurate glucose prediction.

The spectral absorbencies obtained from these two clinical trials (Stage 2 and Stage 3) only contained information on the glucose level. The spectra from the subjects could have derived from many different carbohydrate-rich components, such as protein, fat, body tissues and others. The metabolism and physiology may also have limited the predictions of glucose by NIR.

Both the clinical trials of Stage 2 and Stage 3 showed that the predictability of  $R_p$  and  $rmsep$  were better when no PDS and Savgol preprocesses were applied. The results also demonstrated that these preprocesses may not have been suitable for these spectral applications. This might have been due to the high level of noise from the spectral signals of the inter-subject. These preprocesses might have filtered the useful information instead of the noise signals since the spectra varied substantially.

In addition, the spectra from 1381 to 1701nm, where the signal was blocked, also caused some effects on the predictions. Figure 6-5 showed the predictions of using the spectra range of '905 to 1380nm' by using Savgol. The results were similar to the prediction with the full range of '905 to 1701nm,' without having used a preprocess. This demonstrated that the wavelength range of 1381 – 1701nm may have been useful for the prediction, although the NIR light was blocked. This also confirmed that a wider spectrum could average the noise for reducing the error. Thus, the prediction of the glucose level should have used a wider spectrum. However, due to the effect of the region, 1381-1701nm, the reflectance NIR spectroscopic measurement technique should be applied, where the measurement probe was also recommended, for avoiding the NIR light block.

## **6.4 Conclusions**

This prediction involved intra-subject (within subject) data. It showed that when intra-subject data were included in the predictions, the predicted results seemed more consistent. This was because the noise caused by the inter-subject was relatively large. This supported the hypothesis that non-invasive blood glucose measurement could apply to intra-subject data, in which the physiological effect was relatively small. The results also showed that the NIR measurement was also applicable for non-diabetic people, while the range of glucose levels was relatively narrower.

The NIR light was semi-covered to limit the effect of the surrounding environment. However, the results showed no significant improvement because the

existing visible/shorter wavelength light in the surrounding area did not affect the NIR light. A wider spectral signal could have provided a more stable result, in which a wider spectrum would have averaged the noise, reducing the effect. The noise signals (many ripples and spectra deflection occurred) mainly occurred in the range of 1381 to 1701nm, which was blocked by the fingers.

Physiological effects are unpredictable and vary from time to time due to the body's reaction to the environment. Thus, consideration of the physiology for NIR non-invasive blood glucose measurements would be needed. The next stage mainly focused on physiological effects and was measured by the reflectance approach.

## Chapter 7

### Stage 4: Longitudinal Measurement for Diabetics

#### 7.1 Diabetic clinical trial from a community clinic

After the previous three studies, the measurements had been changed to use the reflectance approach. The penetration limitation of this spectrometer, through the transmittance measurement, caused incomplete spectra to be obtained. Although Jeon et al. (135) recommended the use of transmittance NIR measurement, NIR light at a wavelength of 1381 to 1701nm could not pass through the fingers. The clinical trial focused on Type-1 and Type-2 diabetes. A comparison that was specially designed for *in vivo* comparison was introduced, so as to screen out or minimize background noise and other uncertain noise due to physiological influences.

##### 7.1.1 Objectives

- To find out if intra-subject measurement was better than inter-subject measurement for NIR prediction;
- To evaluate reflectance NIR measurement via a fibre optic probe;
- To evaluate new clinical trial methods for the comparison of both inter- and intra-subjects and
- To evaluate intra-subject prediction over the long-term.

### **7.1.2 Apparatus and equipment**

A new reflection probe connected to a fibre optic cable was introduced for the same spectrometer. The reflection probe was connected to a tungsten light source through a standard SMA905 connector. This fibre bundle consisted of seven fibres which linked the probe to the spectrometer. The NIR light was transmitted through the fibre optics to the probe. The NIR signal was reflected back through the seventh fibre in the centre of the probe. For a detailed specification, refer to Appendix A.6.

NIR sources – a tungsten halogen light (10Watt power) from Avantes was used. The light was transmitted through the fibres and then reflected to the spectroscopy. Refer to Appendices A.6 - A.7 for detailed specifications.

An AccuChek Active finger-prick glucose meter was used for the measurement of the capillary blood glucose levels as reference, in which the AccuChek controls are at 2.0 – 3.6 mmol/l, and 7.2-9.7mmol/l (refer to Appendix A.10 for the specifications). This device had been evaluated by the biochemical blood glucose test in the first and the last days of the clinical trial. The same thermometer with a k-type thermocouple was used for fingertip surface temperature measurement, with an accuracy of two decimal places.

Four customized individual finger plastic moulds were introduced for each subject to fix and restrict the movement of each finger during the NIR measurement. This assisted in maintaining the measurement consistency on the index, middle, ring and little fingers, as shown in Figure 7-1.

A micrometer with 0.01 mm accuracy was used for finger thickness measurement.



**Figure 7-1: NIR spectroscopic probe measurement with customized finger mould**

### **7.1.3 Subjects**

Twenty-seven diabetic patients voluntarily joined the three-month clinical trial. One patient dropped out. The remaining 26 patients were required to visit the clinic 30 times for blood glucose and other measurements. Inclusion criteria for the subjects were:

The patients should be recruited from individuals that are either Type 1 or Type 2 DM, and they

1. should not have any blood disease or abnormal RBC, WBC;
2. should not have a serious hand skin problem, such as a skin ulcer;
3. should be non-pregnant;
4. should not take any anti-coagulants 10 hours prior to the blood glucose measurement and
5. should not take aspirin 10 hours prior to the blood glucose measurement.

#### **7.1.4 Procedures**

During the clinical trial (Day 2 to Day 29), patients were requested to provide a 24-hour dietary record. NIR spectra (each finger took about 30-40 seconds for obtaining 15 sets of NIR spectra record; each spectral set was the average from 64 spectral readings) were obtained. Finger-prick blood glucose levels were recorded as well. Finger surface temperatures were measured before and after NIR measurements.

On the visits for the first day and the last day, patients were requested to provide their dietary record of the last 24 hours before the measurement. Blood pressure, body height and weight were recorded. Venous blood was also sampled from the forearm on the first and the last day. The other measurements taken followed the same procedures as Day 2 through Day 29.

All subjects were required to take a rest for 20-40 minutes before any measurement. This helped to reduce any unnecessary interference from blood flow or body temperature due to any exercise before visit. All the measurements were taken at the same location and under same conditions. Refer to Appendix B.4 for detailed procedures.

#### **7.1.5 Characteristics**

At the first and the last visits, all subjects gave a blood sample for the plasma glucose test in which the accuracy of the finger-prick blood glucose meter was evaluated.

Other blood measurements were also performed to check any common blood diseases which might have affected the measurement. Many researchers mentioned



that blood components such as protein, fat (triglyceride) and RBC could affect NIR blood glucose measurements. However, it was not practical to measure different blood components continuously over a short period of time. Thus, any effect of the above-mentioned components for the NIR blood glucose measurement was not counted, although these would be considered major interferences.

Fingertip surface temperatures were measured, and the room temperature (within 300mm diameter from the measurement probe) was recorded for each subject, for each visit. Fingertips were chosen for the measurement because they are filled with blood capillaries and not subject to any time lag.

The average finger thickness was obtained from five measurements over different days since many researchers pointed out that tissue was one of the key influences on NIR measurement.

In order to reduce the effect due to the force and the different measurement depths, a marker had been drawn on the probe, in which each person had been measured at the same depth of deformation, 0.5mm, for each measurement. This was taken from the recommendation of Chen et al. (105), although their results were not very encouraging.

The spectrometer used was set at its original factory calibration (i.e., total darkness, 0% of light intensity against total brightness, 100% of light intensity) since the measuring probe was highly sensitive to the external environment, i.e., various probe orientations could have caused different NIR-calibrated results. This would have led to a large measurement error when calibrated under typical room conditions.

## **Measurement**

Two different glucose measurements were conducted:

### 1. Fasting blood glucose test

Tests for the first day and the last day were conducted in the early morning after overnight fasting.

- a. Finger-prick blood glucose measurement
  - i. Twice a week measurements for each subject and
  - ii. Total of 30 blood glucose measurements were obtained.
- b. Record of the subjects for the first and the last measurements
  - i. Sex (1<sup>st</sup> day only), age (1<sup>st</sup> day only), body height, body weight, BMI, finger surface temperature;
  - ii. NIR spectra;
  - iii. Blood glucose level, type of diabetes (1<sup>st</sup> day only);
  - iv. HbA1c, Hemoglobin level;
  - v. Total cholesterol, Total protein, Triglycerides, HDL, LDL;
  - vi. Red blood cell (RBC) count, white blood cell (WBC) count and blood platelet count and
  - vii. Blood pressure – Systolic and Diastolic,

### 2. Record of the subjects for the second day to 29<sup>th</sup> day were as shown below:

- a. Fingertips surface temperature;
- b. NIR spectra;

- c. Finger-prick blood glucose levels and
- d. Finger thickness measurement (selected arbitrarily from five different sample days).

The spectrometer recorded spectral signals after a stable spectrum appeared. Repeated measurements were performed for all fingers of the left hand of each subject.

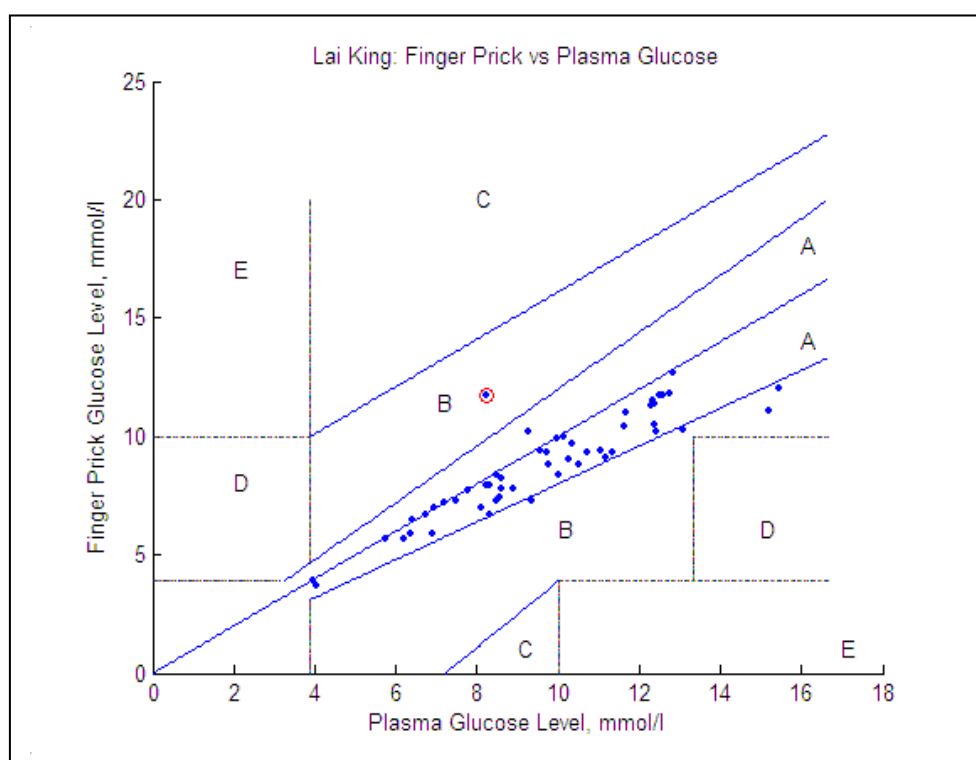
### **7.1.6 Analytical technique**

PLS regression was mainly used for the blood glucose prediction. Different preprocesses (simple mean-centred, PDS and Savgol) are compared in Chapter 8.

Both prediction of intra-subject and inter-subject were compared. All the absorbance spectra were collected from the spectrometer. They were collected in Microsoft Excel format. A total of 15 sets of data per subject, per finger measurement were collected. The 15 sets (each set was obtained from the average of the 64 spectra) of spectral records were trimmed down to 10 spectral sets (retained the 4<sup>th</sup> through the 13<sup>th</sup> spectral sets). A total of 39,000 spectral data sets were arranged for the analysis. The trimming action helped to reduce noise interference during the measurement, which might have been affected by the touching and removing of the probe to the fingers.

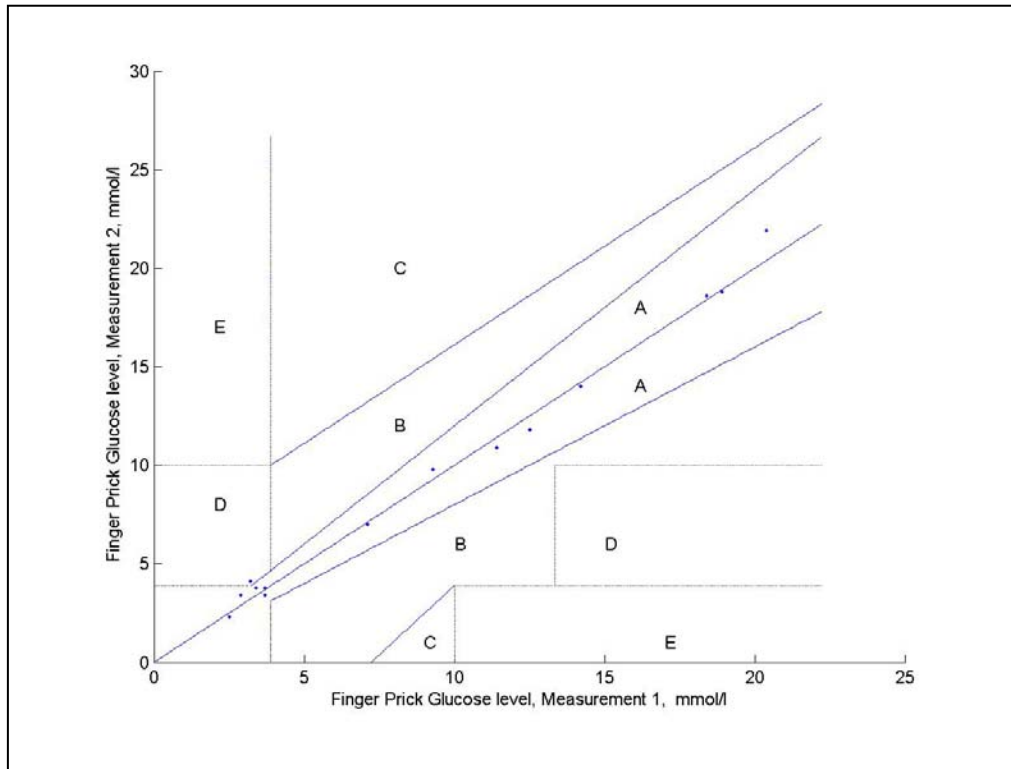
## 7.2 Results

Twenty-six diabetic subjects were measured 30 times in three months. Casual glucose measurements were carried out apart from the first and last visits, in which the subjects were required to fast overnight for 10-12 hours. The results mainly were represented by the scatter plot with Clarke Grid Error plot. Rp and rmsep were used for the predictability comparison. PLS with simple mean-center preprocess, Savgol and PDS were used for the prediction. The finger-prick glucose meter was first calibrated and evaluated by a biochemical analysis. The finger surface temperatures ranged from 19.5 to 38.3 degrees Celsius. The results are shown below.



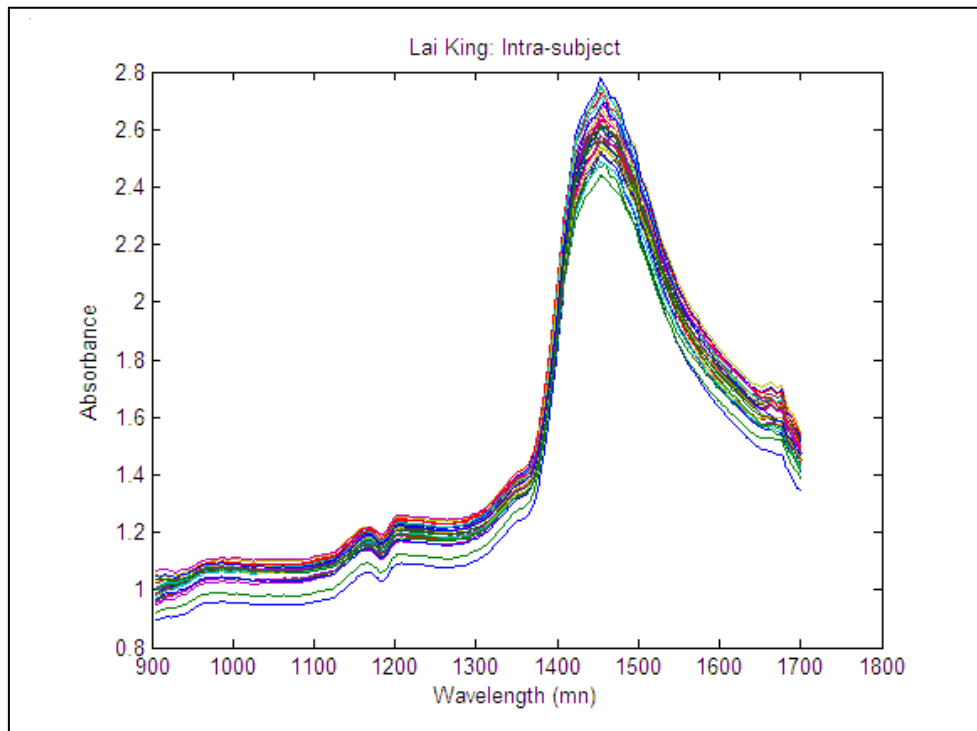
**Figure 7-2: Finger prick against venous blood glucose level, forearm (Plasma Glucose),  $R = 0.9$ ,  $rmse = 1.40\text{mmol/l}$ .**

Figure 7-2 showed that the scatter plot of the finger-prick versus the forearm venous plasma glucose level values on the first and the last days of the clinical trial were close to each other. This checked the reliability of the finger-prick glucose meter for the clinical trial. The results showed that all finger prick readings were located within the clinically acceptable regions, A and B, and over 90% of the finger-prick readings were inside Region A (80% accuracy region). The R correlation coefficient was 0.90. The root mean square error (rmse) was 1.40mmol/l. By omitting the point, circled in red in Figure 7-2, R reached 0.94; while rmse was reduced to 1.32mmol/l, in which the difference between the finger-prick and plasma glucose levels ranged from 0.1 to 4.1mmol/l. However, the results were biased in the lower part of Region A, which showed that the finger-prick glucose meter might have obtained a relatively lower glucose level.



**Figure 7-3: Finger-to-finger glucose levels comparison by finger-prick glucose meter**

Figure 7-3 showed that the finger-prick glucose levels between fingers were close (at about 0.1-1.5 mmol/l apart). The error of rmse was 0.58mmol/l. The result of the R correlation coefficient was 0.996, which almost reached one, that is totally correlated. Thus, the glucose levels of the fingers in the left hand side could be shown to be the same. The variation was relatively smaller than the results between plasma glucose level and the finger-prick glucose levels. Thus, it was not necessary to obtain readings from all of the fingers.



**Figure 7-4: Absorbance against wavelength (from left thumb of Subject 26, intra-subject)**

Figure 7-4 showed the spectra plot of the intra-subject (within subject) data from the left-handed thumb of Subject 26. The plot demonstrated the results obtained from reflectance NIR measurement. The spectra obtained were smoother than the spectra from the previous two studies (Stages 2 and 3), in which the measurements were performed using the transmittance method.

The ripples of the above spectra were relatively small compared with the previous two studies. The range of the 1381 to 1701 nm provided an overtone. This demonstrated that NIR signals were reflected by the fingers, and the signals reached the detector. There was no deflection which showed that the NIR light was blocked.

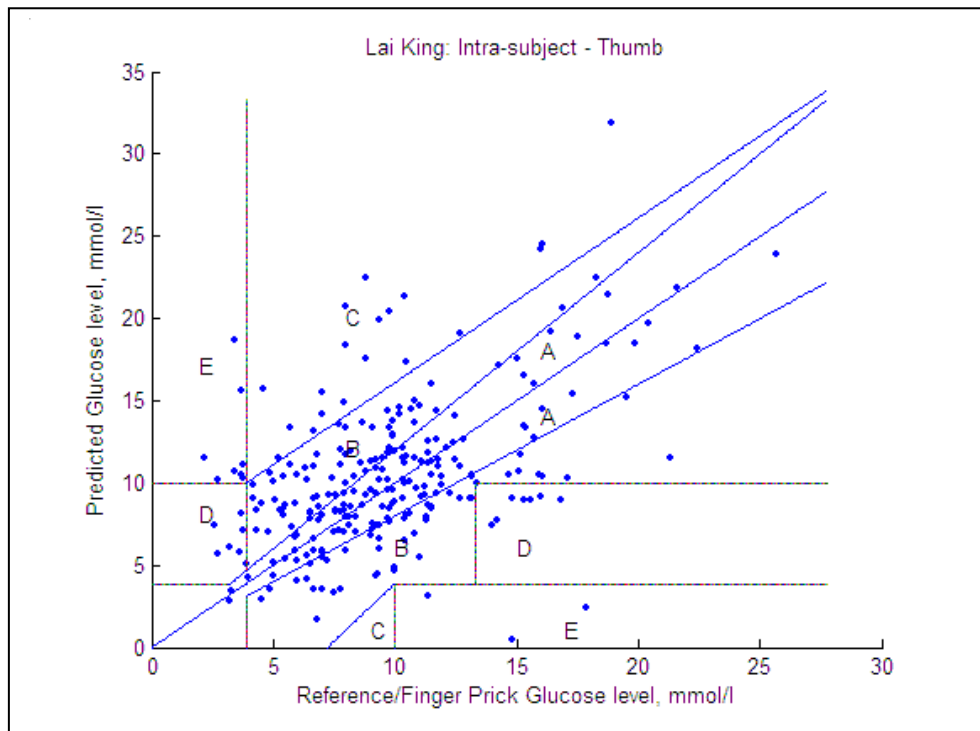
### **7.2.1 Prediction by PLS**

The prediction was preprocessed by Savgol, and predicted by PLS. For the individual subject, every third data set was used for the prediction on his/her 30 data sets, while the rest were used for the calibration. All of the 26 individual predicted results (thumb, index, middle, ring and little finger respectively) were scatter plotted in the following figures.

Spectra of the individual subject were preprocessed by simple mean-centred preprocess and Savgol preprocess. Two-thirds of the preprocessed data were calibrated with the corresponding finger-prick glucose levels via PLS. The remaining one-third of the preprocessed data, which were inputted into the model generated by the calibration, was used for the prediction against the rest of the finger-prick glucose levels for validation.

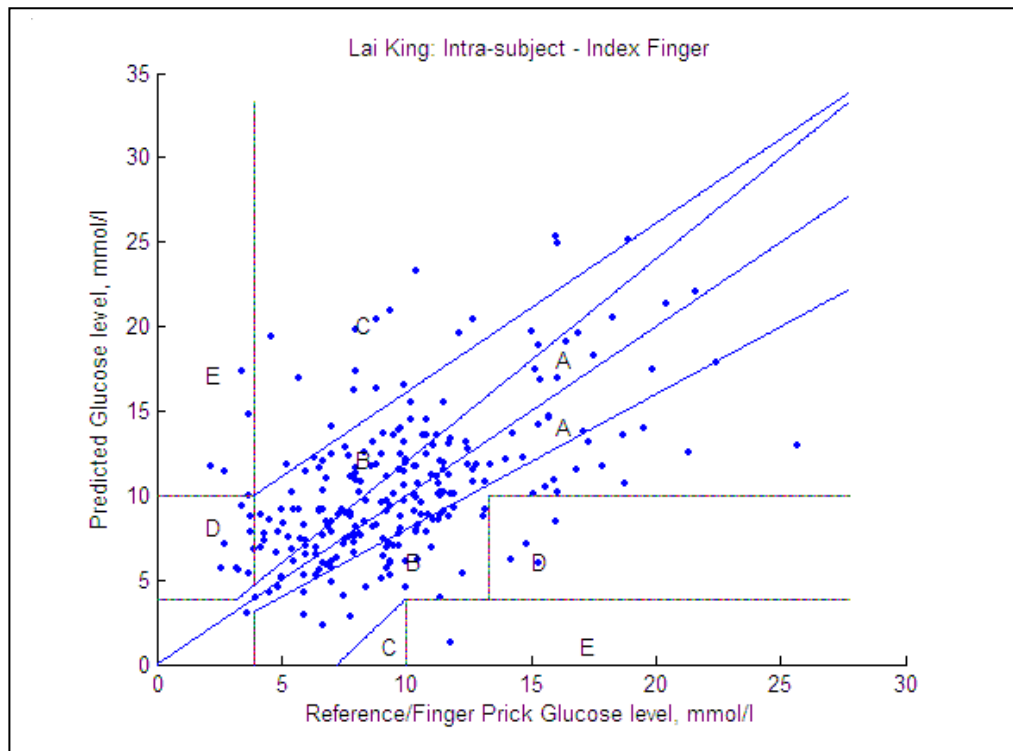
The predicted results of the entire individual diabetic patients were then scatter plotted together in Figures 7-5 to 7-9, where the plots of the predicted blood glucose from different fingers – thumbs, index, middle, ring and little fingers are shown for comparison.





**Figure 7-5: Prediction scatter plot from the community clinic – Thumb, plot of all the predicted glucose levels together against the reference/finger-prick glucose level.**

The results shown in Figure 7-5 revealed that the scatter plot of the non-invasive blood glucose prediction amongst thumbs was more diverse, with  $R_p = 0.5$  and  $rmsep = 4.43\text{mmol/l}$ . About 80% of the prediction was located in the clinically acceptable regions, A and B. where about 50% occurred in Region A, which showed an 80% accuracy. About 20% were located in Regions C, D and E.



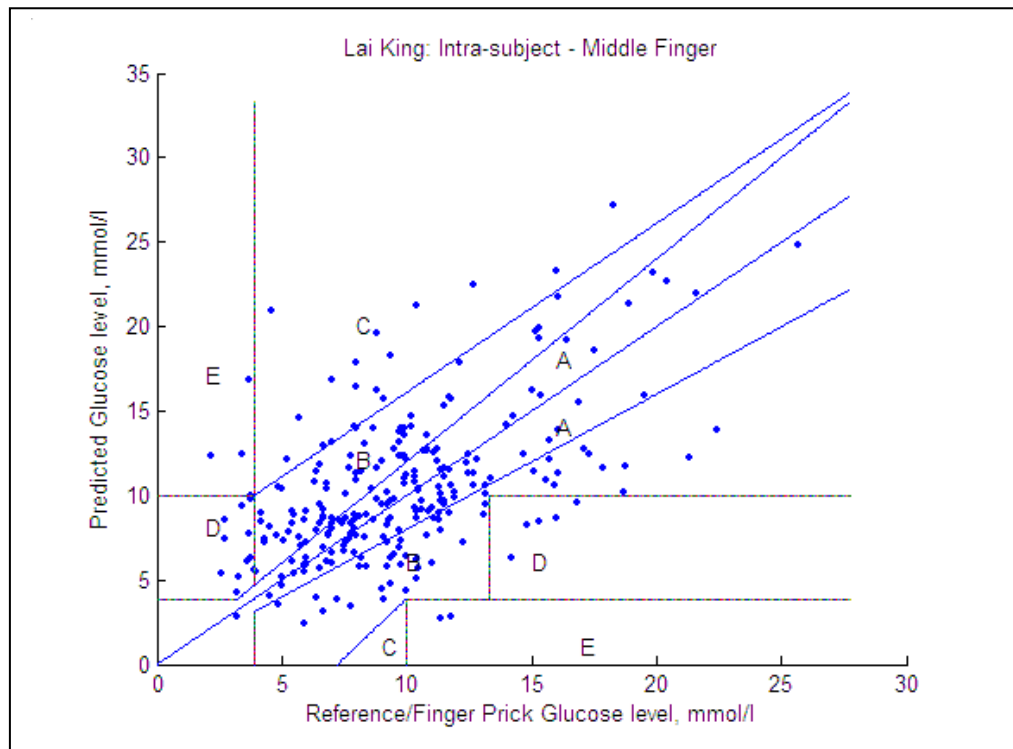
**Figure 7-6: Prediction scatter plot from the community clinic – index finger, plot of all the predicted glucose level together against the reference/finger-prick glucose level.**

Figure 7-6 showed the prediction from which the calibration was obtained from the different dates of the individual subjects (intra-subject). The overall results showed that  $R_p$  was only 0.5, and the  $rmsep$  was 4.28mmol/l. In the index finger, the non-invasive blood glucose prediction was also widely dispersed with the predicted values located in the following regions:

Region A: 40% of data

Region B: 40% of data

Region C, D and E: 20% of data



**Figure 7-7: Prediction scatter plot from the community clinic – middle finger, plot all the predicted glucose level together against the reference/finger-prick glucose level.**

The results showed that  $R_p = 0.54$  and  $rmsep = 4.12$  mmol/l in the prediction from the middle fingers in Figure 7-7. It was also widely dispersed with the predicted points located in the following regions:

A and B: 80% of data

C, D and E: 20% of data

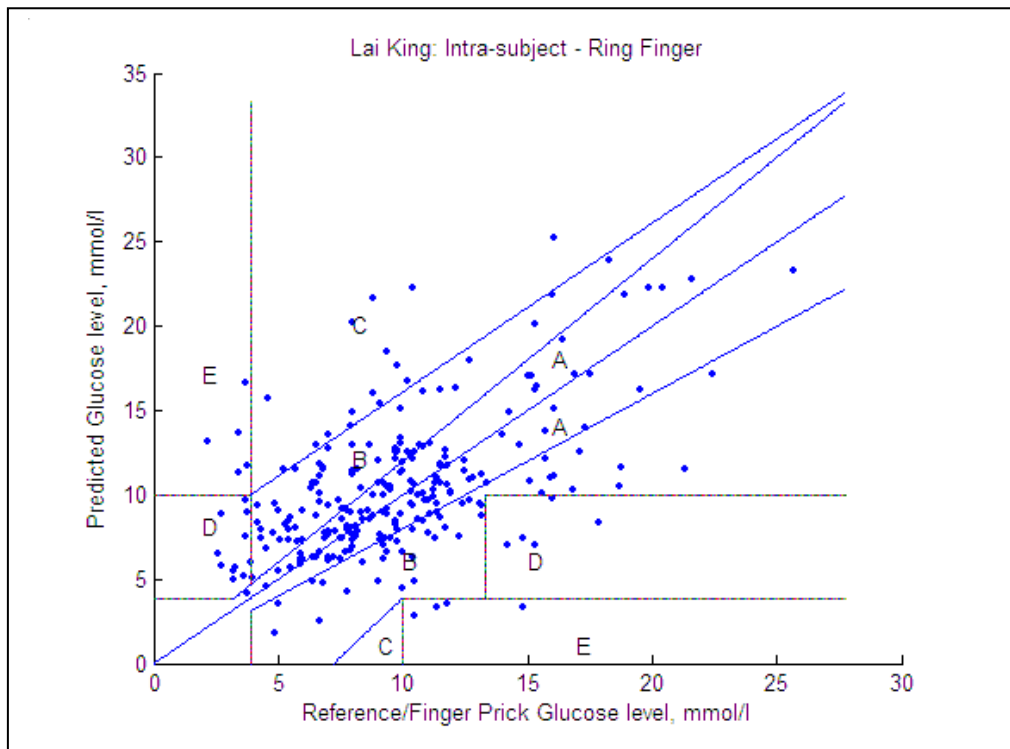


**Figure 7-8: Prediction scatter plot from the community clinic– ring finger, plot all the predicted glucose level together against the reference/finger-prick glucose level.**

The results showed that  $R_p = 0.54$  and  $rmsep = 4.03\text{mmol/l}$  amongst ring fingers in Figure 7-8. Regions A and B contained about 85% of the data points while regions C, D and E contained the rest (15%).

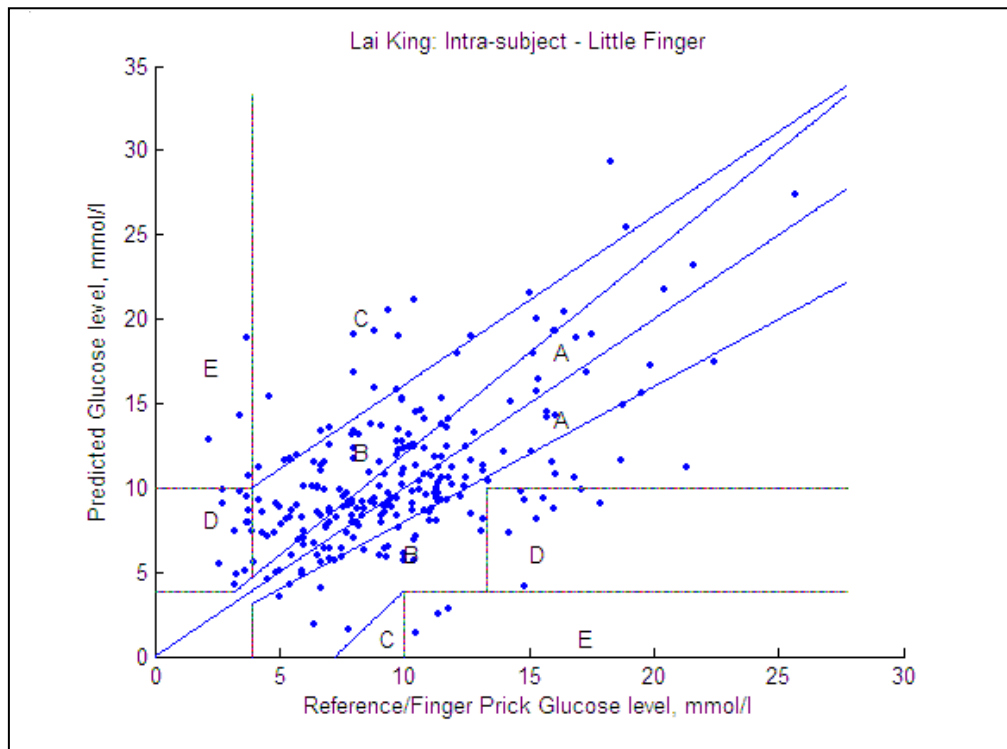


**Figure 7-9: Prediction scatter plot from the community clinic – little finger, plot all the predicted glucose level together against the reference/finger-prick glucose level.**

The results showed that  $R = 0.54$  and  $rmsep = 4.14$  mmol/l amongst little fingers in Figure 7-9. About 90% of the data fell into Regions A and B; the other 10% were located in Regions C, D and E. In comparison with each of the other Figures, 7-5 to 7-9, results showed that the middle, ring and little finger might have obtained a better predictability since there were more data in Regions A and B, and their  $R$ s were relatively higher and  $rmsep$ s relatively smaller.

## 7.2.2 Comparison and summary

For the summary of Figures 7-5 to 7-9, Rps and rmseps were compared as follows:

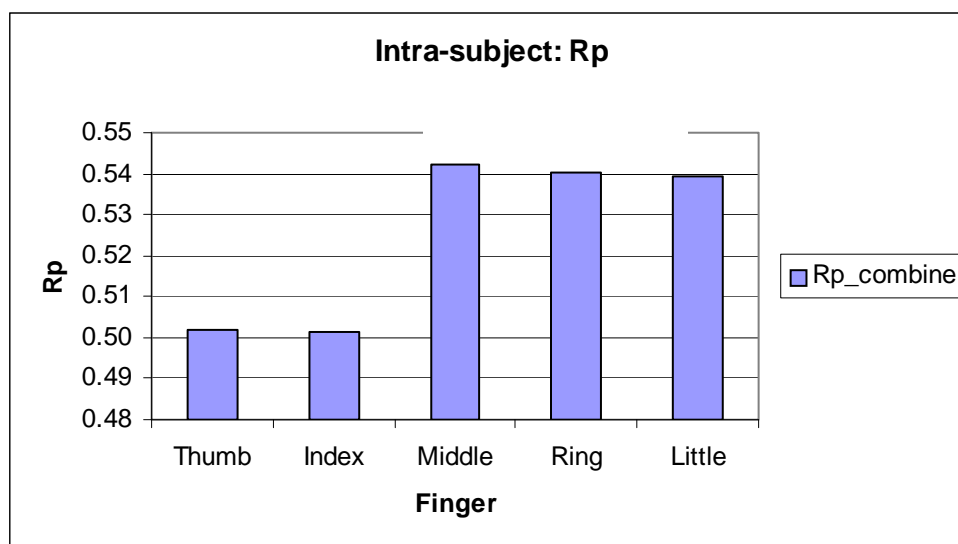


**Figure 7-10: Intra-subject, R correlation coefficient of prediction (Rp) comparison**

In Figure 7-10, Rp-combined was represented by Rp of the predicted glucose levels and the corresponding reference finger-prick glucose levels of all subjects.

$$\text{i.e., } R_{p\_combine} = R_p(\text{sub1}_t, \text{sub2}_t, \dots, \text{sub26}_t)$$

where

$\text{sub}_x_t$  = predicted glucose levels and the corresponding finger-prick glucose levels of subject  $x$  via thumb, index, middle, ring and little fingers, respectively

$$x = 1, 2, \dots, 26$$

$t$  = thumb, index, middle, ring and little finger

Rps were as low as 0.5, which indicated a poor prediction. This showed that there were still many sources of noise which existed in the intra-subject predictions, which might have come from the physiological effects due to the long period of the clinical trial. The results also showed that middle, ring and little fingers provided a slightly higher Rp value.

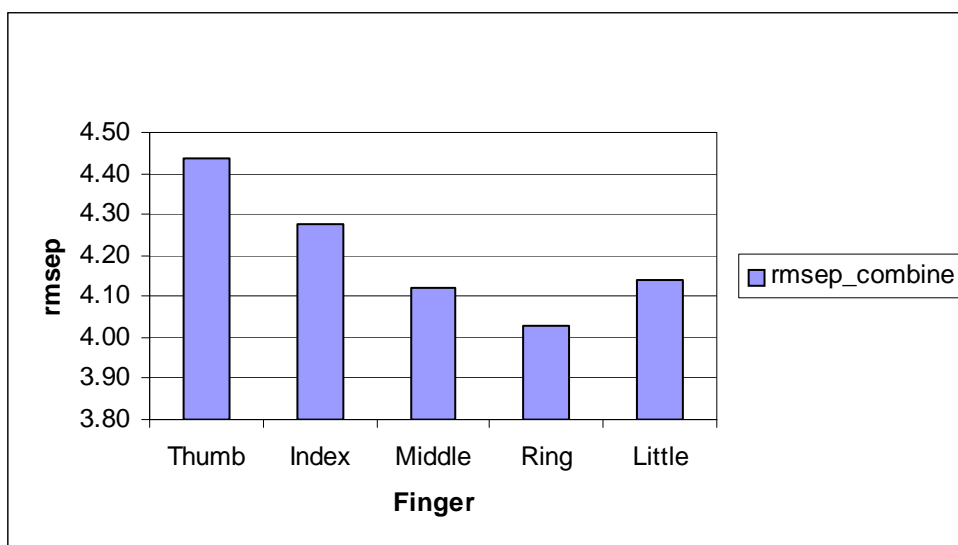


**Figure 7-11: Intra-subject, on his/her 30 data sets, root mean square error prediction (RMSEP) comparison.**

Figure 7-11 showed the rmsep of the intra-subject prediction. The rmsep-combined was represented in all of the predicted glucose levels to the reference finger-prick glucose levels.

i.e.,  $rmsep\_combine = rmsep(sub1\_t, sub2\_t, \dots, sub26\_t)$

where

subx<sub>t</sub> = predicted and the corresponding finger-prick glucose level of subject x via thumb, index, middle, ring and little fingers, respectively

x = 1, 2, ..., 26

t = thumb, index, middle, ring and little fingers

The middle, ring and little fingers showed a smaller rmsep, which demonstrated that they were the best three. The results of rmsep were match to the results of the Rp. However, the rmsep were high, with ranges higher than 3.5mmol/l.

### **7.3 Discussion**

The predicted results showed that poor Rp and rmsep were obtained, although most of the predicted points fell with Regions A and B, the clinically acceptable regions. These predictions showed that non-invasive NIR blood glucose prediction was hardly repeatable under *in vivo* measurements. Rp could only reach 0.55 among 26 intra-subject predictions.

The results indicated that intra-subject predictions also faced many uncertainties during the three-month clinical trial. However, there was an improvement against the previous two clinical trials.

#### **7.3.1 Reflectance against transmittance NIR spectroscopy**

Reflectance NIR spectroscopy was carried out in this clinical trial. This was because transmittance NIR measurements obtained incomplete signals. Jeon et al. (135; 157),



in 2004 and 2006, recommended transmittance NIR spectroscopic measurement for non-invasive blood glucose measurement. However, their comparisons between the transmittance and reflectance were based on different sample thicknesses, where the reflectance NIR spectroscopy used 10mm samples thickness and the transmittance NIR spectroscopy used 1 and 2 mm sample thicknesses under *in vitro* experiment at conditions. This showed a comparative bias in the transmittance measurement since they had also mentioned that the 1 mm sample thickness provided better results than the 2 mm sample thickness for transmittance action. Due to the disadvantages of the transmittance NIR measurement, reflectance NIR spectroscopy was recommended in Stage 4.

The clinical trial used finger tips for blood glucose measurement through both NIR spectrometer and the finger-prick glucose meter. Using finger tips for the measurement had the following advantages and disadvantages:

### **7.3.2 Pros and cons of using fingertips for NIR measurement**

The advantages of using the fingertip for NIR and finger-prick glucose measurements instead of other parts of the body for NIR measurement are as follows:

1. Hair will not affect the NIR measurement;
2. A high-density of capillaries is located in the fingers;
3. Little or no time lag when compared under the same measurement place  
and
4. Data can be easily obtained from different fingers.

The disadvantages of using the fingertip for NIR measurement:

1. Measurements are easily affected by the surrounding environment, such as finger temperature, which is relatively low in comparison with other parts of the body, i.e., higher temperature variation occurs in fingers and
2. The toughness/softness of the tissue of the pressing/contact area may change from time to time. i.e., the tension of the tissue may change. As a result, it may affect the consistency of the force being applied to the contact area. Thus, consistent force contact may not be useful for NIR probe measurement due to tissue deformation. Consistent force contact is useful for short-term measurement, in which less tissue deformation occurs. For long-term measurement, the consistent force may also be altered by the inconsistent reaction of the tissue deformation.

### **7.3.3 Consideration of the measurement on arms**

Calibration and prediction using blood from the arms could be relatively poor when NIR measurement had been taken from fingers, since there would be a time lag between the glucose level from the finger-prick and from the arm, as mentioned in Chapter 2. The error due to time lag could add to the prediction, just like the prediction in Stage 2.

However, fasting blood glucose from the arm for a laboratory test would be recommended for a blood glucose test. The plasma glucose level test in this stage was used to check whether the finger-prick blood glucose results were valid as the plasma test would be the valid measurement of blood glucose levels. Thus, there

were two tests for arm blood glucose level on the first day and the last day of the clinical trial during Stage 4. The results of the plasma test had confirmed that this finger-prick glucose meter was suitable for the measurement and clinical trial.

#### **7.3.4 Finger prick glucose meter**

The results in Figure 7-1 showed that the finger prick glucose meter used for the clinical trials was clinically acceptable. The majority of the finger-prick readings were located within an 80% accuracy region when compared with the plasma glucose readings. This helped to ensure the reliability of the finger-prick glucose meter. According to the Food and Drug Administration (FDA), USA (158) for an international standard (ISO DIS 15197), the finger-prick glucose meter should attain  $\pm 20\%$  for a higher value and  $\pm 1.1$  mmol/l for glucose value under 5.6 mmol/l accuracy against the venous blood glucose test by biochemical measurement. This finger-prick glucose meter fulfilled the specification required by the FDA. Thus, it was used to obtain reference/true glucose levels for this clinical trial (Stage 4).

The finger-prick glucose meter was also used to check the glucose difference between fingers. As reported in Figure 7-2, there was not much difference in the blood glucose levels between the fingers. The error of blood glucose levels between fingers was lower than the error of the blood glucose levels between plasma glucose and finger-prick glucose levels. Thus, the finger-prick method was only applied for one finger instead of five fingers from the left hand.

### **7.3.5 Measurement locations and blood effect**

However, as mentioned by McGarraugh et al. (127), a time lag occurred between glucose measurement in the finger and the arm (about 5-20 minutes behind the finger's glucose levels) or other parts of body, introducing error.

The comparison of the glucose reading between the finger and the arm was performed under fasting conditions for about 10 hours in Stage 4. As it was not practical to abstract the venous blood every day and in each visit, the venous blood was only taken from the first and the last days (the first visit and the last visit), in order to ensure the accuracy of the finger-prick glucose meter.

NIR glucose measurement might have been influenced by blood diseases, such as an abnormal number of red blood cells, protein or cholesterol which may have caused the spectroscopic measurement to deviate. Therefore, many blood component readings, as mentioned above, were obtained in the first and last visits.

### **7.3.6 Force for the measurement area**

The force of the contact point of the measurement area affected the deformation of the contact point of the tissue. The constant force applied to the measurement area provided a little help over a short period of time, while it would be likely to produce a poor prediction after a long period (159). This is because the tension of the body tissue is different after a certain time. Different deformations of the finger tissues may cause different reflections or refractions, so it may affect the strength of signal capturing. Constant depth measurement may provide a little help for the non-

invasive blood glucose measurement. However, this may only keep for a short period due to the influence of physiology.

NIR light can be reflected, refracted, passed through and absorbed by the fingers. Irregular force adding on the finger may deform the blood capillaries; in which unsteady blood flow rate and undistributed finger tissue deformation may produce additional noise to the signals. Thus, unsteady NIR signals may be obtained. This unsteady signal may produce additional uncertainty to the blood glucose prediction.

### **7.3.7 Temperature effect**

Many researchers had mentioned that temperature had a significant effect on the NIR measurement in non-invasive blood glucose prediction. Therefore, some attempts had been made to manipulate the contacting temperatures in order to reduce the temperature effect or temperature variation of the measurements. In this clinical trial, no temperature manipulation action was applied, but the temperature of the contact points was recorded as shown in Appendix C. The regulation of the temperature might have caused the manipulation of the NIR reading, which was highly dominated by the temperature, i.e., the spectra obtained might have contained energy added to or extracted from the temperature regulating action. Thus, the readings of the NIR spectra might have become hardly distinguishable between the outside, manipulated temperature and from the normal body signal generated naturally.

Temperature itself might not significantly affect the predictions since there were many uncertain physiological influences, in which temperature was only a part. Large temperature variations might not represent a large spectral variance among *in*

*in vivo* spectral signals. According to the predicted results, there seemed to be no direct relation to the temperature difference. This means that the blood glucose prediction of the *in vivo* subject with lower temperature variation may not provide a better result than with larger temperature variation signals.

### **7.3.8 Physiological effect against Reliability**

The physiological effect of the human being is the one which cannot be eliminated and is constantly changing. Variables, such as finger temperature, react to the surrounding environment. This caused difficulty for NIR non-invasive blood glucose measurements and prediction. Thus, the error was relatively increased over a longer period of calibration and prediction.

Thus, the reliability of the non-invasive blood glucose measurement by using NIR with PLS prediction was poorer in the long term, regardless of the other physical noise sources. The predicted results for the long-term require a large adjustment for compensation. Physiological differences within a single subject can affect the NIR measurement. A higher chance of physiological differences occurs for longer-period clinical trials. Thus, the NIR spectra obtained may contain different information, which mostly becomes noise in relation to the NIR spectroscopic measurement.

Accordingly, the NIR measurement among inter-subjects caused a poorer prediction, as stated in Stage 2. This was because the physiological difference between subjects should be relatively larger than the difference within subject (intra-subject) when compared over time. Therefore, the research by using intra-subject

data should result in a higher reliability. Chapter 10 discusses further the effects of the intra-subject and inter-subject to NIR spectroscopic measurement.

This showed that intra-subject prediction seemed better than inter-subject prediction, when comparing the  $R_p$  and  $rmsep$  between Stage 2 (inter-subject) and this stage. The prediction also showed a slight improvement when compared with Stage 3. However, this analysis needed to be further confirmed since the comparisons were based on different measurement approaches and different sampling sets.

### **7.3.9 Spectral variations**

The spectra plot shown in Figure 7-4 provided a smaller spectral variation when compared against Stage 2 and Stage 3. The plot showed that the variance of the intra-subject NIR spectra was relatively low. This showed that intra-subject measurements might have lower interference. This also indicated that intra-subject measurement resulted in less noise for non-invasive blood glucose measurement.

The predictions in Figures 7-5 to 7-9 showed glucose levels predicted from the thumb, index, middle, ring and little fingers, respectively. Most of the predicted glucose levels were located in the clinically acceptable region. This demonstrated that the NIR glucose prediction was positive for *in vivo* application. However, the predictability of  $R_p$  was only at around 0.5; improvement is needed. This might have been due to the long period of the three-month clinical trial. This demonstrated that prediction was affected in the long-term.

The best Rp and rmsep predictability were from ring fingers' data. One reason was that the majority of the finger-prick readings were obtained from the ring fingers. This might have shown some closer relationship between NIR and finger-prick glucose readings under closer area. Another reason was that the thickness variance of the ring fingers was the smallest (with variance = 1.06mm), which might also play an influential role in glucose prediction.

## **7.4 Conclusions**

Non-invasive NIR spectroscopic blood glucose measurement is scarcely repeatable for the long-term due to physiological effects. Reflectance NIR measurement is recommended for *in vivo* non-invasive blood glucose measurement. The results of intra-subject trials seemed better than the results of inter-subject from Stage 2; further confirmation is needed.

The sampling data arrangements were applicable for both inter- and intra-subject comparisons under the same situations. Thus, further analysis for this clinical trial will be reported in Chapters 8 through 10.



## Chapter 8

### Evaluation of Preprocesses

A preprocess is normally needed for PLS to improve the prediction. The signal of the spectra is treated by preprocess first, prior to making the prediction. Piece-wise Direct Standardization (PDS) is one of the more powerful preprocesses and has the advantage of reducing the variation of the signal, thereby reducing the variance of the signal/spectra. On the other hand, the Savitsky-Golay smoothing and differentiation (Savgol) can provide another form of signal preprocessing by reducing many background noise sources, thus reducing their interference. They both can provide successful preprocessing before any predictive action.

This chapter further discusses Savgol and PDS, with mean-centred preprocess as a basis, and by comparing the predictability of  $R_p$  and  $rmsep$ . As discussed in the previous studies, it seemed that the smaller the variance, the better the prediction. The intra-subject data of Stage 4 were used for analysis and discussion. The pros and cons of using a preprocess for PLS analysis in NIR blood glucose measurement are also discussed in this chapter.

## 8.1 Objectives

- To compare preprocesses for PLS predictions among PDS and Savgol by using simple mean-centred preprocess as basis;
- To evaluate whether high variation spectral signals are poorer for prediction and
- To confirm the preprocess choice of Stage 3 for NIR spectroscopic measurement by PLS prediction.

## 8.2 Predictions and comparisons

Rp and rmsep were used for predictability comparisons between Savgol and PDS. A simple mean-centred preprocess (SMCP) was used as basis, in which it worked with PLS alone. It was also used with Savgol and with PDS, respectively for PLS prediction. The predictions were obtained by calibrating the spectra of the four measured fingers among the spectra of the five measured fingers. The remaining one finger was used for the prediction. The process then continued with different spectra combinations. These comparisons were different to the previous clinical trials as the spectra obtained were relatively less noisy. No signal was blocked in the region of 1381 to 1701nm.

As discussed in Stages 2 and 3, different preprocesses provided different filtering power over various signals. The following sections discuss the selection of a suitable preprocess for PLS analysis and evaluate the right preprocess for NIR spectroscopic measurement.

### 8.3 PLS prediction with simple mean centred preprocess

As mentioned before, SMCP was used as basis for the comparison between PDS and Savgol. Figure 8-1 shows the results of PLS prediction with SMCP, in which predicted results were obtained by calibrating the spectral data from the other four fingers. For example, when predicting the glucose level of the thumb, the spectra of the index, middle, ring and little fingers were used for the calibration with the finger-prick glucose levels. The spectra of thumb were applied for the prediction.

After all of the predictions, all of the predicted glucose levels and the reference finger-prick glucose levels were examined to obtain  $R_p$  and  $rmsep$ , and they were also plotted on bar charts for comparison.

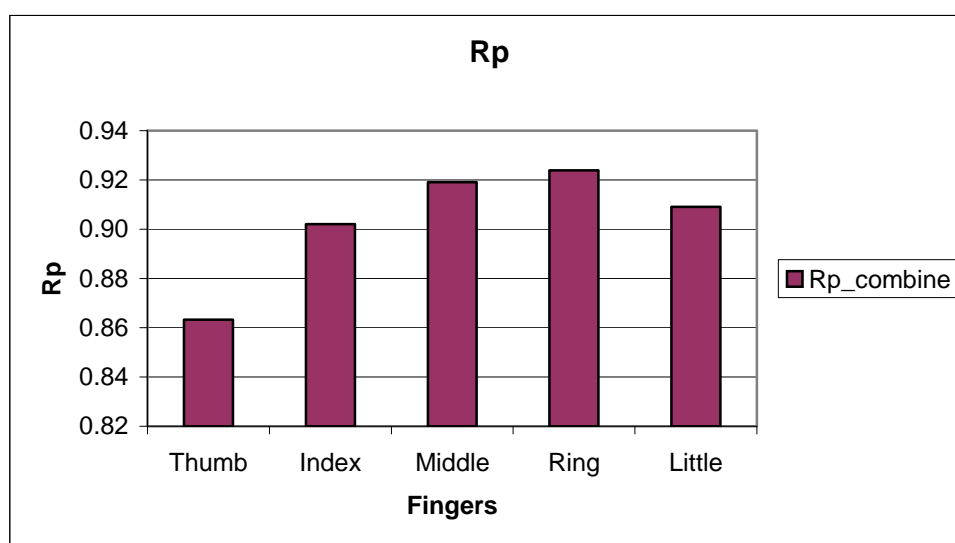


**Figure 8-1: Bar chart of R correlation coefficient of prediction comparison,  $R_p$ ; PLS with simple mean-centred preprocess for the intra-subject.**

All the  $R_p$  were higher than 0.86; the best one appears for the ring finger, which showed  $R_p = 0.92$ . The poorest  $R_p$  was the thumb, in which  $R_p = 0.86$ . This

provided a basis for PLS prediction. Thus, PLS, with preprocess added, should offer an improvement for the predictability. In addition to the  $R_p$  correlation, rmsep is another prediction consideration. The following section reports the results of rmsep.

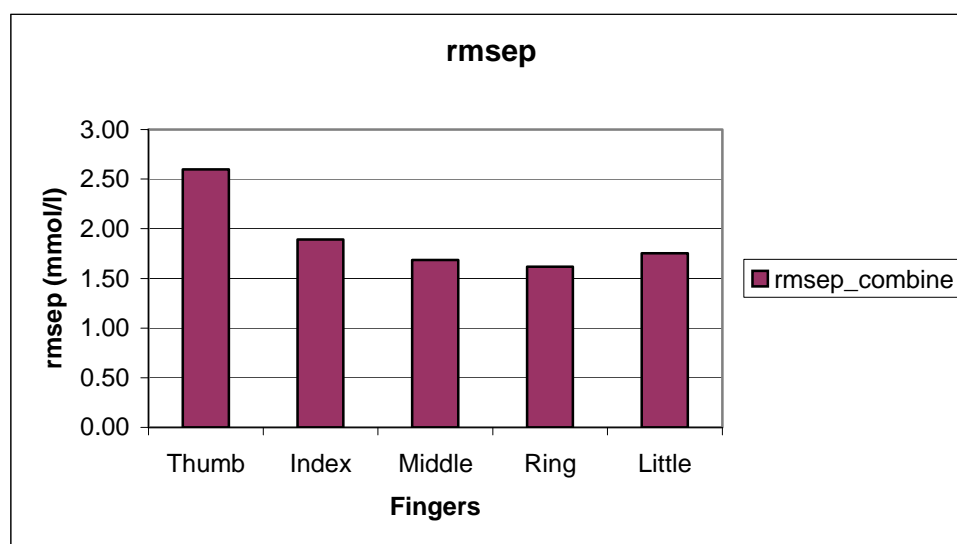


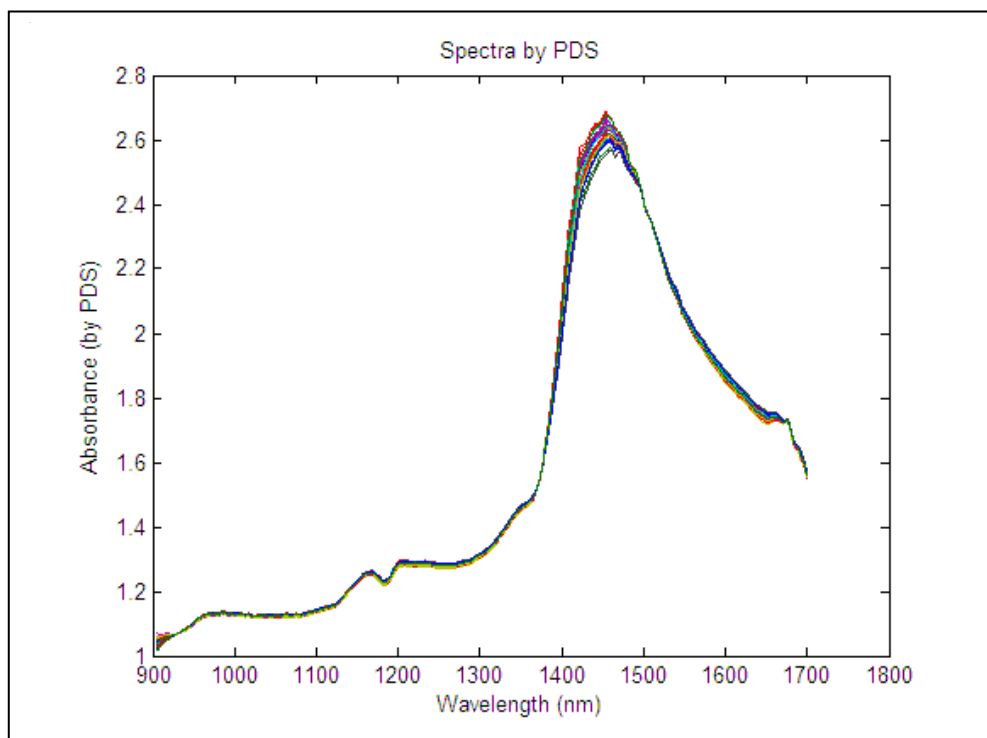
**Figure 8-2: Bar chart of root mean square error of prediction, rmsep; PLS with simple mean-centred preprocess for the intra-subject.**

The smaller the rmsep, the better the prediction will be. Figure 8-2 showed the same results for  $R_p$  shown in Figure 8-1. The best predicted glucose levels were located in the ring finger. The poorest one was the prediction from the thumb. This confirmed that the error of the prediction from the ring finger was the least. In addition, all results of rmsep were lower than 2mmol/l, except the thumb.

## 8.4 PDS preprocessing

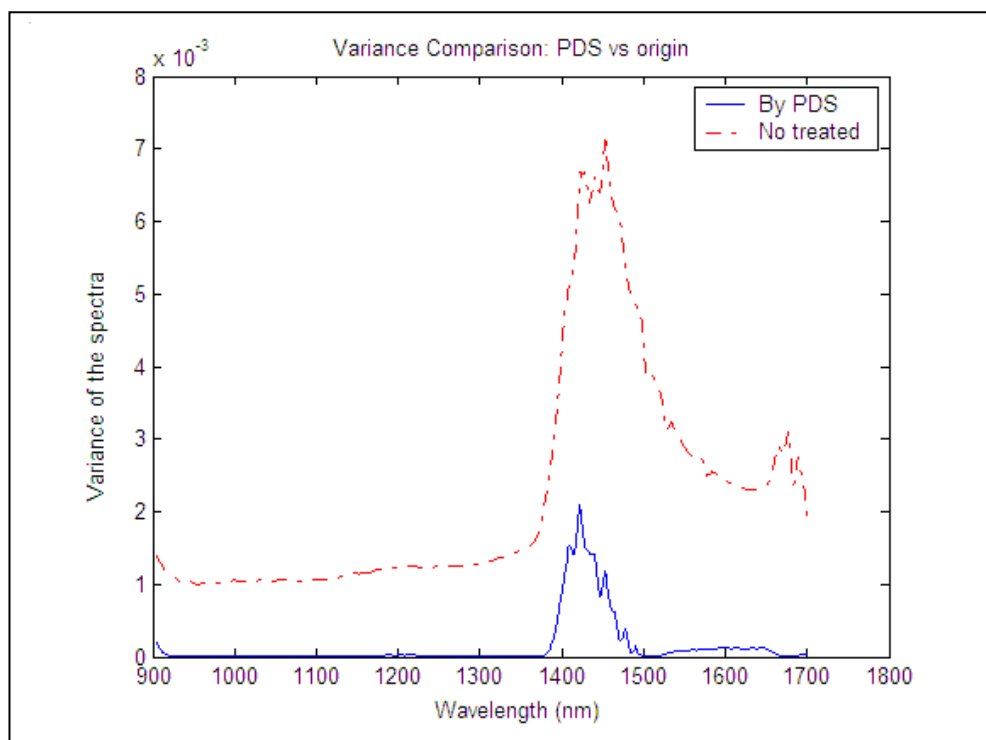
Piece-wise direct standardization (PDS) helped to reduce the variance before performing the PLS prediction. Figure 8-3 shows spectral plots obtained from

Subject 27 and preprocessed by PDS. The shape of the spectra was same as the spectra before it was preprocessed. Besides, all the spectra were close in range to each other, and some were almost overlapping, without zooming in.



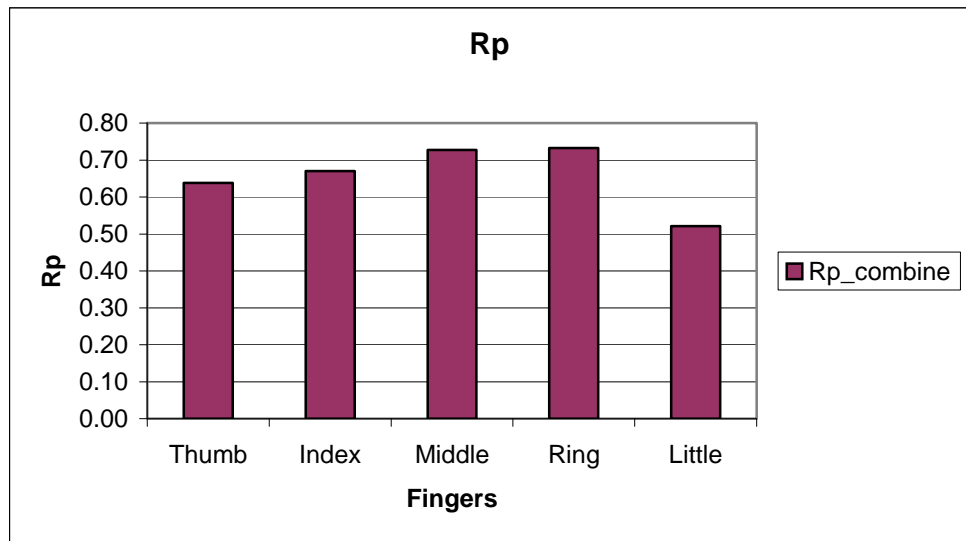
**Figure 8-3: Spectra plot after the preprocessing of the PDS**

The variance of the absorbance was finer when compared with the variance of the NIR spectral plots in Figure 7-4. PDS reduced the difference between spectra. The large, varied portion was located at about 1400-1500nm, where the OH element was represented. The other portions were relatively close to each other. Figure 8-4 shows the variance comparisons between PDS preprocessed spectra and non-treated spectra (SMCP).



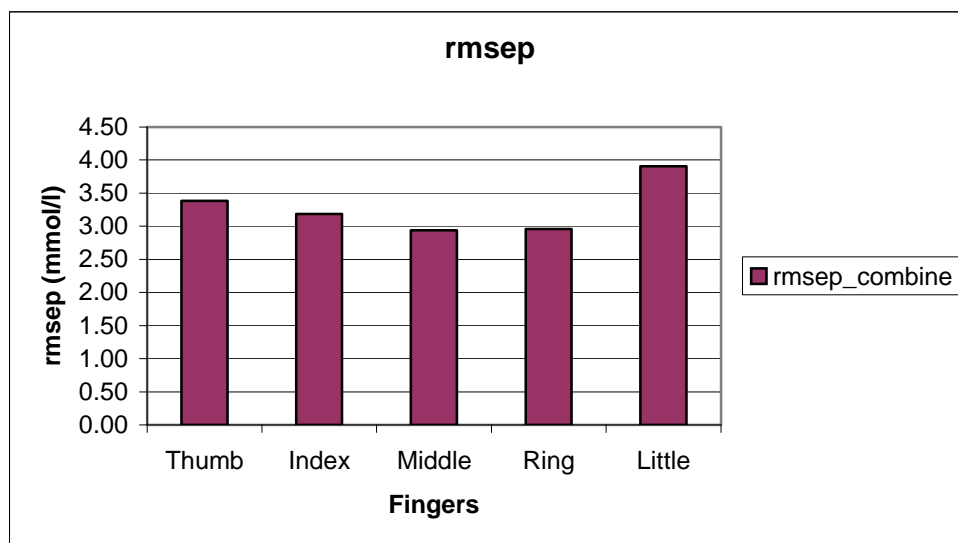
**Figure 8-4: Variance Comparison Plot of NIR spectra - PDS preprocess vs. Non-treated (simple mean-centred preprocess)**

According to the figure, the large variances existed at about 1400 - 1500nm in both spectral signals. However, results indicated that the variance of the non-treated (SMCP) spectra is higher than the PDS preprocessed spectra at 3.5 times the wavelength of 1420nm, in which the whole spectral variance of non-treated was higher than the spectra of PDS preprocessed. This also demonstrated that PDS was able to reduce the spectral variance. The following figures report the predicted results of PLS, in which the spectra were preprocessed by PDS.



**Figure 8-5: Rp correlation coefficient, PLS with PDS preprocess**

Figure 8-5 illustrated the Rp of the predicted glucose levels, in which the spectra had been preprocessed by PDS. However, the Rp obtained were not encouraging, with a value lower than 0.8 (ranging from 0.52 to 0.73). The middle and ring fingers gave the best two Rp which were coherent with the previous PLS prediction of SMCP. The Rp of the little finger was the worst; this showed a discrepancy from the previous PLS prediction. The result showed that PDS might interrupt the spectral signals, thus the preprocessed signals might have contained unrelated information. This also stated that even though PDS preprocesses reduce the variation of spectra, they may vary the spectral information. Thus, the correlation would be poorer.



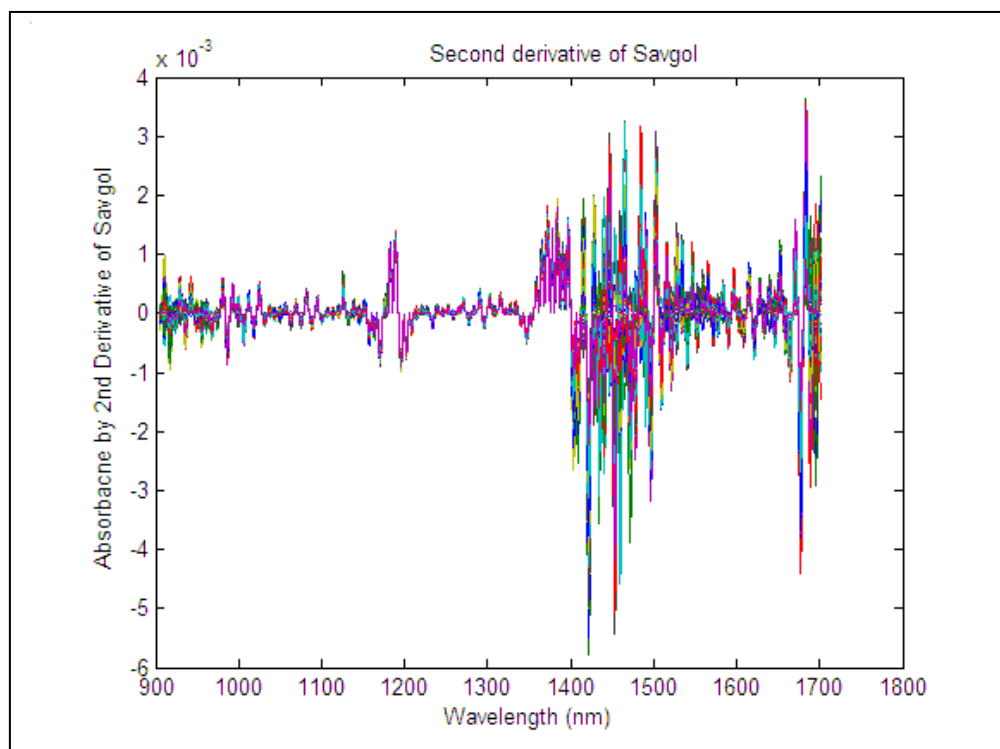
**Figure 8-6: RMSEP (Root Mean Square Error Prediction), PLS with PDS preprocess**

Figure 8-6 showed the rmsep of the fingers by PLS with PDS preprocess. All of the rmsep were larger than 2mmol/l, and they ranged from 2.9 to 3.9mmol/l. The middle and ring fingers showed, relatively, the lowest rmsep value. However, the rmsep obtained were about 1mmol/l poorer than the previous prediction, which used SMCP. This indicated that PDS affected the spectral data. It might have shrunk the unrelated information, which caused a poor prediction. Although many researchers mentioned that preprocess helped to improve the PLS prediction, the selection of a suitable preprocess would be vital. Otherwise no preprocess (except the common preprocess of SMCP) should be used for PLS prediction. PDS was not a suitable preprocess for NIR spectroscopic measurement for human fingers.



## 8.5 Savgol preprocess

This section reviews the analysis of spectral data by Savgol preprocess. Figure 8-7 shows the spectral signal preprocessed by the second derivative of Savgol. After Savgol, the spectra become noise-like signals. The variation of the NIR spectra was much narrower after being preprocessed by Savgol. The spectra magnitude was relatively smaller (by 10 to the power of minus 3) than the signal preprocessed by PDS. The highest variance was also located around 1400-1500nm, where the similarities with the previous preprocessed variance were shown (Figure 8-4).



**Figure 8-7: Absorbance against Wavelength after 2nd derivative with Savitsky-Golay smoothing and differentiation (Savgol)**

All of the second derivative Savgol preprocessed spectra were then plotted as a variance plot in Figure 8-8. The variance plot clearly showed the largest variance

and the shape was like the spectral signal. The variance was about 1/20000 of the variance signal (in magnitude) of that preprocessed by PDS (Figure 8-4). This implied that Savgol may have provided a larger noise filtering power.

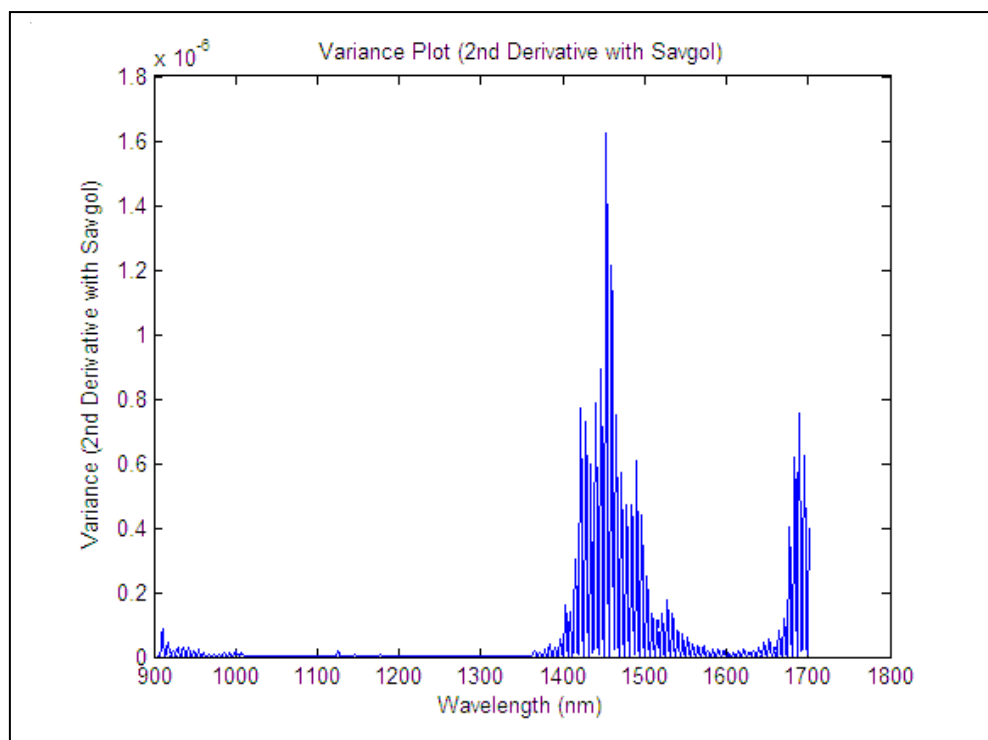


**Figure 8-8: Variance Plot of 2nd Derivative with Savitsky-Golay smoothing and differentiation (Savgol)**

This also showed that Savgol was suitable for reducing the variation of the NIR spectral signal for finger spectroscopic measurement. The largest variance, located around wavelength 1400 - 1500nm, explained that the OH might have been the most significant effect in spectroscopic measurement among the fingers.

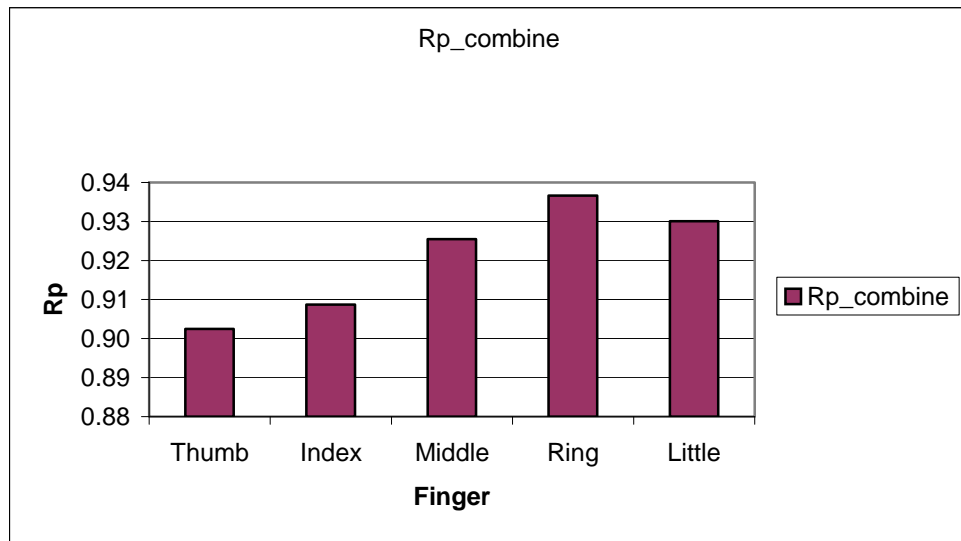


**Figure 8-9: Correlation coefficient of prediction (Rp) comparison; Rp\_combine: Rp obtained by all predicted glucose levels and the corresponding finger-prick glucose levels.**

Figure 8-9 showed the comparison of the Rp of the thumb, index, middle, ring and little fingers. The “Rp\_combine” represented the correlation coefficient between all the predicted glucose levels and the corresponding finger-prick glucose levels.

i.e.,  $R_p(\text{sub1}_t, \text{sub2}_t, \dots, \text{sub26}_t)$

where  $\text{sub}_i_t$  = the predicted glucose levels and the corresponding finger-prick glucose levels of the thumb of subject  $i$

$$i = 1, 2, \dots, 26$$

Results showed that middle, ring and little fingers were higher in correlation between the prediction and the finger-prick glucose levels, where the ring finger was the best. All Rp ranged from 0.90 to 0.94.

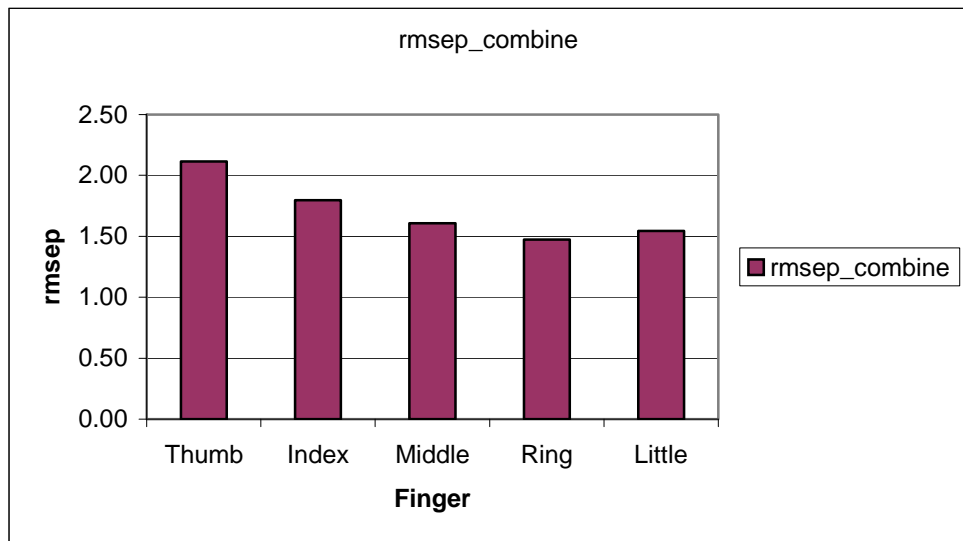


**Figure 8-10: RMSEP (Root mean square error prediction) comparison; rmsep\_combine: the rmsep between the predicted glucose levels and the finger-prick glucose levels.**

Figure 8-10 showed the comparison of rmsep. The “rmsep\_combine” was the rmsep of all the predicted values.

i.e.,  $\text{rmsep}(\text{sub1}_t, \text{sub2}_t, \dots, \text{sub3}_t)$

where  $\text{subi}_t$  = predicted glucose levels and the finger-prick glucose levels of the individual finger of subject  $i$ .

$i = 1, 2, \dots, 26$

$t = \text{thumb, index, middle, ring, little fingers}$

As before, the middle, ring and little fingers showed the lower value rmsep among the five fingers. The results provided the consistency of the Rp and rmsep. This suggested that the middle, ring and little fingers might have provided a higher predictability. The prediction showed that rmsep was from 1.49 to 2.10mmol/l. For the thumb, both Rp and rmsep provided the poorest predicted results.

## **8.6 Discussion**

Preprocessing is a method to reduce the signal gap or minimize noise from the signal prior to analysis. The purpose of the preprocessing in this case was to assist PLS to obtain better prediction. Preprocessing helped to arrange the data set and to filter out the unnecessary noise for obtaining a higher predictability. However, the results from different preprocesses could be very different.

### **8.6.1 Spectral variation**

According to the results from Figures 8-3, 8-4 and 8-8, they indicated that the spectra preprocessed by Savgol provided a relatively smaller variance than that by PDS. These preprocess actions provided different data arrangements for PLS prediction. Small variance showed that the spectra were close to each other; thus, comparing the best fit for the PLS prediction. Therefore, prediction from Savgol (SMCP + Savgol) should be the best. PDS (SMCP + PDS) should be the second and non-treated (SMCP) should be the poorest. However, the facts showed that the PLS prediction of PDS was the poorest.

The results showed that PDS compressed the variation. However, the compression interrupted the spectral signals. Although the variation of spectra was relatively larger, the original signal had no disruption. Therefore, the predictability was higher. Savgol preprocess was the best one to reduce the variation. The variance preprocessed by PDS was 1200 times larger than the variance of Savgol preprocessed. In addition, the largest variance was at about 1400 to 1500nm. This also indicated that OH groups provided the largest influence on the spectra, whether

they had been preprocessed or not. The result also demonstrated that Savgol did not disrupt the spectral signal much when compared with the shape of the original spectra.

### **8.6.2 Simple mean-centred preprocess (SMCG)**

SMCG is a very common practice to centralize a large data set for PLS prediction. This action helps to centralize the large data set to become mean centred. The results obtained through PLS with SMCG were the basis for comparison with the other two preprocesses, PDS and Savgol. The higher  $R_p$  and lower rmsep demonstrate the better predictability.

The results showed the highest  $R_p$  and lowest rmsep were in the ring fingers. This indicated that the ring finger resulted in the best prediction. The predicted values were close to the reference value for more than 92%, whereas the ring fingers gave the best correlation. This echoes the previous study stated in Chapter 7 - ring fingers were of relatively smaller thickness variation, and also most of the finger-prick readings came from them. However, there was only a range of 0.06 between lowest and highest  $R_p$ . The results here were quite consistent.

For rmsep, the best rmsep was also in the ring fingers, whereas rmsep was at 1.6mmol/l. The worst prediction was the thumb, which showed rmsep at 2.6mmol/l. This confirmed that the ring finger provided the best prediction. The poorest prediction was from the thumb. This might have been due to the thumb being relatively thicker.

### 8.6.3 PDS

The predicted results showed that PDS preprocessed data provided worse prediction through PLS. All the  $R_p$  were relatively lower than by using SMCP by about 20%. All rmsep were higher than 2.8mmol/l. The poorest prediction was in the little finger. This proved quite different from the previous predictions. This implied that PDS might have disrupted the arrangement of the spectral signals. The newly PDS preprocessed signal might not have contained the proper information needed for glucose level prediction. It may not have been suitable for *in vivo* spectroscopic signals although it could have helped the prediction for the glucose solution concentration.

Herrero and Ortiz (148) recommend PDS for PLS prediction, but the current results showed that PDS might not be suitable for *in vivo* NIR spectroscopic measurement via the reflectance approach, predicted by PLS. Even though the calibrated results might have provided a very high correlation between reference/true glucose levels and calibrated spectral signals, the PDS preprocess might have misled the spectral signals. As a result, it might have implied a poorer PLS prediction. This also indicated that the small variation obtained by PDS was not suitable for this clinical trial.

### 8.6.4 Savgol

For Savgol, the results were positive. The  $R_p$  were higher than 0.8 and the rmsep were lower than 1.5mmol/l. Savgol preprocess was suitable for this application. As mentioned, the variance of the spectra via Savgol was smaller than that via PDS. This demonstrated that Savgol provided the closer signal needed for PLS prediction

in this case. This also reinforced the results of Stage 3 which also demonstrated that Savgol was the best for PLS prediction (among polynomial like spectral signals). Therefore, the Savgol preprocess was applicable for PLS prediction via reflectance NIR for non-invasive blood glucose measurement.

## **8.7 Conclusions**

In conclusion, PLS prediction with the Savgol preprocess should have been used for reflectance NIR spectroscopic blood glucose measurement via a probe. The smaller variance of the spectra after preprocessing might not have given a better predictability if the inappropriate preprocess was chosen. However, the small variance still represented a better prediction. It supported the result of the preprocess comparison in Stage 3.



## **Chapter 9**

### **Evaluation of the Effect of Sampling Size Ratio of Calibration to Prediction**

In addition to the effect of preprocessing the prediction, the sampling size for the calibration will also affect the results of the prediction. The larger the calibration, the better the prediction will be in theory. However, the results may be totally different if many uncertainties exist in the obtained signals. In addition, many researchers of non-invasive blood glucose measurements have a tendency to select different calibration and prediction sampling sizes for prediction. This may lead to an increase in the cost and time required for the clinical trial. The following sections report on the relationship between the calibration sampling size and the prediction sampling size.  $R_p$  and  $rmsep$  are used for the prediction comparison.

#### **9.1 Objectives**

- To find out the calibration sets required for non-invasive blood glucose prediction via NIR spectroscopic measurement;
- To compare the sampling size ratio needed and
- To report the predictability under various calibration sets.

## 9.2 Calibration size comparison

The calibration size can affect the prediction result as it is one of the processes for constructing the prediction. For clinical trials, a suitable sampling size and ratio is important. This not only can reduce the cost but optimize the effectiveness. As mentioned, a larger calibration sampling size may not result in a better prediction for the high-noise signals. The following, analyzed designs use the same sampling sets, which were separated into different combinations. Just like in Chapter 8, there was a calibration of the spectra of four fingers in order to obtain a model. Afterwards, another, separate set of spectra was used to model the prediction.

### 9.2.1 Calibration - large scale

This section reports on the largest sampling scale for the calibration of this clinical trial. There were a total of five sets of spectral signals. Thus, the largest sampling scale in this case was four sets (i.e., calibration sample size-to-prediction sample size = 4:1). For the prediction of a single finger, the other four fingers were used as the calibrations. For example, the prediction of the thumb was made using the other four fingers' spectra as calibration. In addition, as recommended in Chapter 8, simple mean-centred and Savgol preprocesses were used to treat the spectral signals before PLS prediction. The following shows a detailed arrangement for this application:

1. Spectra of the index, middle, ring and little fingers, with corresponding finger-prick glucose levels, were calibrated by PLS; next, the spectra of the **thumb** were inputted into the model generated by the calibration for the glucose prediction;

2. Spectra of the thumb, middle, ring and little fingers, with corresponding finger-prick glucose levels were calibrated by PLS; next, the spectra of the **index finger** were inputted into the model generated by the calibration for the glucose prediction;
3. Spectra of the thumb, index, ring and little fingers, with the corresponding finger-prick glucose levels, were calibrated by PLS, after which, the spectra of the **middle finger** were inputted into the model generated by the calibration for the glucose prediction;
4. Spectra of the thumb, index, middle and little fingers, with the corresponding finger-prick glucose levels, were calibrated by PLS, after that, the spectra of the **ring finger** were inputted into the model generated by the calibration for the glucose prediction and
5. Spectra of thumb the, index, middle and ring fingers, with the corresponding finger-prick glucose levels, were calibrated by PLS, afterwards, the spectra of the **little finger** were inputted into the model generated by the calibration for the glucose prediction.

The  $R_p$  represented how close the correlation between the predicted glucose levels and reference/finger-prick glucose level was. Figures 8-9 and 8-10 in the previous chapter showed the results of  $R_p$  and  $rmsep$  by calibrating on the largest scale, as mentioned. The results showed that calibration for the prediction of the sampling size of 4:1 provided the best predictability with  $R_p = 0.91$  to  $0.93$  and  $rmsep = 1.49$  to  $2.10$  mmol/l, among predicted fingers.

The results showed that the prediction could have achieved a standard where the  $R_p$  were higher than 0.9 and  $rmsep$  lower than 2mmol/l. This confirmed that NIR had the potential to be the non-invasive blood glucose measurement. Besides, it also indicated that the effect of the tissue thickness was not significant to the NIR measurement. This was because the predictions were calibrated and predicted by using different fingers of different thickness, but the prediction was still able to achieve the mentioned  $R_p > 0.9$  and  $rmsep < 2mmol/l$ . Therefore, the errors were mainly from a change of the internal blood/body tissue due to the metabolism and the reaction of the physiology due to both the internal and external responses. Although physiology was related to time, and the body reaction to internal and external environmental changes, the results were designed to limit the physiological effect. This implied a proper calibration and prediction comparison for the non-invasive glucose measurement.

Therefore, the effect of the finger thickness might not have played a significant enough role to affect the prediction. According to the results shown in Figures 8-9 and 8-10,  $R_p$  and  $rmsep$  were closest to each other, among all of the fingers for the prediction. The maximum error ( $rmse$ ) was about 2.1mmol/l. This also illustrated that finger thickness was not the key effect for the prediction of glucose levels.

### **9.2.2 Calibration - small scale**

The predicted results were obtained by using PLS with simple mean-centred and Savgol preprocesses. For the prediction of a single finger, the other four fingers were used as the calibrations. For example, for the prediction of the thumb, the other four

fingers' spectra were used as calibration, i.e., four individual calibrations. The following reports the calibration and prediction arrangement in detail:

1. Spectra of the **index finger** and the corresponding finger-prick glucose levels were calibrated by PLS, then spectra of **thumb** were inputted into the model generated by the calibration for the glucose prediction;
2. Spectra of the **middle finger** and the corresponding finger-prick glucose levels were calibrated by PLS, then spectra of **thumb** were inputted into the model generated by the calibration for the glucose prediction;
3. Spectra of the **ring finger** and the corresponding finger-prick glucose levels were calibrated by PLS, then spectra of **thumb** were inputted into the model generated by the calibration for the glucose prediction;
4. Spectra of the **little finger** and the corresponding finger-prick glucose levels were calibrated by PLS, then spectra of **thumb** were inputted into the model generated by the calibration for the glucose prediction;
5. Spectra of the **thumb** and the corresponding finger-prick glucose levels were calibrated by PLS, then spectra of **index finger** were inputted into the model generated by the calibration for the glucose prediction and
6. The rest of the finger combinations were arranged for the predictions, as shown in the following paragraph and the row of "One Set" in Table 9-1.

The spectra of **finger x** and corresponding finger-prick glucose levels were calibrated by PLS, then spectra of **finger y** were inputted into the model generated

by the calibration for the glucose prediction. After the arrangement of sampling size ratio of calibration-to-prediction (1:1) was analyzed, the higher calibration-to-prediction sampling size ratios were also analyzed. They were 2:1 and 3:1, as well. The overall combinations of calibration to prediction ratio are shown in Table 9-1.

**Table 9-1: Calibration-to-prediction arrangement where each column represents each finger and the calibration combination; 1 = thumb, 2 = index finger, 3 = middle finger, 4 = index finger, 5 = little finger**

Calibration size	Fingers				
	1	2	3	4	5
Four sets	2345	1345	1245	1235	1234
Three sets	234	134	124	123	123
	235	135	125	125	124
	345	345	245	135	234
Two sets	23	13	12	12	12
	24	14	14	13	13
	25	15	15	15	14
	34	34	24	23	23
	35	35	25	25	24
	45	45	45	35	34
One set	2	1	1	1	1
	3	3	2	2	2
	4	4	4	3	3
	5	5	5	5	4

The numbers below each finger represented the combination of 1 = thumb, 2 = index finger, 3 = middle finger, 4 = index finger, 5 = little finger. For example, for three sets of calibration to predict glucose levels of thumb, the combination sets of

calibration were 234 (i.e., index, middle and ring fingers), 235 (i.e., index, middle and little fingers) and 345 (i.e., middle, ring and little fingers). The spectra of the other fingers were continued for the calibration and prediction. After obtaining each predicted glucose level,  $R_p$  and  $rmsep$  were calculated for predictive analysis.

The spectra of the other fingers were continued for calibration and prediction as arranged in Table 9-1. After obtaining each predicted glucose level, they were used for analysis with  $R_p$  and  $rmsep$ . Figure 9-1 shows the results of  $R_p$  of the small scale calibration and prediction (1:1).

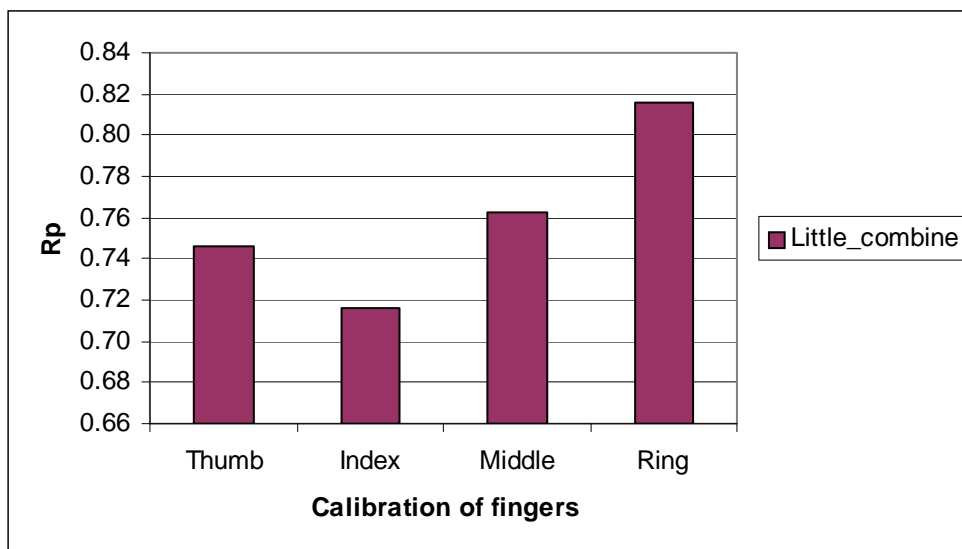


**Figure 9-1: R correlation coefficient of prediction,  $R_p$ ; little finger  $R_p$  by using the calibrations of the thumb, index, middle and ring fingers, respectively.**

Little\_combine represented “the  $R_p$  of all prediction from little fingers,” in which the prediction obtained was by a combination of the calibration of the thumb, index, middle and ring fingers.

$$\text{i.e., little\_combine} = R_p(\text{sub1\_tL}, \text{sub2\_tL}, \dots, \text{sub26\_tL})$$

where  $\text{subi\_tL}$  = predicted and finger prick glucose level of the little finger of subject  $i$  and calibrated by finger  $t$ .

$$i = 1, 2, \dots, 26$$

L = little finger

t = thumb, index, middle and ring finger, respectively

Figure 9-1 represented the small-scale calibration, in which  $R_p$  ranged from 0.71-0.81 for the prediction of the non-invasive blood glucose level in little fingers. The best glucose level prediction of little fingers was based on the calibration of ring fingers. The poorest one was the one calibrated by the index fingers. When compared with the previous figure, Figure 8-9 ( $R_p$  is 0.91-0.93), the  $R_p$  of Figure 9-1 also showed poorer correlation between the predicted glucose level and the finger-prick glucose level. The other small-scale calibrations are reported and compared in Figure 9-3.

Figure 9-2 illustrates the rmsep of the small scale calibration. There,  $\text{little\_combine}$  represents “the rmsep of all predicted and finger-prick glucose levels”

$$\text{i.e., little\_combine} = \text{rmsep}(\text{sub1\_tL}, \text{sub2\_tL}, \dots, \text{sub26\_tL})$$

where  $\text{subi\_tL}$  = predicted and the corresponding finger-prick glucose levels of the little finger by using the calibration of thumb, index, middle and ring finger.

$$i = 1, 2, \dots, 26$$

L = little fingers

t = thumb, index, middle, ring fingers, respectively.



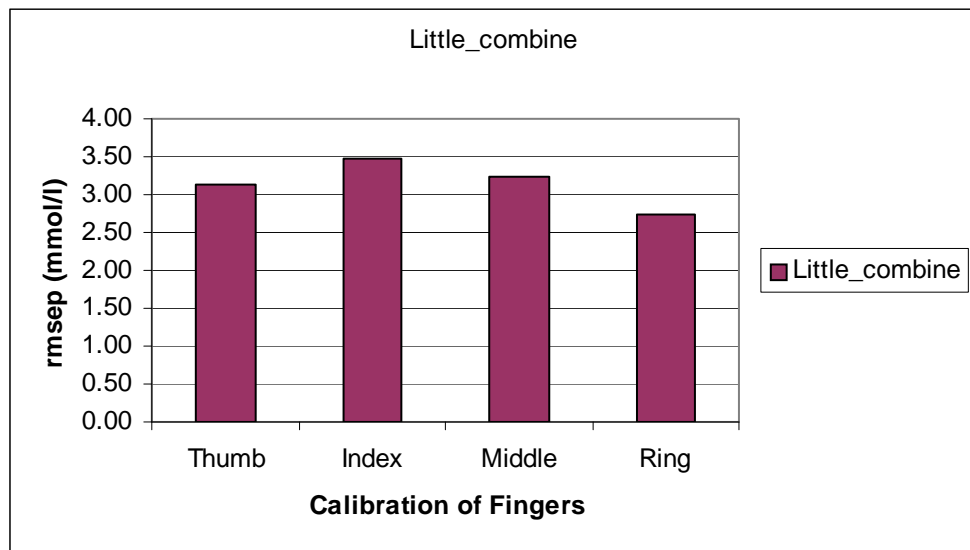


**Figure 9-2: Root mean square error prediction, rmsep; little finger rmsep by the calibrations of thumb, index, middle and ring fingers.**

The rmsep shown in Figure 9-2 ranged from 2.7 to 3.5mmol/l for the prediction of blood glucose levels of little fingers. The same results were obtained when compared with Rp, where the prediction from the calibration of ring fingers was the best and the poorest was from the calibration of index fingers. When compared with the previous figure (Figure 8-10 of Chapter 8), the rmsep in Figure 9-4 was relatively large. This result demonstrated that rmsep was higher for the smaller sampling size of the calibration size.

Figure 9-3 and Figure 9-4 show the comparison between different calibration sizes. The x-axis is the number of sets in which “1” represents one set of calibration, “2” represents two sets of calibration, “3” represents three sets of calibration and “4” represents four sets of calibration to one set of prediction.

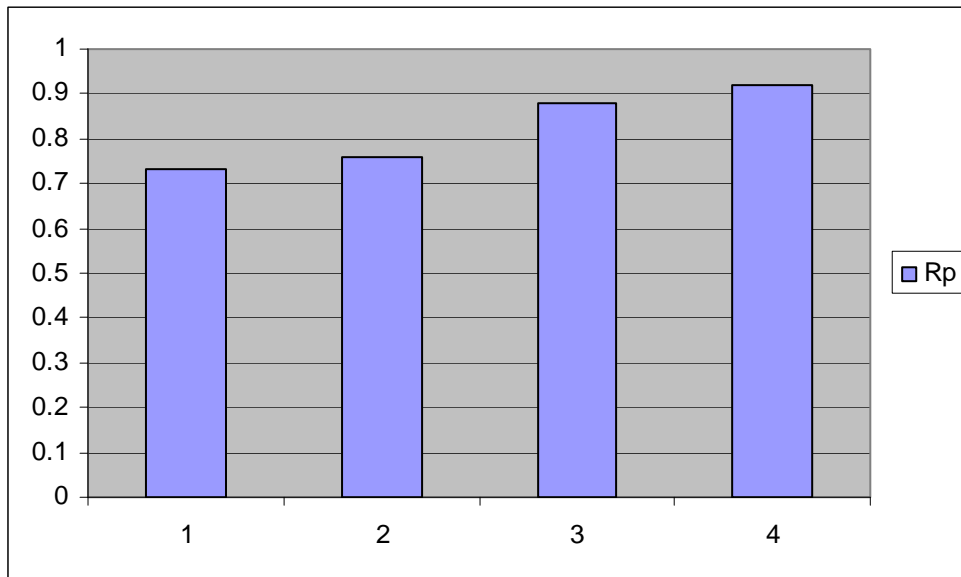


**Figure 9-3: R<sub>p</sub> of prediction from different calibrations sets: 1-4**

Figure 9-3 showed that R<sub>p</sub> was the highest at 0.92 when four sets of the calibration to one set of prediction were used. The poorest was at R<sub>p</sub> = 0.73 which was one set of calibration data to predict one set of glucose level. The figure also indicated that the larger calibration set to prediction set provided a higher correlation. The best correlation of R<sub>p</sub> was 20% higher than the poorest one.

Figure 9-4 shows the similar case which used rmsep for the comparison. The results showed that using more sets of data for calibration (in this case four sets of calibration data) obtained the lowest rmsep at 1.71mmol/l. The poorest one was at 3.62mmol/l, when the calibration used only one set.

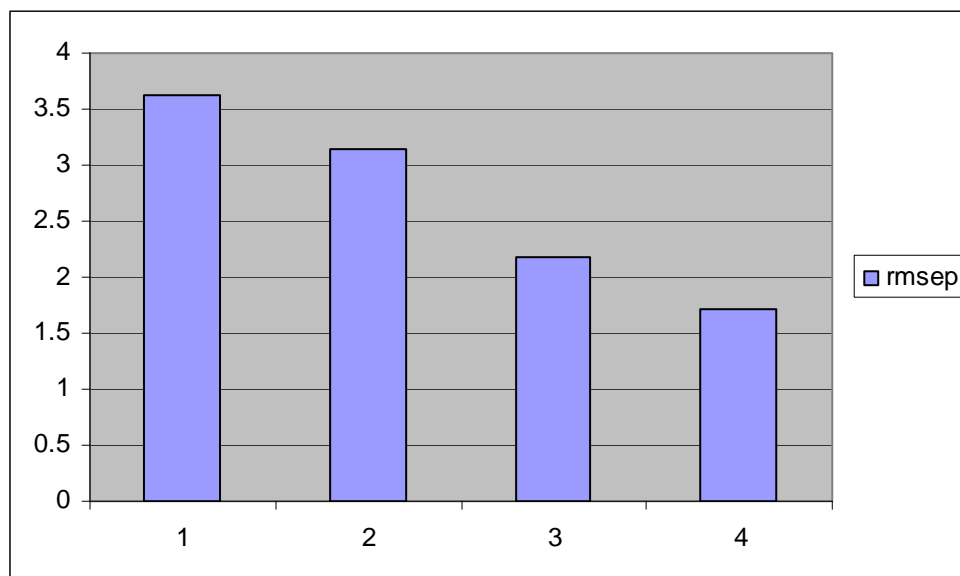


**Figure 9-4: rmsep of prediction from different sets of calibrations 1-4**

Both results for  $R_p$  and rmsep showed that a larger calibration size-to-prediction size could assist to obtain higher  $R_p$  and lower rmsep.

### 9.3 Discussion

The analysis demonstrated that with the larger calibration size, then the higher  $R_p$  and lower rmsep were under intra-subject analysis, in which the time span between the measurement of the calibrations and the prediction was within five minutes, i.e., the time span for NIR spectroscopic measurement was about five minutes for the five fingers. The results were from the 30 visits on different days within three months. The following further discusses how the calibrating sampling size could influence the prediction.

### **9.3.1 Sampling size for calibration**

The reliability of the non-invasive blood glucose measurement is still a matter to be resolved. The results of large calibration-to-prediction ratio showed higher reliability in prediction.  $R_p$  and  $rmsep$  could be improved by increasing the calibration size. The larger the calibration data set, the fewer unwanted influences to the prediction. However, the analysis was limited to ratios of 1:1 to 4:1 (sampling size of calibration data-to-prediction data).

The calibration size affected the predictability of the glucose levels. This was because the large data group could provide a more complete calibration model for the prediction. These calibration data were obtained from NIR spectra of different fingers, in which their finger-prick glucose readings were relatively equal at the time of the measurement, as reported in Section 7-2 of Chapter 7. The measuring of different fingers was able to increase the sample size for obtaining a more complete calibration model. This designation of the clinical trial also provided a situation for prediction without physiological effect (or minimum physiological effect) since the NIR spectroscopic measurements were completed within five minutes for the five fingers during each visit.

Ring fingers provided the best prediction. The little and middle fingers were the second and third best for NIR prediction, respectively. The poorest were the thumb and index fingers. The measurement of the thumbs might cause relatively larger physiological influence because of the larger thickness variations. The variance of the thumb thickness was the largest, and tends to be the most frequently

used for handling workload, after the index fingers. Thus, the physiological difference might be larger, so the prediction was poorer.

In Figures 8-9 and 8-10, all the  $R_p$  were higher than 0.8 and rmsep were lower than 2mmol/l, which meant that the correlation between the non-invasive NIR glucose prediction and the corresponding finger-prick glucose was within the clinically acceptable range of the Clarke Grid Error plot. According to the FDA, ISO 15197 shows that new blood glucose meter accuracy should be within 20% of the blood glucose concentration, in which blood glucose should be higher than 75 mg/dl (4.17mmol/l)(158; 160).

In Figure 8-10, the best rmsep was about 1.49mmol/l. The result was quite close to the result of the “finger-prick glucose level against the venous plasma glucose level” which the rmse was 1.40mmol/l, as shown in Figure 7-2. This showed that the non-invasive blood glucose prediction might be substituted for the finger-prick measurement, provided the calibration was within a short period of time, such as five minutes, which showed that no physiological boundaries exist.

Using fingers for the calibration helped to increase the sample size, and it also demonstrated that the tissue thickness boundary might not provide significant effect for NIR measurement. However, the physiological differences were a key influence after a long period of time, such as three months. This was why many non-invasive glucose predictions, in a short period following the OGTT, could reach a high predictability.

### **9.3.2 Calibration**

Calibration is a process to determine the relationship between the spectra and finger-pricked glucose levels. Many researchers have pointed out that calibration was important for the PLS prediction. Thus, they modified many different preprocesses, as they believed that the better the calibration, the better the prediction. In addition, the sampling size for calibration-to-prediction is important, too. This is because precise information for calibration can assist in obtaining precise predicted values. As mentioned, a larger sample size for calibration-to-prediction provided more complete information for model construction. Further, the broader data range covered also boosted up the calibration because the calibration was more complete, for a wider distribution.

### **9.4 Conclusions**

This chapter has showed the preliminary result of the calibration size-to-prediction size ratio, where the higher calibration size-to-prediction size provided the better predictability, but it might only be applicable to the ratios of 4:1, 3:1, 2:1 and 1:1, respectively. This also demonstrated that 3:1 of calibration size-to-prediction size is enough for obtaining  $R_p > 0.8$  and  $rmsep < 2$  mmol/l, while 4:1 was even better.

### **9.5 Future Work**

A large scale calibration-to-prediction experiment may need to be carried out to obtain a more detailed calibration to prediction size. Thus, a more precise ratio can be obtained. On the other hand, scientists may choose to follow the results of the ratio for their prediction analysis.

## **Chapter 10**

### **Physiological Evaluation by Inter- and Intra-subject**

Many scientists claim that intra-subject prediction is more accurate than inter-subject prediction, while some research groups have still obtained good, predictable results based on the inter-subject data. This shows some degree of contradiction to their claims. There is still no conclusion for whether NIR spectroscopic blood glucose measurement should be based on inter-subject analysis or intra-subject analysis. The following sections report and discuss the predictions of both inter-subject and intra-subject, with clinically supported data.

#### **10.1 Objectives**

- To compare the predictability of the inter- and intra-subject data;
- To evaluate the effects of physiology (including finger surface temperature) among inter- and intra-subject;
- To evaluate the effect of finger thickness and
- To assess the comparisons between inter- and intra-subject under this clinical trial.

## **10.2 Inter-subject glucose prediction**

This section shows the results of inter-subject prediction by PLS. All the predicted results of thumb, index, middle, ring and little fingers were scatter plotted in a Clarke Grid Error plot. The  $R_p$  and  $rmsep$  of the overall, predicted glucose levels were used for the comparison.

The data were obtained from the clinical trial of Stage 4, where calibration was formed by using the NIR spectra of the fingers, where fours were for calibration and ones were for prediction. The following sections report the results and further the discussion regarding the clinical trial which included both inter-subject data and intra-subject data.

### **10.2.1 Results**

The variances of the spectra are plotted in Figure 10-1 for the comparison between intra-subject and inter-subject among the same subject group. The figure shows that the variance of the inter-subject spectra was larger than the variance of the intra-subject spectra.



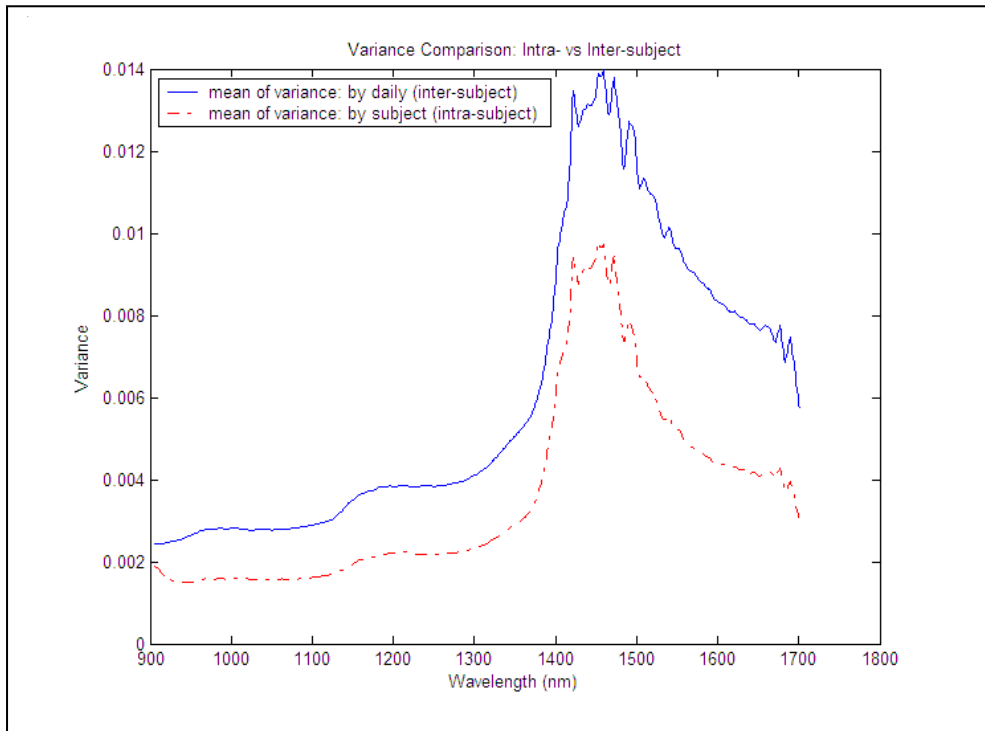


**Figure 10-1: Variance comparison between intra- and inter-subjects**

The figure was formed by using the average of the variance of the spectra from intra-subject (red dot line) and from inter-subject (blue solid line) for the comparison. The daily variance (inter-subject) was plotted by variance of the spectra of each subject, at the same scheduled visit (the time span was within one-half week). The subject variance (intra-subject) was plotted by the variance of the spectra of each subject of all their visits. The spectral peaks were approximately at the wavelength of 1450nm, where the spectra showed the highest variance. This indicated that OH was the most significant effect among the whole spectral range. This might be due to the high water (about 70% of H<sub>2</sub>O) content in the human body. This then would lead to the high variance.

In addition, higher spectral variance might have resulted in poorer prediction. According to the results of Stages 2 and 3, these showed that the larger spectral variance (without preprocess) had a poorer prediction rate. However, the results were based on different calibration sets of two different clinical trials. These results might have only reflected the difference between the long-term and short-term NIR spectroscopic measurement. Further discussion for the inter- and intra-subjects, under the same data sets, are reported in the following sections. Figures 10-2 to 10-6 show the scatter plot of the predicted glucose levels against the finger-prick glucose levels (by using inter-subject data).

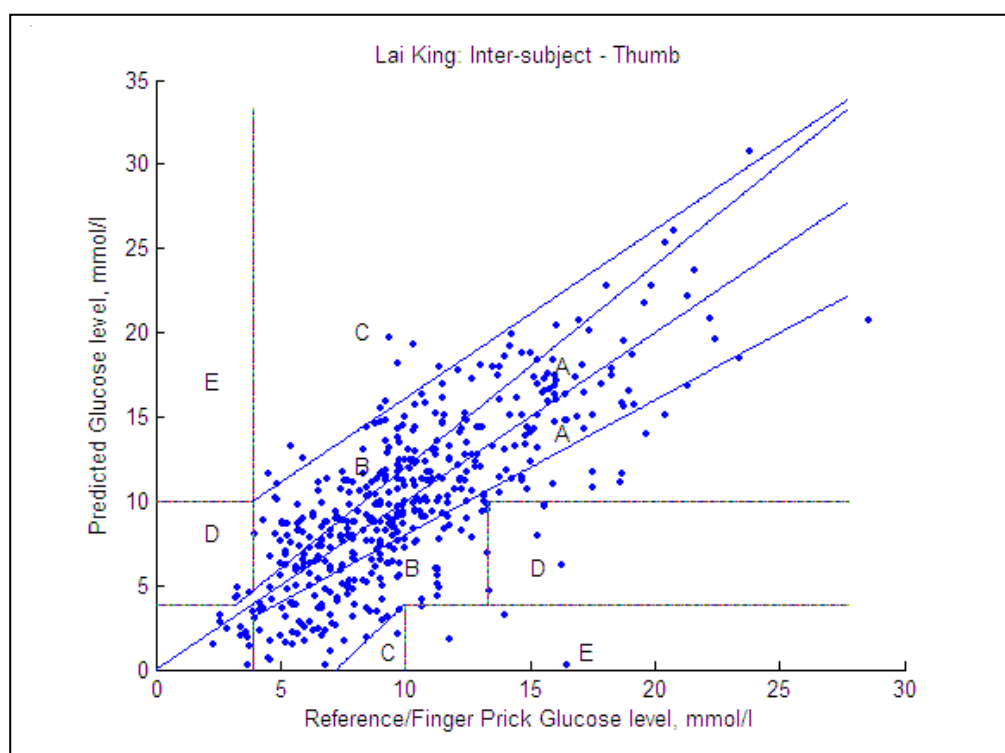


**Figure 10-2: Inter-subject: calibrated by index + middle + ring + little fingers to predict blood glucose level of thumbs.**

Figure 10-2 demonstrated the predicted glucose levels of thumbs, which were calibrated by the remaining four fingers of the left hand. The predicted glucose levels were widely spread and mainly fell in Regions A and B, which contained 90% of the predictions. About 60% was inside Region A. The  $R_p$  was 0.73 and rmsep was 3.66mmol/l. Region C contained 5% of prediction, Region D contained 4% and Region E contained 1%.

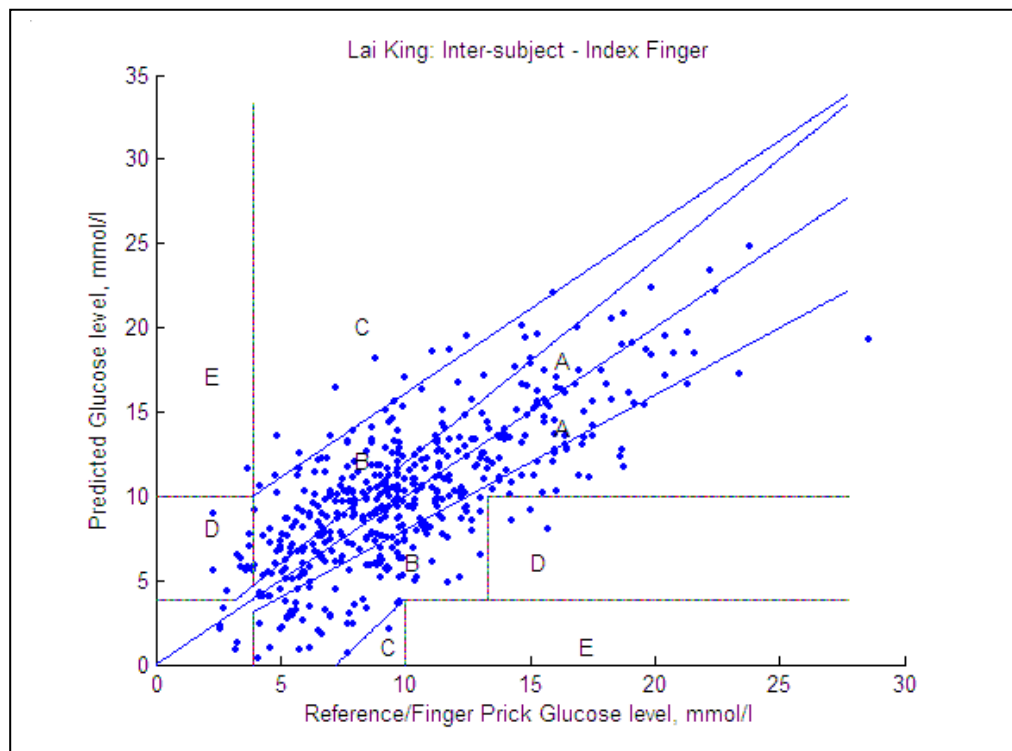


**Figure 10-3: Inter-subject: calibrated by thumb + middle + ring + little fingers to predict blood glucose level of index fingers.**

Figure 10-3 represented the scatter plot of the glucose prediction from the index finger. The results of  $R_p = 0.73$  and  $rmsep = 3.14\text{mmol/l}$ . The rmsep was

relatively smaller, but lower in  $R_p$ , too. 90% of prediction was within the clinically acceptable regions of A and B, in which 70% is in Region A.

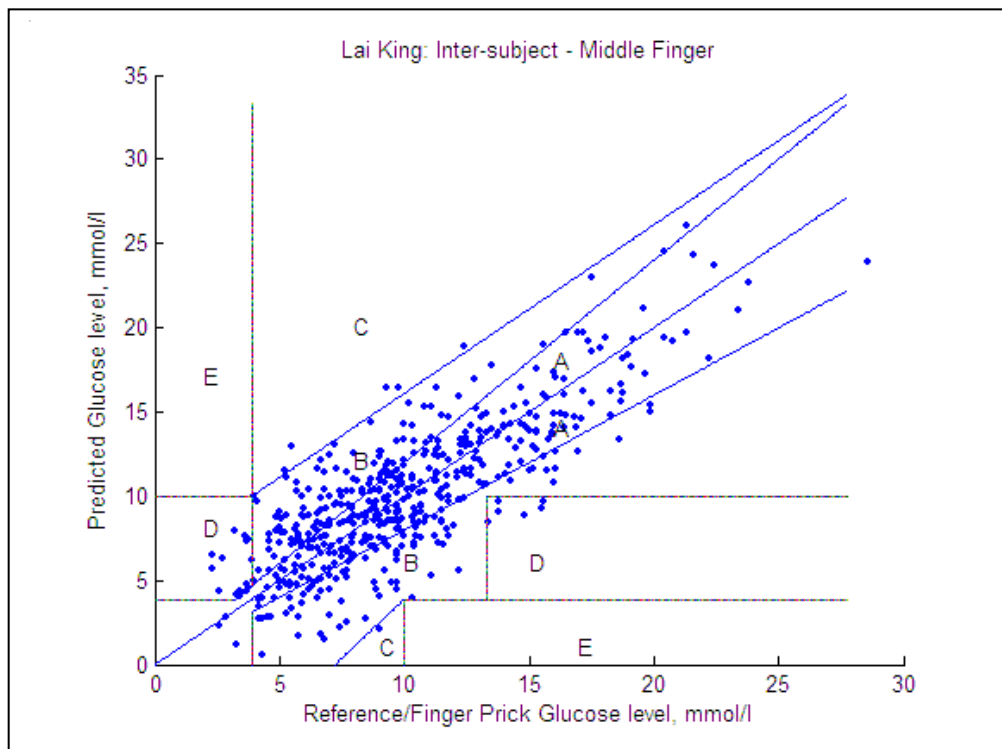


**Figure 10-4: Inter-subject: calibrated by thumb + index + ring + little fingers to predict the blood glucose level of middle fingers.**

Based on  $R_p$ ,  $rmsep$  and the scatter plot, it demonstrated that the index finger had higher predictability. For the middle fingers,  $R_p = 0.8$  and  $rmsep = 2.64$  mmol/l, as shown in Figure 10-4. The plot was more confined when compared with the plots of the thumb and index fingers. The predictions from the middle fingers showed that 95% of predictions were within the clinically acceptable regions, A and B, in which 65% were in Region A. Results showed that higher predictability was in the middle finger among thumbs, index and middle fingers.

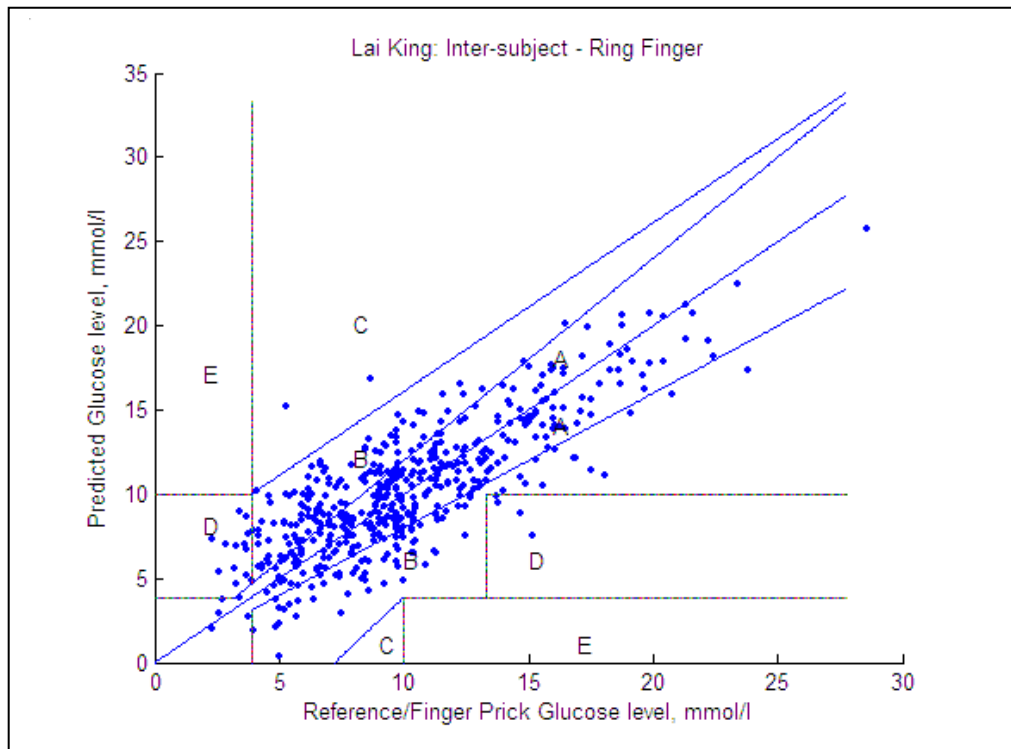


**Figure 10-5: Inter-subject: calibrated by thumb + index + middle + little fingers to predict blood glucose level of ring fingers.**

Figure 10-5 showed the scatter plot from predicted results of the ring fingers. Their  $R_p$  and  $rmsep$  were 0.80 and 2.60 mmol/l, respectively. This indicated that most of the predicted results were located in the clinically acceptable region. There were 98% of the predictions within the clinically acceptable regions, A and B, of which 70% is in Region A. Using ring fingers for NIR spectroscopic measurement might provide the best predictability, i.e., higher correlations and lower errors were found in ring fingers.

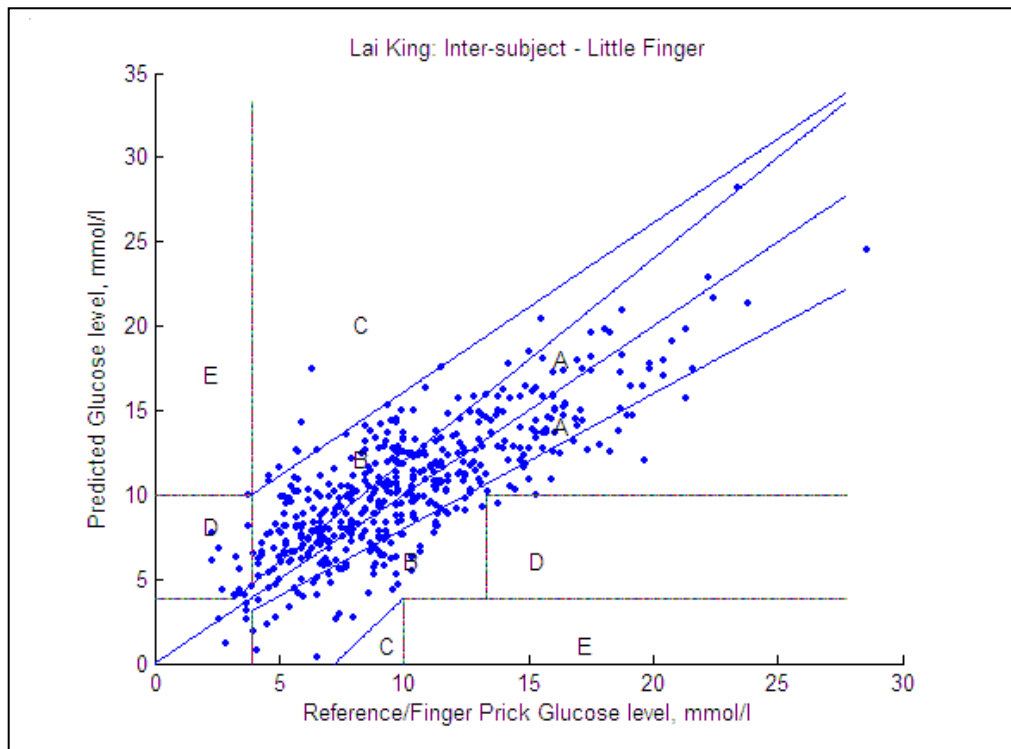


**Figure 10-6: Inter-subject: calibrated by thumb + index + middle + ring fingers to predict blood glucose level of little fingers.**

The little finger is the smallest finger in many cases. Figure 10-6 showed that the results from little fingers were worse than the results from the ring fingers. Of all of the predictions, 98% of the predictions were within the clinically acceptable region, A and B, of which 65% was in Region A.  $R_p$  was 0.78 and  $rmsep$  was 2.7mmol/l.

The summary of the inter-subject of glucose prediction using calibration of the other four fingers is shown in Figure 10-7. This shows the  $R_p$  comparison in which the time span between subjects was about one week.

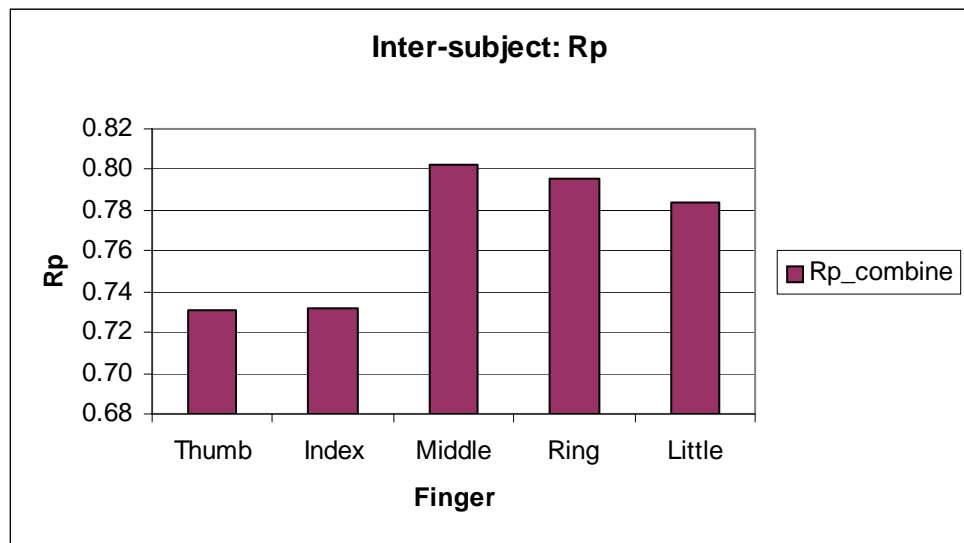


**Figure 10-7: Rp of predicted blood glucose level from each finger by using the other four fingers as the calibration.**

“Rp\_combine” represents the Rp of all the corresponding predicted and finger-prick glucose levels.

$$\text{i.e., } Rp\_combine = Rp(\text{day1}_t, \text{day2}_t, \dots, \text{day30}_t)$$

where  $\text{day}_x_t$  = predicted and the corresponding finger prick glucose level from the Day  $x$  (within one week time span) on the thumb, index, middle, ring and little fingers, respectively

$$x = 1, 2, \dots, 30$$

$t$  = thumb, index, middle, ring and little fingers

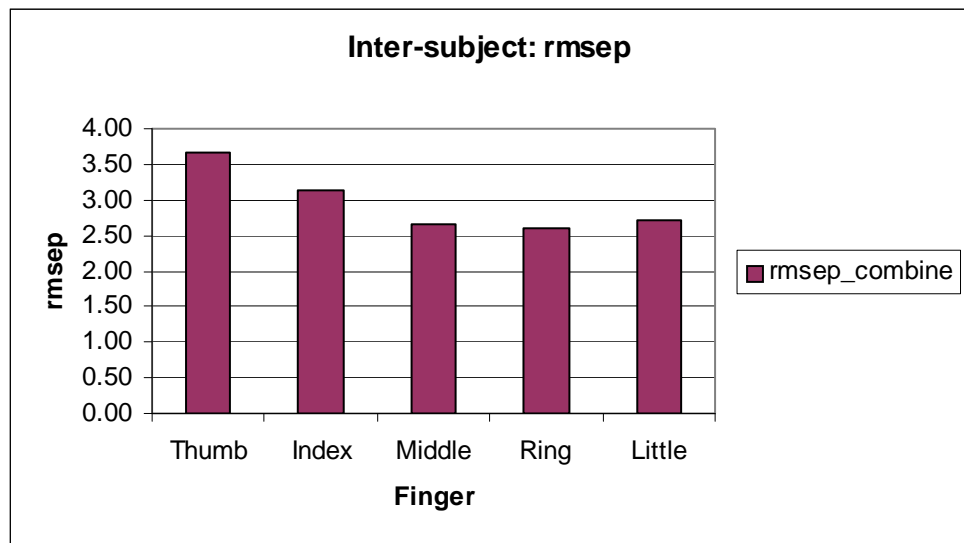


**Figure 10-8: RMSEP of predicted blood glucose level from each finger by using the other four fingers as the calibration.**

“rmsep\_combine” represents the rmsep of all the corresponding predicted and finger-prick glucose levels.

$$\text{i.e., } \text{rmsep\_combine} = \text{rmsep}(\text{day1\_t}, \text{day2\_t}, \dots, \text{day30\_t})$$

where day<sub>x</sub>\_t = predicted and the corresponding finger-prick glucose levels from the Day x (within one week time span) on the thumb, index, middle, ring and little fingers, respectively

$$x = 1, 2, \dots, 30$$

$$t = \text{thumb, index, middle, ring and little fingers}$$

The results of the R correlations coefficient  $R_p$  ranged from 0.73 to 0.80. The rmsep ranged from 2.49 to 3.52mmol/l. The correlations were lower than 0.8, which



provided less than 80% chance of the prediction. The following section discusses glucose prediction via intra-subject data.

### **10.3 Intra-subject glucose prediction**

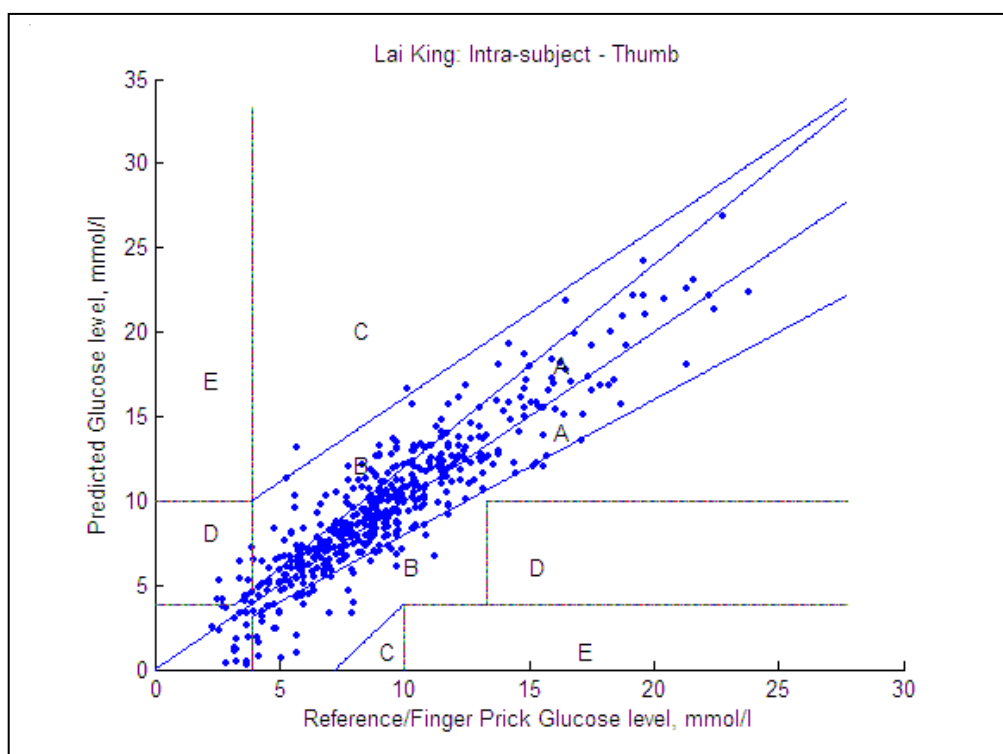
Intra-subject prediction used NIR spectra and blood glucose data of the individual subject from about a three-month period. The predicted blood glucose levels are scatter plotted in Figures 10-9 to 10-13 using the Clarke Grid Error plot.

#### **10.3.1 Results**

There are glucose level predictions via thumbs, as shown in Figure 10-9, while the calibrations were carried out by using spectra from the index, middle, ring and little fingers. Almost 98% of the predictions were located within the clinically acceptable regions of A and B. The major errors were due to the predictions of the lower glucose levels (under 4mmol/l). The predicted glucose levels located in Region D were classified as dangerous because of a failure in predicting the error according to the Clarke Grid Error plot. Rp was 0.9 and rmsep was 2.11mmol/l.

In comparison with the prediction from inter-subject data of the thumbs, Rp and rmsep of the predictions from the thumbs of the intra-subjects showed significant improvement of about 23% and 42%, respectively. This result initially showed that intra-subject data for the prediction was more stable and reliable among NIR spectroscopic blood glucose level prediction. Thus, research of non-invasive blood glucose by using NIR spectroscopy should use an intra-subject data set.

**Figure 10-9: Intra-subject, calibrated by index + middle + ring + little fingers to**



**predict blood glucose level of thumbs.**

According to Figure 10-9, Region D should not be used to detect the blood glucose level when measured by NIR spectroscopy. This method demonstrated difficulty in obtaining the low blood glucose levels, in which a large factor of error

also exists in many finger-prick glucose meters as well. The following figures continue to report the predicted results from different fingers, based on the calibration from other fingers.

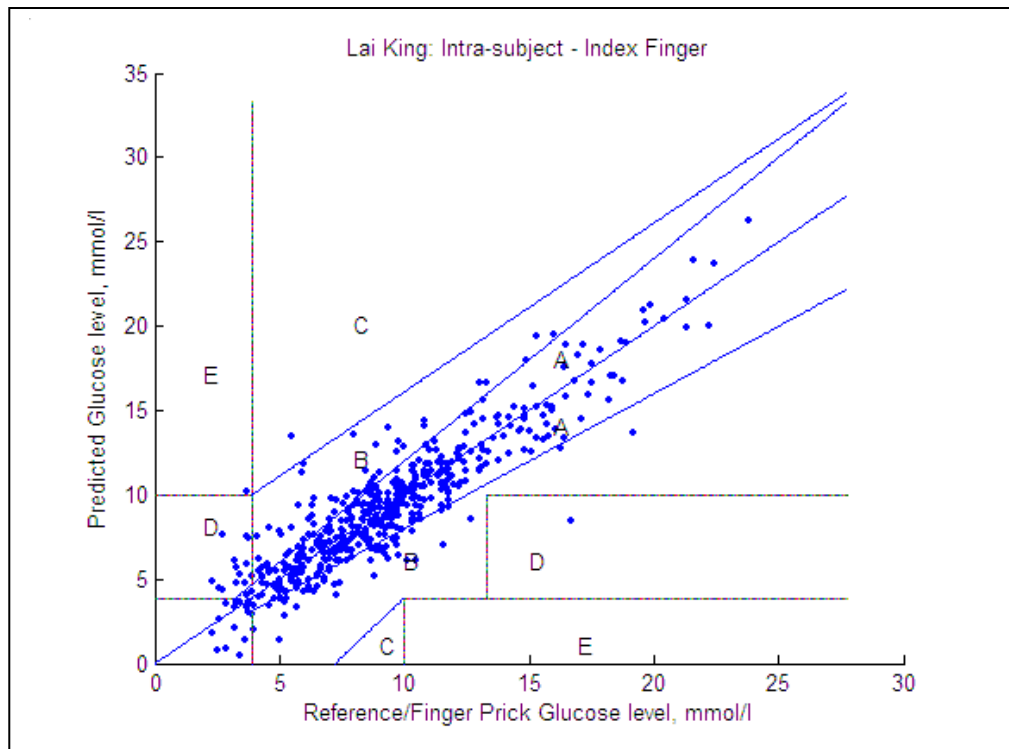


**Figure 10-10: Intra-subject: calibrated by thumb + middle + ring + little fingers to predict blood glucose level of index fingers.**

Figure 10-10 shows the predicted blood glucose levels against finger-prick blood glucose levels from the index fingers. Over 98% of the predicted points were located within the clinically acceptable regions, A and B. The hypoglycemia prediction was worse when compared with the predicted results of the thumbs.

However, the scatter points were more centralized, thus the  $R_p = 0.91$  and  $rmsep = 1.80$ , in which predictions were better than in the thumbs.

When compared with the prediction of the index finger of inter-subject, there was an improvement of 25% in  $R_p$  and 74% lower in  $rmsep$ . This reinforces the proposition that intra-subject data were recommended for the NIR blood glucose prediction.

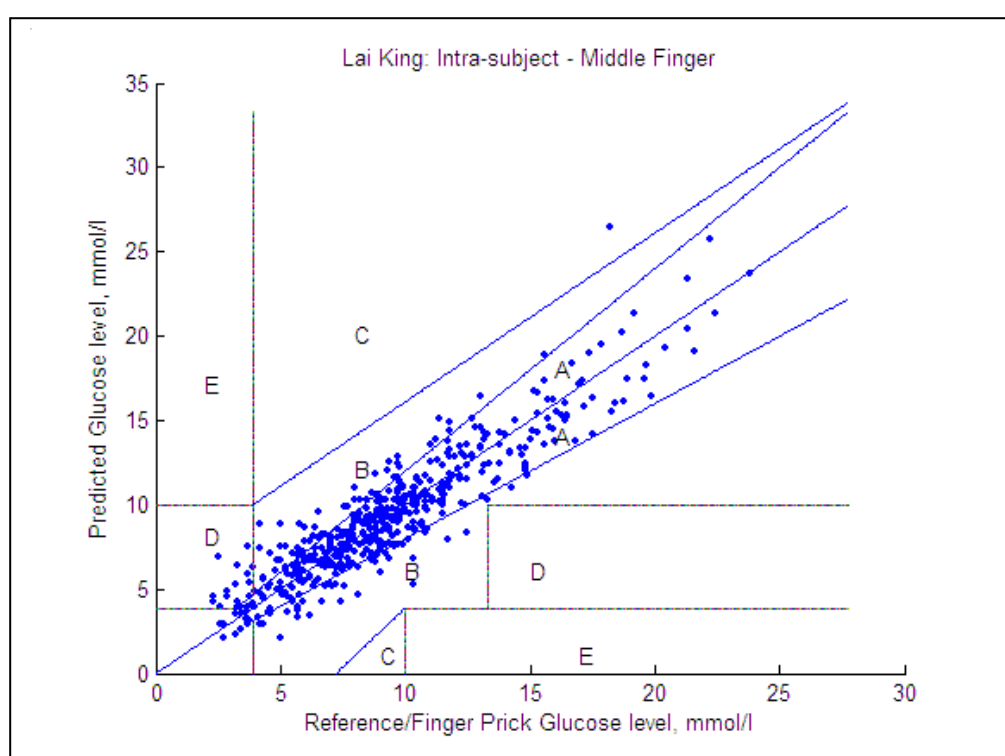


**Figure 10-11: Intra-subject: calibrated by thumb + index + ring + little fingers to predict glucose level of middle fingers.**

For middle fingers, Figure 10-11 showed that  $R_p = 0.93$  and  $rmsep = 1.61$  mmol/l. The results indicated that the  $R_p$  of the intra-subjects were 16% higher than that of the inter-subjects. It was also 64% lower than the inter-subject in  $rmsep$ .

Amongst the thumb, index and middle fingers, Rp and rmsep from the middle finger were the best ones. Despite the error in Region D, there was only one point outside the clinically acceptable regions of A and B.

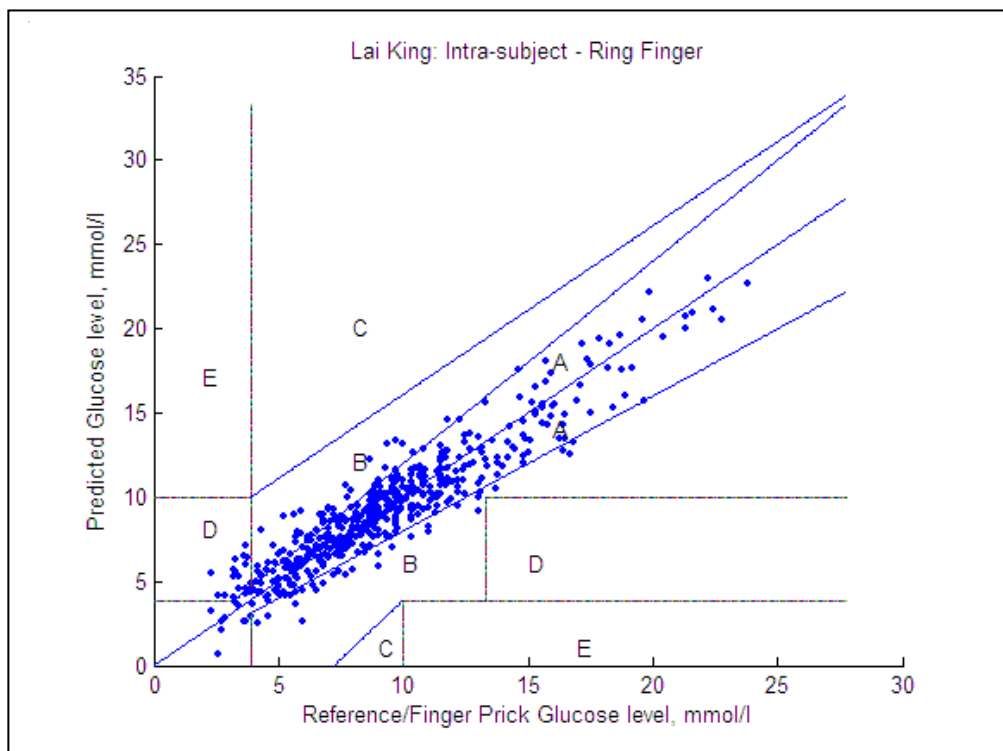


**Figure 10-12: Intra-subject: calibrated by thumb + index + middle + little fingers to predict glucose level of ring fingers.**

For the results from the ring fingers in Figure 10-12, values of  $R_p = 0.94$  and  $rmsep = 1.49\text{mmol/}$  were obtained. The  $R_p$  of intra-subject predictions was 15% higher than  $R_p$  from the inter-subjects. For  $rmsep$  comparison, intra-subject prediction provided 43% lower value than the inter-subject prediction.

The predicted results were mainly located in Regions A and B, while some of the predicted results were located in Region D (the hypoglycemia region). Despite the error in Region D, all of the predicted glucose levels were within the clinically acceptable regions. This demonstrated that non-invasive blood glucose by NIR spectroscopic measurement was mostly achievable if using the ring fingers. It also indicated that more accuracy occurred in the non-hypoglycemia region.

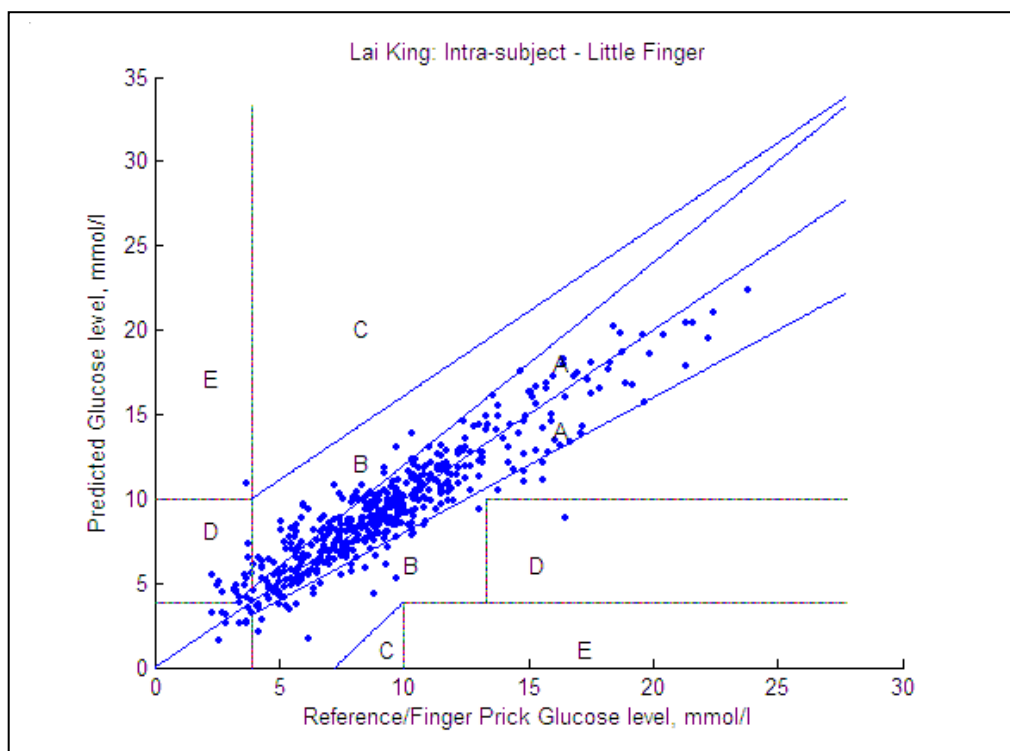


**Figure 10-13: Intra-subject: calibrated by thumb + index + middle + ring fingers to predict glucose level of little fingers.**

Figure 10-13 showed that  $R_p = 0.93$ , which was 16% higher than the prediction from the inter-subject study. Their results of  $rmsep = 1.54\text{mmol/l}$ , in which the intra-subject prediction provided was 43% lower than the inter-subject's

prediction (rmsep = 2.7mmol/l). Predictions of little fingers showed the second best of the predictions among the five fingers.

Regarding intra-subject data, all the predictions (according to results of Rp and rmsep) were better than the inter-subject's results. This demonstrated that using intra-subject data was more achievable than using inter-subject data for prediction among NIR spectroscopic non-invasive blood glucose measurements.

## **10.4 Discussion**

The results implied that using intra-subject data for non-invasive blood glucose prediction was more achievable. The design of the clinical trial and its arrangement demonstrated that it was suitable for the comparison between intra- and inter-subjects, where the same data sets had been used. The arrangement helped to limit many effects from physiology and environment so that they could be properly compared with each other. The following sections discuss the details for the intra- and inter-subjects' prediction.

### **10.4.1 Intra- and inter-subject**

Intra-subject analysis is superior to inter-subject analysis, theoretically. However, there is no clinical proof that using intra-subject data is better than using inter-subject data for blood glucose prediction. This is due to the difficulty in identifying the many uncertain parameters, especially the influence of physiology. The clinical trial of Stage 4 was designed to limit the effects of physiology (further discussion for

clinical data analysis is reported in Table 10-1). The result was clinically demonstrated that using intra-subject data provided a smaller error, i.e., better prediction. Conversely, many researchers still use the inter-subject data for NIR non-invasive blood glucose analysis. The physiological difference was greater in the inter-subject cases. This led to the high variation which was caused by different interferences occurring, as shown in Figure 10-1. This demonstrated that the variance of the spectra from inter-subject data was larger, which showed the data might contain more varied signal accumulations. Thus, this may potentially lead to a higher prediction error.

The clinical trial was carried out under a constant environment, in the same location. Thus, the only remaining deviation might have been due to the subject or between subjects. This was mainly from the physiological differences of intra- and inter-subjects. With this clinical trial and data arrangement, both intra- and inter-subjects were able to make comparisons since many uncertainties had been minimized for the predictions.

Predictions from ring fingers received the highest  $R_p$  and lowest rmsep in both intra- and inter-subjects' cases. One possible reason was due to the fact that over 85% of the finger-prick blood glucose reading was obtained from ring fingers. Although many finger-prick readings between various fingers were smaller than the "own meter error," NIR measurement for the calibration might reach a closer correlation and smaller error for ring fingers. In addition, ring fingers in this clinical trial provided the smallest thickness variations. Therefore, the internal physiological



influence due to blood vessels, body fluids and other component differences might be relatively small, too.

The change of the blood/tissue components in fingers might affect NIR spectroscopic glucose measurement. More differences in the components might cause higher variations of NIR absorption and reflection. Thus, more noise and higher variation might be occurring in the inter-subject readings.

#### **10.4.2 Time drift and machine drift**

NIR spectroscopic measurement for the five fingers was done within five minutes, so the time drift and machine drift effect were also only within five minutes, but this happened for 30 different subject measurements. In order to minimize these drifts, the NIR spectra were obtained from 15 sets of spectra per each finger of each subject where one set of the data was obtained from the average of 64 individual spectra. Ten sets of data (fourth to thirteenth set) from the 15 sets of spectra were used to produce the final average set. Thus, time drift and machine drift effects should be kept to a minimum, although this small effect could also be eliminated by PLS, as stated in the experiment for Stage 1.

Therefore, non-invasive blood glucose prediction via NIR spectroscopy was shown to be highly achievable in a short period of time (within five minutes), since the physiological effects were relatively small as well.

### **10.4.3 Physiological effect**

For comparisons between intra-subject and inter-subject data, time drift was not taken into consideration since it had been eliminated or reduced by PLS, as reported in Chapter 4, and reduced by large data averaging, as stated in Section 10.4.4. Thus, the physiology became the major effect since the tissue/skin of the fingers could not have a significant effect on NIR, as stated in Section 10.4.1.

The results of  $R_p$  and  $rmsep$  of the inter-subject data were poorer than for the intra-subject data. Their predicted values were widely scattered, as shown in Figures 10-1 to 10-5. This was due to the large variations of the physiology amongst different subjects. This led to the conclusion of the clinical trial, which clearly showed that the use of NIR spectroscopy for intra-subject data could provide a more precise blood glucose prediction.

The physiological differences are mainly due to individual metabolism, blood components and other bodily fluid circulations for body regulation. The NIR spectrometer mainly detects the OH- and CH- groups. These elements can be found everywhere in the human body. Thus, differences in components affect NIR spectral signal measurement. Therefore, it is hard to get the blood glucose level via NIR spectroscopy, particularly for a highly different physiological status.

### **10.4.4 NIR spectra vs. body tissue**

NIR spectra were obtained by NIR light being shined onto the measurement area, while a partial light had been reflected onto the spectrometer. The light that reflected back had been absorbed and scattered by the body tissue and body fluid, including

blood and other body components. The light being reflected back to the spectrometer contained different information from the area. The PLS helped decode this information from the acquired NIR signal. One part of the PLS analysis was to maximize the correlation between the measured NIR spectra and the corresponding finger-prick glucose levels, and the other part was to form a calibrated model for glucose predictions.

For inter-subjects and intra-subjects, by using the different thickness of the fingers for the calibration, the results showed that the thickness of the tissue of the finger might not have affected the NIR reading significantly. From the Clarke Grid Error plot from Figures 10-1 to 10-5, over 80% of the predicted glucose levels were located inside the clinically acceptable regions, A and B. This demonstrated that the inter-subject prediction was also clinically acceptable.

Although, it had been reported that thickness of the tissue was one of the key factors affecting NIR non-invasive blood glucose prediction, a more specific, major factor was the physiological differences, as well as the internal fluids of the lipids and the proteins in the blood and body tissues. This explained why many of the experiments which used dead animal skin as the boundary obtained a high correlation between the reference glucose and the predicted glucose. There was no metabolism occurring. The skins existed in a state of constant influence with regards to the glucose prediction. Thus, it was easily eliminated.

#### **10.4.5 Effect of finger thickness**

As mentioned, there was no significant effect caused by the finger thickness. This was because the predicted blood glucose levels were obtained by calibrating the NIR measurement of different fingers, which were varied in thickness. The results were supported by Raghavachari, who stated that NIR was poorly absorbed by the body's tissues (8), thus the intervention by the body tissue was limited. Therefore, the result was more likely due to differences in physiology instead of finger thickness.

The average thickness of each NIR measured finger had been recorded by the micrometer. The readings were used to check the average finger thickness. This was because the finger thickness might have played an important role in affecting the NIR reading (115). The results of the clinical trial from Stage 4 demonstrated that the thickness of the finger might not have had a major effect on NIR glucose predictions, but the difference of internal fluid, or the difference of physiology, might have resulted in a greater influence to the NIR glucose prediction over a longer period of time. This was because there were high predicted results obtained from various fingers with different thicknesses, and the results were also close to each other.

This consequently indicated that the effect of the different finger thickness was not significant for NIR measurement with PLS analysis, in which the glucose prediction was calibrated by using NIR spectra from different fingers with various thicknesses. The analysis also limited the physiological effects for the comparison.

The study also showed that a higher error was associated with hypoglycemia (when blood glucose was lower than 4 mmol/l, prediction was poor). This might have been due to the relatively lesser amount of data and the relatively greater noise for the relatively smaller amount of glucose components in the tissue and body fluids, as mentioned by Maruo et al. (87).

#### **10.4.6 NIR spectra by PLS**

It is difficult to compare NIR spectra between inter-subject and intra-subject blood glucose prediction. This is because the spectra taken from the subjects came from different groups of subjects or were taken from the same group from different time slots. This may lead to the comparisons of two separate groups, in which many uncertain factors would have been obtained, such as different physiologies (the significant effect on NIR blood glucose measurement). As a result, it may lead to wrongly comparing the blood glucose levels under many different parameters. i.e., for glucose levels comparisons between inter- and intra-subjects, the NIR spectra of A may be taken to compare with the NIR spectra of B, with different background noise/variables. Thus, NIR spectral data cannot be randomly separated into two groups for comparison because many uncertain factors exist due to the small amount of glucose in blood.

The clinical trial of Stage 4 recruited 26 volunteer subjects. Every subject was measured 30 times. After the NIR spectra were obtained, as well as the corresponding finger-prick glucose levels, the data sets became 26 x 30 sets of data arrangement, i.e., 26 subjects with each individual having 30 sets of spectra and

finger-prick readings. Each set of data contained five sets of spectra from the corresponding five fingers on the left hand of each subject and one set of finger-prick glucose levels. Table 10-1 shows the data set arrangement.

The predictions were carried out under the same group of subjects and their readings were obtained under same conditions. Therefore, the only two factors left, which might explain the differences between intra- and inter-subject predictions, were the physiological differences between the subjects, and the physiological variations between the individual over the three-month timeframe.

**Table 10-1: Data arrangement of stage 4 clinical trial**

Subject 1, day 1	Subject 2, day 1	...	...	Subject 26, day1
Subject 1, day 2	Subject 2, day 2	...	...	Subject 26, day 2
⋮	⋮	⋮	⋮	⋮
⋮	⋮	⋮	⋮	⋮
Subject 1, day 30	Subject 2, day 30	...	...	Subject 26, day 30

Although most of the conditions were the same, the signals between subjects (inter-subjects) were highly varied, which caused poor glucose predictions. Under these circumstances, the data for either intra-subject or inter-subject could be formed as reported below.

For inter-subject prediction, by applying PLS to each row, the glucose prediction of the inter-subjects of each measurement day was calculated. Then, the

predicted glucose levels were used to calculate the Rp and the rmsep. For intra-subject prediction, a similar action was carried out; while the PLS was applied to each column, the predicted glucose levels were then used for the Rp and rmsep calculations. This demonstrated that the above-mentioned data arrangements could have provided a suitable comparison for NIR glucose prediction between two different things, such as data from inter- and intra-subjects.

#### **10.4.7 Temperature effect**

The results showed that even though temperature affected the NIR measurement (84), the effect could have been reduced by the designed data arrangement, as stated in Table 10-1, and by PLS prediction using the Savgol preprocess. This arrangement not only weakened the effect of temperature, but the physiological influence as well.

Some researchers showed that the temperature effect could be reduced by controlling the temperature in the area of measurement. However, temperature control may cause another reading error in the NIR measurement, which was due to the heating radiation of the equipment.

In an experiment from Arimoto et al. (151) through glucose solutions, various temperatures showed an effect on the absorbance of the NIR spectra. Their results showed that PLS calibrations under different temperatures could eliminate the effect of temperature in NIR measurement for glucose solutions prediction. However, it was complicated for human subject. Therefore, many research groups tried to standardize the surface temperature for higher predicted results (125; 126;

161). It was found that the temperature effect on NIR measurement through human subjects might not be easily eliminated.

The results of this chapter showed that high  $R_p$  and low  $rmsep$  were obtainable by minimizing the physiological influence, including that of temperature. This clearly demonstrated that the smaller the physiological influence, the higher the prediction accuracy that could be attained. Thus, naturally consistent temperatures from intra-subjects (i.e., lesser physiological impact) for non-invasive blood glucose measurement would be recommended. However, physiological effects, over a long period of time, exist in humans. This showed that NIR spectroscopic measurement for blood glucose levels should only be applied for short-term measurement, unless no significant physiological effects existed.

## **10.5 Conclusions**

The specially designed data arrangement and clinical trials provided a clear, clinical comparison between inter- and intra-subject. The analysis showed that NIR spectroscopic measurement should use intra-subject data for prediction where higher  $R_p$  and lower  $rmsep$  are obtained.

The physiological difference (including temperature) affected the predicted results. Thus, only short-term (within five minutes in this case) non-invasive NIR spectroscopic measurement could be achieved. Long-term NIR blood glucose measurement could only succeed without physiological influence.



The results also showed that finger thickness might not have provided a significant effect for NIR spectroscopic measurement, but that the blood or other body fluids could have been responsible for errors due to metabolism.

## **10.6 Future work**

There is still a great demand for an accurate, non-invasive method for measuring the blood glucose of diabetic patients, both on a daily basis and over the long term. The data in this thesis indicate promising directions of research. It is hoped that by reducing confounding factors, such as finger thickness and the physiological differences, more accurate methods of glucose measurement can be developed to help clinicians and patients.

Furthermore, a large scale experiment to check the limitations for the calibration-to-prediction ratio should be carried out. This can help scientists to narrow their focus for long-term NIR measurement and overcome the existing boundaries of long-term NIR measurement, due to physiological effects

# Chapter 11

## Conclusions

### 11.1 Introduction

Highly accurate, consistent non-invasive blood glucose measurement still cannot be achieved due to the physiological differences within subjects over the long-term, as well as the physiological differences between subjects. It has been demonstrated that by using PLS, and comparing the predictability by using  $R_p$  and  $rmsep$ , intra-subject prediction was more achievable for NIR non-invasive blood glucose research.

Short-term measurement may be more easily achieved when compared with long-term measurement, except no physiological effects will exist.

In addition, the results also established that the calibration size should be larger than or equal to the ratio of 3:1 (calibration size-to prediction size) if  $R_p$  needs to be higher than 0.8 and  $rmsep$  to be lower than 2mmol/l for short-term measurement.

NIR glucose measurement via fingertips was achievable. The background interference could be reduced by using a more specific measurement such as fibre optics with a small probe and by using the reflection method.

The effect of physiology from inter-subject data was greater than that from intra-subject.

### 11.1.1 Objectives of each stages

There were four stages for non-invasive blood glucose research by using NIR spectroscopy described in this thesis. They were tested by using glucose solutions, followed by three different clinical trials.

#### Stage 1: Ground Work among Glucose Solutions

- To find out the relationship of the NIR spectra and the glucose concentrations;
- To evaluate the repeatability of the NIR measurement in glucose concentrations over a long period and
- To study time drift and machine drift effects for glucose measurement in the long term.

#### Stage 2: Studies among Diabetics

- To find out the relationship between NIR spectra and blood glucose levels from diabetic patients;
- To evaluate the possibility of NIR measurement for *in vivo* glucose measurement and
- To find out a suitable method for the NIR measurement.

### Stage 3: Short-term Measurement among Non-diabetics

- To evaluate NIR measurement amongst non-diabetic subjects with meal tolerance;
- To evaluate the possibility of using NIR glucose measurement in non-diabetic subjects;
- To evaluate any improvement of the non-invasive blood glucose measurement by using a modified spectrometer and
- To undertake a preliminary study of the physiological effect over a short-term period.

### Stage 4: Longitudinal Measurement for Diabetics

- To find out if intra-subject measurement is better than inter-subject for NIR prediction;
- To evaluate the reflectance NIR measurement via a fibre optic probe;
- To evaluate new clinical trial methods for the comparison of both inter- and intra-subjects;
- To evaluate intra-subject prediction in the long term;
- To compare preprocesses for PLS predictions among PDS and Savgol by using simple mean-centred preprocess as a basis;
- To evaluate whether high variation spectral signals lead to poor prediction;

- To confirm the preprocess choice of Stage 3 for NIR spectroscopic measurement by PLS prediction;
- To find out the calibration sets required for the prediction of non-invasive blood glucose prediction via NIR spectroscopic measurement;
- To compare the sampling size ratio needs;
- To report the predictability under various calibration sets to the prediction set;
- To compare the predictability of the inter- and intra-subject data;
- To evaluate the effect of physiology (including finger surface temperature) among inter- and intra-subjects;
- To evaluate the effect of finger thickness and
- To assess the comparisons between inter- and intra-subject under this clinical trial.

### **11.1.2 Summary of significant results**

1. The results demonstrated clinically that intra-subject prediction was more reliable than inter-subject prediction for NIR spectroscopic non-invasive blood glucose research;
2. Short-term prediction (within five minutes in this case) was achievable while long-term measurement needs to be improved;
3. The most common, major errors for NIR spectroscopic measurement were due to physiological differences;

4. The tissue thickness might not generate a significant effect for the prediction, but the effect might be due to metabolism and physiological differences. This explains why the measurement using dead skin/tissue by other scientists was able to reach higher predictability;
5. Based on Chapter 8, it could be concluded that not all preprocesses were suitable for NIR glucose measurement. Savgol is one of the most suitable preprocesses for PLS prediction among non-invasive blood glucose measurement via NIR spectroscopy;
6. The larger the calibration sampling size to prediction sampling size, the better the prediction was in terms of  $R_p$  and  $rmsep$  comparison. However, this case was limited to ratios of 1:1, 2:1, 3:1, 4:1 (calibration sampling size : prediction sampling size) and
7. The design of the clinical trial and the data arrangement of Stage 4 took into account different situations among intra- and inter-subject data for NIR spectroscopic blood glucose measurement.

### **11.1.3 Conclusions**

#### Stage 1: Ground Work among Glucose Solutions

From the experiment, the results showed that the higher the glucose concentration, the lower the spectral absorbance was in the spectrum. However, NIR spectroscopic measurements deviated due to machine drift and time drift after two months. This caused errors in NIR spectroscopic measurements. These drifts could be reduced or eliminated by adoption of the PLS technique.

NIR spectroscopic measurement under PLS analysis showed promising results on the glucose solution test in both short- and long-term experiments. Thus, it might be applicable for NIR measurement in diabetic patients.

#### Stage 2: Studies among Diabetics

NIR Blood glucose measurement seemed partly achievable in this stage. However, high physiological noise affected the predicted results. The use of preprocesses might not provide appropriate assistant to PLS in glucose predictions. Time lag influence between the glucose level from venous arm and finger-prick sampling might also affect the prediction. The results demonstrated that blood glucose in diabetic patients was measurable using NIR, with necessary, further fine-tuning.

Due to many uncertainties from the physiological effects among different diabetic patients and the two-month clinical trial duration, a short-term clinical trial might be helpful in reducing the physiological effects, in which consecutive measurements should be carried out.

#### Stage 3: Short-term Measurement among Non-Diabetics

This prediction involved data of intra-subject (within subject). It showed that when intra-subject data were included for the predictions, the predicted results seemed more consistent. This was because the noise caused by the inter-subject effects were relatively larger. This supported the thesis that non-invasive blood glucose measurement should apply to data for intra-subjects, in which physiological effects

were relatively small. The results also showed that NIR measurement was applicable for non-diabetic people, while the range of glucose levels was narrower.

The NIR light was semi-covered for limiting the effect from the surrounding environment. However, the results showed no significant improvement because the existing visible/shorter wavelength light in the surrounding area did not affect the NIR light. A wider spectral signal could have provided a more stable result, in which a wider spectrum would have averaged the noise, reducing the effect. The noise signals (many ripples and spectra deflection happened) mainly occurred in the range of 1381 to 1701nm, which was blocked by the fingers.

Physiological effects are unpredictable and vary due to the body's reaction to the environment. Thus, considerations of physiology for NIR non-invasive blood glucose measurements are needed. The next stage mainly focused on physiological effects and was measured by the reflectance approach.

#### Stage 4: Longitudinal Measurement for Diabetics

Non-invasive NIR spectroscopic blood glucose measurement is hardly repeatable for the long-term due to physiological effects. Reflectance NIR measurement is recommended for *in vivo* non-invasive blood glucose measurement. The results of the intra-subject study seemed more applicable than the results of the inter-subject study from Stage 2 in NIR glucose prediction. The sampling data arrangements were applicable for both inter- and intra-subject comparisons under the same situations.



In summary, PLS prediction with a Savgol preprocess should be used for reflectance NIR spectroscopic blood glucose measurement via a probe. The smaller variance of the spectra after preprocessing might not give a better predictability if an inappropriate preprocess was chosen. However, a small variance still represents a better prediction. It supported the result of the preprocess comparison of Stage 3.

This showed the preliminary results of the calibration size-to-prediction size ratio, where the higher calibration size to prediction size provided better predictability, but it might only be applicable to the ratios of 4:1, 3:1, 2:1 and 1:1. This also demonstrated that 3:1 of calibration size-to-prediction size ratio was enough for obtaining  $R_p > 0.8$  and  $rmsep < 2$  mmol/l, while 4:1 was even better.

The specially designed data arrangement and clinical trial provided a clear, clinical comparison between inter- and intra-subject studies. The analysis showed that NIR spectroscopic measurement should use intra-subject data for prediction where higher  $R_p$  and lower  $rmsep$  were obtained.

Physiological differences (including temperature) affect the predicted results. Thus, only short-term (within five minutes in this case), non-invasive NIR spectroscopic measurement could be achieved. Long-term NIR blood glucose measurement could only succeed without physiological influences. The results also showed that finger thickness might not provide significant effects for NIR spectroscopic measurement, but that significant effects might be due to blood or other body fluids in the context of metabolism.

## Appendix A: Apparatus and Equipment

### A.1 NIR spectroscopy - NIR-128L-1.7-USB

The spectrometer used was purchased from Controls Development, with the following specifications:

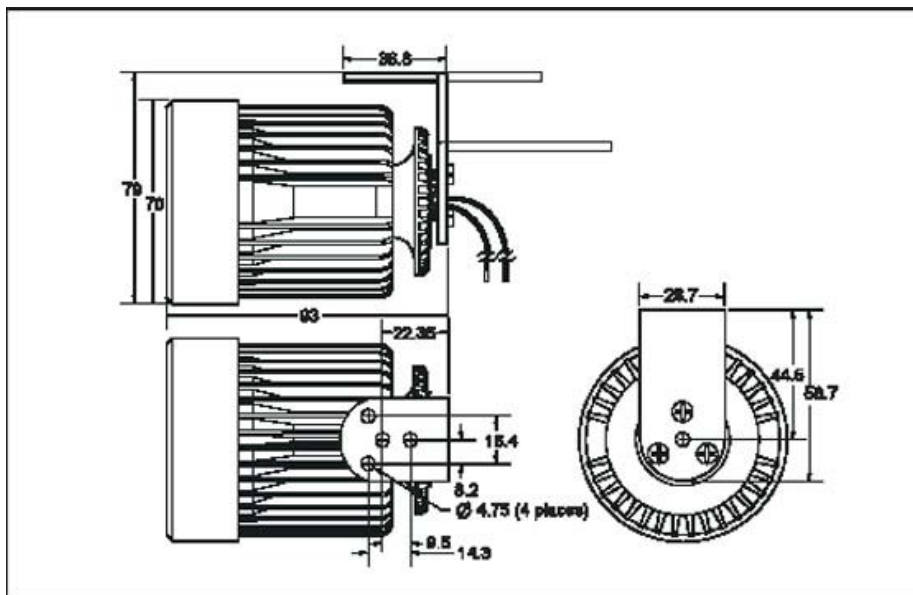
Wavelength range	905-1701 nm
Wavelength Stability	Better than 0.05 nm over 48 hours.
Input Fiber	400 micron core Low OH 50 micron slit standard
Optics	Fast f/2.0 or f/3.0 proprietary design
Detector	128 element InGaAs Array, temperature stabilized
Stray Light	<0.1%
Photometric Stability	±0.05%, over 60 minutes, light source with optical feedback ±0.15%, over 60 minutes, light source without optical feedback
Integration Time	6 micron-seconds to 0.5 second
Outputs	Modular connector, trigger, two strobes, light source shutter control and two fiber optic switch controls
Interface	USB
Computer Type	386, 486 and Pentiums IBM compatible
Power Requirements	85 - 265 VAC; 120 - 870 VDC; 47 Hz - 63 Hz
Size	11.2" L x 3.5" H x 7.5" W
Weight	Approximately 8 pounds (3.6 kg)

Information obtained from Controls Development

## A.2 Tungsten Halogen Light

The tungsten halogen light was purchased from Controls Development in conjunction with the spectrometer. The specifications are shown below.

1. Model: TH/DR, 35Watt with gold reflector in a cast aluminum housing.
2. 2" diameter's light beam is provided.
3. Rugged Aluminum Construction
4. Multi-Position Mounting Bracket



Picture quoted from Controls Development

### A.3 Optical Stand

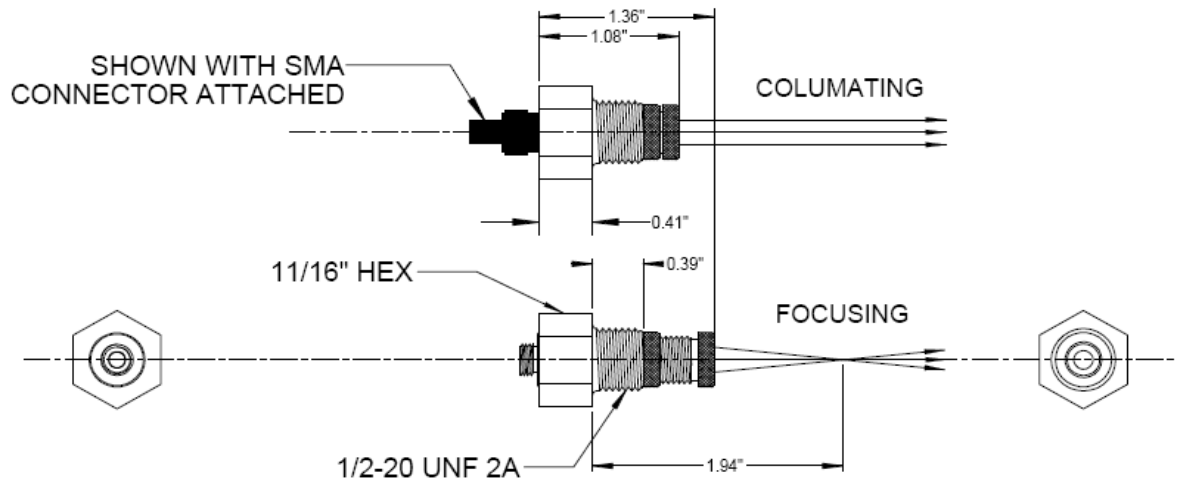
The Stand is used to connect to the fibre optics focusing lens and to fix the Tungsten Halogen Light for the sample measurement. Supplied by Controls Development.



Picture quoted from Controls Development

## A.4 Fibre Optic Focusing Lens

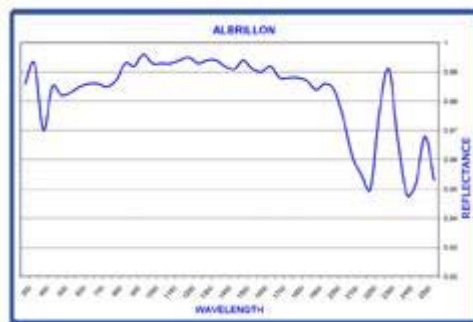
The lens integrated with the fibre optic to connect to the spectrometer for signal receiving and transmission. The design of  $\frac{1}{4}$ " aperture, rugged stainless steel housing with the dimensions are shown below.



Picture quoted from Controls Development

## A.5 White Reflectance Reference

The white reference is made of Halon/Albrillon surface which provides a spectrally flat surface for the light reflection. 50mm diameter with reference data are shown below.



CIE COLOR VALUES			
	Y	x	y
A; 2	98.40	.4479	.4078
C; 2	98.38	.3105	.3168
D; 2	98.38	.3131	.3297
A; 10	98.40	.4516	.4061
C; 10	98.35	.3108	.3195
D; 10	98.36	.3142	.3314

Picture quoted from Controls Development

## A.6 Reflection Probe - SMA905

The reflection probe was purchased from Avantes which connected between a tungsten halogen light and the spectrometer for the reflectance measurement. It contains 7 fiber optics for the light transmission and reflection purposes as shown on the specification below.

<b>Fibres</b>	7 fibres 400 $\mu\text{m}$ core, 6 light-fibres, 1 read fibre, N.A.= 0,22. Standard 2m length, splitting point in the middle.
<b>Wavelength range</b>	350-2000 (VIS/NIR)
<b>Connectors</b>	SMA905 connectors (2x)
<b>Probe end</b>	Stainless steel cylinder, 50 mm long x 6,35 mm diameter.
<b>Tubing</b>	The optical fibres are protected by a silicon inner tube and a flexible chrome plated brass outer tubing. The tubing also gives stress relief. OD: 5.0 mm
<b>Temperature</b>	-30°C to 100°C. (High Temperature Probe FCR-7UV200-2-ME-HTX)
<b>Bending</b>	Minimum bend radius: Short term (few seconds) 20 mm, long term: 60 mm

Specification quoted from Avantes

## **A.7 Tungsten Halogen Light –Avantes**

The tungsten halogen light was supplied from Avantes. It contains SMA connector for maximizing light coupling into fiber optics and a 10W tungsten halogen lamp. It ventilates by fan cooler.



Picture quoted from Avantes



## **A.8 Petri Dishes**

Petri Dishes were introduced for the measuring the glucose solutions. Orange Brand was used for NIR glucose concentration measurement. They were diameter 90 x 15mm Height, round, sterile and made of Polystyrene (PS) with superior optical clarity and heavy wall for increased strength and stability.

## **A.9 Finger Moulds**

A customized finger mould was used to fix the positions of the subjects' fingers.



## **A.10 Finger Prick Glucose Meter**

Model: Accu-chek Active

Test strips Code: 006

Accu-Chek Control: 2.0 – 3.6 mmol/l, 7.2-9.7mmol/l

## A.11 D-Glucose

Sigma G7528-250G / Batch #: D52k002

D-(+)-Glucose anhydrous sigma ultra, 99.5% (GC)

## A.12 Thermometer

Microprobe Thermometer, BAT – 12, by Physitemp Instruments, Inc

<b>Temperature Range:</b>	-100°C to +200°C
<b>Resolution:</b>	0.1°
<b>Accuracy:</b>	0.1°C ± 1 digit between 0-50°C 0.1% ± 1 digit over full range
<b>Calibration Conformity:</b>	Follows NIST thermocouple tables within 1 digit
<b>Ambient Temperature Compensation:</b>	Auto-compensated to 0.1°C from 0°C to 50°C
<b>Readout:</b>	3 1/2 digits, 1/2" liquid crystal numerals
<b>Input Socket:</b>	Miniature, quick disconnect, copper-constantan
<b>Analog Output:</b>	10mV per degree C, approx.
<b>Power Supply: Model BAT-12</b>	9V transistor battery, available everywhere
<b>Model BAT-12R</b>	AC 115V and Ni-Cad battery with charger
<b>Size, Weight:</b>	5" x 2 1/2" x 6" - 2 lbs., including carrying case

## A.13 Micrometer

Specifications of Series 293, by Mitutoyo Corporation

<b>Measuring Range:</b>	0 to 25mm / 0 to 1"
<b>Resolution:</b>	0.001mm / 0.00005"
<b>Instrumental Error (20°C):</b>	± 2μm (Excluding the quantizing error)
<b>Quantizing Error:</b>	± 1 count
<b>Measurement Force:</b>	5 to 10N
<b>Display:</b>	LCD (6 digits and a minus sign)
<b>Power Supply:</b>	Silver oxide battery (SR44, No. 938882), 1 piece
<b>Battery Life:</b>	1.2 years under normal operation
<b>Operation Temperature Range:</b>	5°C to 40°C
<b>Storage Temperature:</b>	-10°C to 60°C

## **Appendix B: Experiment and Clinical Trials Procedures**

### **B.1 Glucose Solutions Test**

1. Made a large volume glucose solution with 1 mol/l (500ml).
2. Prepared a large amount of distilled water.
3. Marked a petri dish to ensure the position and orientation.
4. Turned on the Tungsten Halogen light for at least 15 minutes to ensure the emitted light stable.
5. Placed the empty petri dish with reference under the light with a fixed position and orientation.
6. Calibrated the background (0%) and the reference (100%) by using NIR-128, which can help to eliminate the background signal.
7. Kept the light on.
8. Use the traditional pipettes (glass) to transfer a fixed volume glucose concentration (1mol/l) to the petri dish.
9. Placed the petri dish under the light again (with the same position and orientation), then started to read the data. Each data (average) was taken from 100 readings.
10. Cleaned the petri dish using distilled water, and dried it with clean tissue paper. (Another approach is to replace a new petri dish)
11. Use the traditional pipettes to add a fixed volume glucose concentration (lower concentration, such as 0.5mol/l, then 0.25mol/l, 0.125mol/l, 0.0625mol/l, and distilled water respectively) to the petri dish. Volume for all solutions was 20 ml.

12. Then repeated 9 to 12 until the test of the distilled water.

During the experiment, the fixed distance of the light to the sample and position must be kept unchanged.

## **B.2 Pilot Studies – Diabetic Subjects**

The clinical trials were performed on type 1 and type 2 diabetic subjects. Ninety-nine patients were recruited in total. Blood sampling was performed after the subjects had been fasting for 10 – 12 hours.

1. A venous blood sample taken for laboratory testing of glucose levels.
2. Measurement of the surface temperature of the index finger
3. Spectrometer calibrations against the background environment.
4. NIR spectroscopic measurement performed.
5. Touching point cleaned by using optical cloth.
6. Item 1 to 5 repeated for each subject.
7. Blood samples sent to the hospital laboratory for glucose measurement.

### **B.3 Pilot Studies – Non-Diabetic Subjects**

The clinical trials were held in the morning after the healthy subjects had fasted for 8-10 hours. The testing was divided into 2 sections, preprandial and postprandial measurement. Finger prick glucose levels were used as the reference. The procedures are shown below.

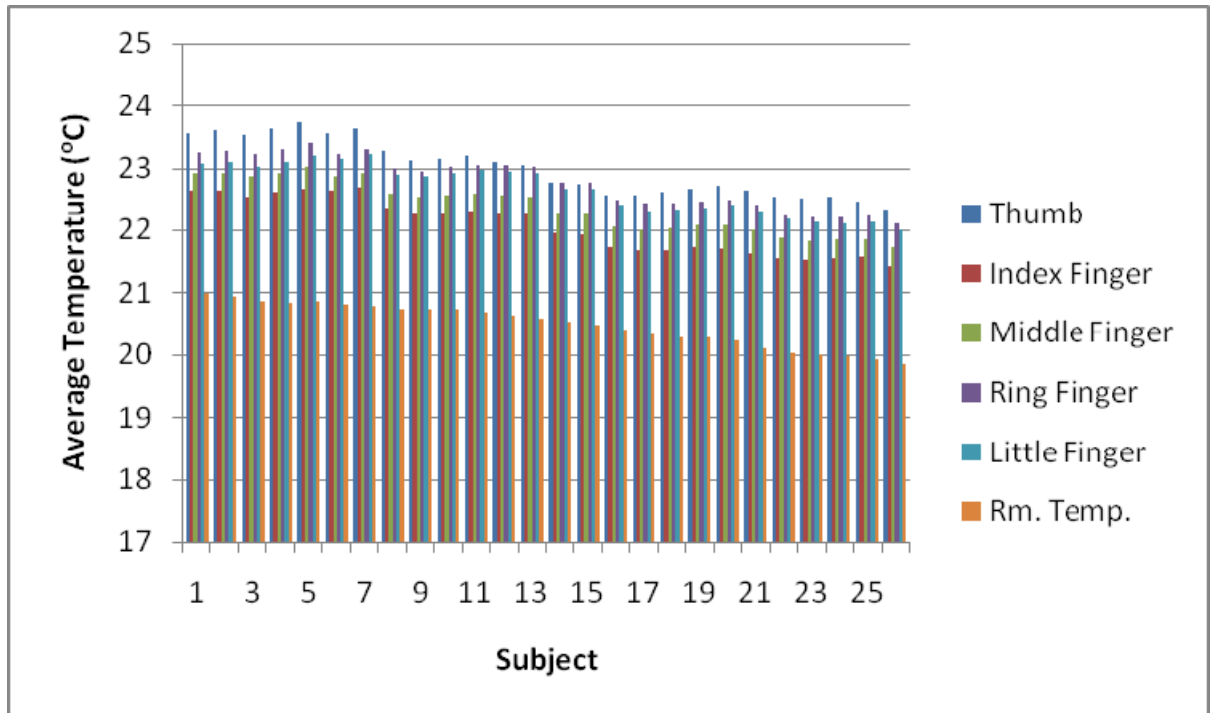
1. Measurement of the finger surface temperature
2. Measurement of the NIR spectra.
3. Finger prick glucose measurement
4. Standard breakfast
5. Returned from the breakfast
6. Provided a sucrose candy before measurement
7. Repeat procedure 1 to 3, in which NIR spectra had been measured twice, ie. two average spectra obtained.

\

## **B.4 Individual Diabetes Glucose Monitoring**

1. **First day and last day** of the procedure-FASTING TEST
  - a. The subjects provided their dietary record within 24 hours.
  - b. Measured blood pressure, heart rate, height and weight (BMI).
  - c. Cleaned with Alcohol swap on the fingers of the left hand.
  - d. Measured the surface temperature of the fingers of the left hand.
  - e. NIR spectra measured from Index, Middle, Ring, Last and Thumb respectively
  - f. Took 6-8ml blood from arm for the plasma test.
  - g. Finger Prick glucose measured.
  - h. Repeated procedures 1 to 6 for each patient.
  - i. Transferred the blood samples (only applicable for first and last day blood sampling) to the lab for testing.
2. Other dates: Casual Glucose test
  - a. The subjects provided their dietary record within 24 hours.
  - b. Cleaned with Alcohol swap on the fingers of the left hand.
  - c. Measured the surface temperature of the fingers of the left hand.
  - d. NIR spectral measured from Index, Middle, Ring, Last and Thumb respectively
  - e. Took 6-8ml blood from arm for the plasma test.
  - f. Finger Prick glucose measured
  - g. Repeated procedures 1 to 6 for each patient.
3. The fingers' thickness had been measured 5 – 7 times by micrometer during the clinical trials period.

## Appendix C: Temperature of Fingers





## References

1. WHO, *Diabetes*, World Health Organization Media Center, **Nov 2008**, Fact Sheet No. 312, <http://www.who.int/mediacentre/factsheets/fs312/en/>.
2. ADA, *Diabetes: Heart Disease and Stroke*, American Diabetes Association, **2006**, <http://www.diabetes.org/diabetes-heart-disease-stroke.jsp>.
3. MedicineNet, *Definition of Finger prick*, MedicineNet, Inc, **2004**, <http://www.medterms.com/script/main/art.asp?articlekey=39540>.
4. Gozani, S, Nerve Damage in Diabetes, *The Harvard Mahoney Neuroscience Institute Letter: On the Brain*, 5, **1996**.
5. Standards of medical care in diabetes--2006, *Diabetes Care*, 29 Suppl 1, **2006**, S4-42.
6. FDA, *Noninvasive Blood Glucose Monitors*, The U.S. Food and Drug Administration, **2003**, <http://diabetes.niddk.nih.gov/dm/pubs/glucosemonitor/index.htm>.
7. Khalil, OS, Spectroscopic and Clinical Aspects of Noninvasive Glucose Measurements, *Clin Chem*, 45, **1999**, 165-177.
8. Raghavachari, R, *Introduction, Near-Infrared Applications in Biotechnology*, Marcel Dekker, New York, **2001**, pp. 1-3.
9. Clarke, WL, Cox, D, Gonder-Frederick, LA, Carter, W and Pohl, SL, Evaluating clinical accuracy of systems for self-monitoring of blood glucose, *Diabetes Care*, 10, **1987**, 622-628.
10. ADA, *All about Diabetes*, American Diabetes Association, **2006**, <http://www.diabetes.org/about-diabetes.jsp>.
11. WHO, *Diabetes Programme: What is Diabetes?* World Health Organization, **2006**, [http://www.who.int/diabetes/BOOKLET\\_HTML/en/index4.html](http://www.who.int/diabetes/BOOKLET_HTML/en/index4.html).
12. WHO, *Diabetes Programme: A rising global burden*, World Health Organization, **2006**.

13. Sarah, W, Sicree, R, Roglic, G, King, H and Green, A, Global Prevalence of Diabetes: Estimates for the year 2000 and projections for 2030, *Diabetes Care*, 27, **2004**, 1047-1053.
14. WHO, *Screening for Type 2 Diabetes*, World Health Organization, **2003**.
15. Diagnosis and classification of diabetes mellitus, *Diabetes Care*, 29 Suppl 1, **2006**, S43-48.
16. *Ketoacidosis*, American Diabetes Association, American Diabetes Association, <http://www.diabetes.org/type-1-diabetes/ketoacidosis.jsp>.
17. Barclay, L and Lie, D, *Dietitian Management Helpful in Obese Patients With Type 2 Diabetes*, Medscape Medical News, **2004**.
18. Mayfield, J, *Diagnosis and Classification of Diabetes Mellitus: New Criteria*, the American Academy of Family Physicians, **1998**.
19. Implications of the Diabetes Control and Complications Trial, *Diabetes Care*, 26, **2003**, 25S-27.
20. *Complications of Diabetes*, Juvenile Diabetes Research Foundation, **2005**, Diabetes Fact Sheets.
21. Turner, APF, Chen, B and Piletsky, SA, In Vitro Diagnostics in Diabetes: Meeting the Challenge, *Clin Chem*, 45, **1999**, 1596-1601.
22. Brown, CD, Davis, HT, Ediger, MN, Fleming, CM, Hull, EL and Rohrscheib, M, Clinical assessment of near-infrared spectroscopy for noninvasive diabetes screening, *Diabetes Technol Ther*, 7, **2005**, 456-466.
23. Gebhart, S, Faupel, M, Fowler, R, Kapsner, C, Lincoln, D, McGee, V, Pasqua, J, Steed, L, Wangsness, M, Xu, F and Vanstory, M, Glucose sensing in transdermal body fluid collected under continuous vacuum pressure via micropores in the stratum corneum, *Diabetes Technol Ther*, 5, **2003**, 159-166.
24. Kulcu, E, Tamada, JA, Reach, G, Potts, RO and Lesho, MJ, Physiological Differences Between Interstitial Glucose and Blood Glucose Measured in Human Subjects, *Diabetes Care*, 26, **2003**, 2405-2409.
25. *User Manual: ACCU-CHEK Active -Test Strips*, Roche Diagnostics GmbH, **2004**.

26. *Glucose*, American Association for Clinical Chemistry, **2005**,  
<http://www.labtestsonline.org/understanding/analytes/glucose/test.html>.
27. Pitzer, KR, Desai, S, Dunn, T, Edelman, S, Jayalakshmi, Y, Kennedy, J, Tamada, JA and Potts, RO, Detection of hypoglycemia with the GlucoWatch biographer, *Diabetes Care*, **24**, **2001**, 881-885.
28. Hathout, E, Patel, N, Southern, C, Hill, J, Anderson, R, Sharkey, J, Hadley-Scofield, M, Tran, L, Leptien, A, Lopatin, M, Wang, B, Mace, J and Eastman, R, Home use of the GlucoWatch G2 biographer in children with diabetes, *Pediatrics*, **115**, **2005**, 662-666.
29. Gandrud, LM, Paguntalan, HU, Van Wyhe, MM, Kunselman, BL, Leptien, AD, Wilson, DM, Eastman, RC and Buckingham, BA, Use of the Cygnus GlucoWatch biographer at a diabetes camp, *Pediatrics*, **113**, **2004**, 108-111.
30. *About the Guardian® RT Continuous Glucose Monitoring System*, Medtronic MiniMed, Inc., **2006**.
31. Jeckelmann, J and Seibold, A, *GlucOnline - a new approach to continuous glucose monitoring*, diabetesprofile, **2002**.
32. Meiki, V and Hanaire-Broutin, H, Indication of CGMS (Continuous Glucose Monitoring System) in the functional investigations of adult type 1 diabetic patients., *Diabetes Metab (Paris)*, **27**, **2001**, 618-623.
33. Choleau, C, Dokladal, P, Klein, J-C, Ward, WK, Wilson, GS and Reach, G, Prevention of Hypoglycemia Using Risk Assessment With a Continuous Glucose Monitoring System, *Diabetes*, **51**, **2002**, 3263-3273.
34. *History: Medtronic MiniMed, Inc.*, Medtronic MiniMed, Inc., **2006**,  
<http://www.minimed.com/about/history.html>.
35. *FDA APPROVES GLUCOWATCH DEVICE FOR CHILDREN WITH DIABETES*, U.S. Food and Drug Administration, **2002**.
36. *FDA Approval Letter: DexCom™ STS™ Continuous Glucose Monitoring System*, Department of Health and Human Services, U.S. Food and Drug Administration, **2006**.

37. *New Device Approval: DexCom™ STS™ Continuous Glucose Monitoring System - P050012*, Department of Health and Human Services, U.S. Food and Drug Administration, **2006**.
38. Leboulanger, B, Guy, RH and Delgado-Charro, MB, Reverse iontophoresis for non-invasive transdermal monitoring, *Physiol Meas*, **25**, **2004**, R35-50.
39. *Animas Glucowatch*, Diabetes Services, Inc., **2005**.
40. Tierney, MJ, *Transdermal glucose monitoring opens a new age of diabetes management*, IVD Technology, **2003**.
41. *Diabetes: Continuous Glucose Monitoring*, (Ed. C. Haines), WebMD, Inc., **2005**.
42. Moschou, EA, Sharma, BV, Deo, SK and Daunert, S, Fluorescence glucose detection: advances toward the ideal in vivo biosensor, *J Fluoresc*, **14**, **2004**, 535-547.
43. Sierra, JF, Galban, J and Castillo, JR, Determination of Glucose in Blood Based on the Intrinsic Fluorescence of Glucose Oxidase, *Anal. Chem.*, **69**, **1997**, 1471-1476.
44. Ballerstadt, R and Schultz, JS, A Fluorescence Affinity Hollow Fiber Sensor for Continuous Transdermal Glucose Monitoring, *Anal. Chem.*, **72**, **2000**, 4185-4192.
45. Rosencwaig, A, *Photoacoustics and Photoacoustic Spectroscopy*, Chemical Analysis, Eds.: P. J. Elving and J. D. Winefordner), John Wiley & Sons, New York, **1996**, pp. 1-5.
46. Rosencwaig, A, *Photoacoustics and Photoacoustic Spectroscopy*, Chemical Analysis, Eds.: P. J. Elving and J. D. Winefordner), John Wiley & Sons, New York, **1996**, pp. 49-50, 83-84.
47. Hao, LY, Ren, Z, Shi, Q, Wu, JL, Zheng, Y, Zheng, JJ and Zhu, QS, A new cylindrical photoacoustic cell with improved performance, *Review Of Scientific Instruments*, **73**, **2002**, 404-410.
48. Duncan, A, Hannigan, J, Freeborn, SS, Rae, PW, Melver, B, Greig, F, Johnston, EM, Binnie, DT and MacKenzie, HA, A Portable Non-invasive Blood Glucose Monitor, *The 8th International Conference On Solid-State Sensors And Actuators And Eurosensors IX* **1995**.

49. MacKenzie, HA, Ashton, HS, Spiers, S, Shen, Y, Freeborn, SS, Hannigan, J, Lindberg, J and Rae, P, Advances in photoacoustic noninvasive glucose testing, *Clin Chem*, 45, **1999**, 1587-1595.
50. Kinnunen, M and Myllyla, R, Effect of glucose on photoacoustic signals at wavelengths of 1064 and 532nm in pig blood and intralipid, *Journal of Physics D: Applied Physics*, 38, **2005**, 2654-2661.
51. Zhao, Z, *Pulsed photoacoustic techniques and glucose determination in human blood and tissue*, Department of Electrical Engineering and Infotech Oulu, University of Oulu, **2002**, pp. 101-104.
52. Huang, D, Swanson, EA, Lin, CP, Schuman, JS, Stinson, WG, Chang, W, Hee, MR, Flotte, T, Gregory, K, Puliafito, CA and et al., Optical coherence tomography, *Science*, 254, **1991**, 1178-1181.
53. Fujimoto, JG, *Optical Coherence Tomography: Introduction*, Handbook of Optical Coherence Tomography, Eds.: b. E. Bouma and G. J. Tearney), Marcel Dekker, Inc, New York, **2002**, pp. 1-3.
54. Esenaliev, RO, Larin, KV and Larina, IV, Noninvasive Monitoring of Glucose Concentraion with Optical Coherence Tomography, *Optics Letters*, **2001**.
55. Larin, KV, Eledrisi, MS, Motamedi, M and Esenaliev, RO, Noninvasive blood glucose monitoring with optical coherence tomography: a pilot study in human subjects, *Diabetes Care*, 25, **2002**, 2263-2267.
56. Larin, KV, Motamedi, M, Ashitkov, TV and Esenaliev, RO, Specificity of noninvasive blood glucose sensing using optical coherence tomography technique: a pilot study., *Physics in Medicine and Biology*, 48, **2003**, 1371-1390.
57. Kinnunen, M, Myllyla, R, Jokela, T and Vainio, S, In vitro studies toward noninvasive glucose monitoring with optical coherence tomography, *Appl Opt*, 45, **2006**, 2251-2260.
58. Koolman, J and Roehm, KH, *Color Atlas of Biochemistry, 2nd Edition*, Thieme, Stuttgart, New York, **2005**, pp. 35-36.

59. Youcef-Toumi, K and Saptari, VA, *Noninvasive Blood Glucose Quantitation using Spectroscopic-based Optical Technique*, MIT: Home Automation and Healthcare Consortium, **1998**,  
<http://darbelofflab.mit.edu/ProgressReports/HomeAutomation/98%20Reports/Youcef-Toumi.pdf>.
60. Cote, GL, Fox, MD and Northrop, RB, Noninvasive optical polarimetric glucose sensing using a true phase measurement technique, *Biomedical Engineering*, **39**, **1992**, 752-756.
61. Cote, D and Vitkin, IA, Balanced detection for low-noise precision polarimetric measurements of optically active, multiply scattering tissue phantoms, *Journal of Biomedical Optics*, **9**, **2004**, 213-220.
62. Ansari, RR, Bockle, S and Rovati, L, New optical scheme for a polarimetric-based glucose sensor, *Journal of Biomedical Optics*, **9**, **2004**, 103-115.
63. Wan, Q, Cote, GL and Brandon, DJ, Dual-wavelength polarimetry for monitoring glucose in the presence of varying birefringence, *Journal of Biomedical Optics*, **10**, **2005**, 024029-024021-024028.
64. Tu, AT, *Raman Spectroscopy in Biology: Principles & Applications*, John Wiley & Sons, **1982**, pp. 7-10.
65. McCreery, RL, *Raman Spectroscopy for Chemical Analysis*, Chemical Analysis, (Ed. J. D. Winefordner), John Wiley & Sons, New York, **2000**, p. 15.
66. Nafie, LA, *Theory of Raman Scattering, Vol. a* (Eds.: I. R. Lewis and H. G. M. Edwards), Marcel Dekker, Inc., New York, **2001**, pp. 1-2.
67. Tu, AT, *Raman Spectroscopy in Biology: Principles & Applications*, John Wiley & Sons, **1982**, pp. 45-47.
68. Workman, J, *Methods and interpretations*, Handbook of Organic Compounds, Academic Press, San Diego, **2001**, p. 78.
69. Berger, AJ, Itzkan, I and Feld, MS, Feasibility of measuring blood glucose concentration by near-infrared Raman spectroscopy, *Spectrochimica Acta Part A*, **53**, **1997**, 287-292.

70. Yonzon, CR, Haynes, CL, Zhang, X, Walsh, JT and Van Duyne, RP, A Glucose Biosensor Based on Surface-Enhanced Raman Scattering: Improved Partition Layer, Temporal Stability, Reversibility, and Resistance to Serum Protein Interference, *Analytical Chemistry*, **76**, **2004**, 78-85.
71. Lyandres, O, Shah, NC, Yonzon, CR and Walsh Jr., JT, Real-Time Glucose Sensing by Surface-Enhanced Raman Spectroscopy in Bovine Plasma Facilitated by a Mixed Decanethiol/Mercaptohexanol Partition Layer, *Analytical Chemistry*, **2005**, A-F.
72. Lambert, J, Storrie-Lombardi, M and Borchert, M, *Measurement of Physiologic Glucose Levels Using Raman Spectroscopy in a Rabbit Aqueous Humor Model*, IEEE, **1998**.
73. Enejder, AM, Seccina, TG, Oh, J, Hunter, M, Shih, WC, Sasic, S, Horowitz, GL and Feld, MS, Raman spectroscopy for noninvasive glucose measurements, *J Biomed Opt*, **10**, **2005**, 031114.
74. Tittel, FK, Richter, D and Fried, A, Mid-Infrared Laser Applications in Spectroscopy, *Appl Phys*, **89**, **2003**, 445-516.
75. Kim, YJ, Hahn, S and Yoon, G, Determination of glucose in whole blood samples by mid-infrared spectroscopy, *Appl Opt*, **42**, **2003**, 745-749.
76. Martin, WB, Mirov, S and Venugopalan, R, Using two discrete frequencies within the middle infrared to quantitatively determine glucose in serum, *Journal of Biomedical Optics*, **7**, **2002**, 613-617.
77. Heise, HM, Marbach, R, Janatsch, G and Kruse-Jarres, JD, Multivariate determination of glucose in whole blood by attenuated total reflection infrared spectroscopy, *Anal Chem*, **61**, **1989**, 2009-2015.
78. Malchoff, CD, Shoukri, K, Landau, JI and Buchert, JM, A novel noninvasive blood glucose monitor, *Diabetes Care*, **25**, **2002**, 2268-2275.
79. Heise, HM and Marbach, R, Human oral mucosa studies with varying blood glucose concentration by non-invasive ATR-FT-IR-spectroscopy, *Cell Mol Biol (Noisy-le-grand)*, **44**, **1998**, 899-912.
80. Heise, HM, Bittner, A and Marbach, R, Clinical chemistry and near infrared spectroscopy: technology for non-invasive glucose monitoring, *Journal of Near Infrared Spectroscopy*, **6**, **1998**, 349-359.

81. Heise, HM, Non-invasive monitoring of metabolites using near infrared spectroscopy: state of the art, *Horm Metab Res*, 28, **1996**, 527-534.
82. Qu, J and Wilson, BC, Monte Carlo modeling studies of the effect of physiological factors and other analytes on the determination of glucose concentration in vivo by near infrared optical absorption and scattering measurements, *Journal of Biomedical Optics*, 2, **1997**, 319-325.
83. *Introduction to NIR Technology*, Analytical Spectral Devices, Inc., **2005**, <http://www.asdi.com>.
84. Kelly, JJ, Kelly, KA and Barlow, CH, Tissue temperature by near-infrared spectroscopy, *Optical Tomography, Photon Migration, and Spectroscopy of Tissue and Model Media: Theory, Human Studies, and Instrumentation* **1995**, pp. 818-828.
85. Heise, HM, Technology for Non-Invasive Monitoring of Glucose, *18th Annual International Conference of the IEEE Engineering in Medicine and Biology Society* (Amsterdam) **1996**.
86. Maruo, K, Chin, J and Tamura, M, Noninvasive Blood Glucose Monitoring by Novel Optical Fiber Probe, *Optical Diagnostics and Sensing of Biological Fluids and Glucose and Cholesterol Monitoring II* **2002**.
87. Maruo, K, Tsurugi, M, Tamura, M and Ozaki, Y, In vivo noninvasive measurement of blood glucose by near-infrared diffuse-reflectance spectroscopy, *Appl Spectrosc*, 57, **2003**, 1236-1244.
88. Maruo, K, Tsurugi, M, Chin, J, Ota, T, Arimoto, H and Yamada, Y, Noninvasive Blood Glucose Assay Using a Newly Developed Near-Infrared System, *Journal of Selected Topics in quantum Electronics*, 9, **2003**, 322-330.
89. Robinson, MR, Eaton, RP, Haaland, DM, Koepp, GW, Thomas, EV, Stallard, BR and Robinson, PL, Noninvasive glucose monitoring in diabetic patients: a preliminary evaluation, *Clin Chem*, 38, **1992**, 1618-1622.
90. Heise, HM and Lampen, P, Transcutaneous glucose measurements using near-infrared spectroscopy: validation of statistical calibration models, *Diabetes Care*, 23, **2000**, 1208-1210.
91. Heise, HM, Bittner, A and Marbach, R, Near-infrared reflectance spectroscopy for noninvasive monitoring of metabolites, *Clin Chem Lab Med*, 38, **2000**, 137-145.



92. Youcef-Toumi, K and Saptari, VA, *noninvasive blood glucose analysis using near infrared absorption spectroscopy*, MIT d'Arbeloff Laboratory for Information Systems and Technology, **1999**, pp. 1-22.
93. Youcef-Toumi, K and Saptari, VA, *noninvasive blood glucose analysis using near infrared absorption spectroscopy*, MIT d'Arbeloff Laboratory for Information Systems and Technology, **2000**, pp. 1-7.
94. Riley, MR and Crider, HM, The effect of analyte concentration range on measurement errors obtained by NIR spectroscopy, *Talanta*, **52**, **2000**, 473.
95. Smith, C, Marks, A and Lieberman, M, *Basic Medical Biochemistry: A Clinical Approach*, Lippincott William & Wilkins, Philadelphia, **2005**, pp. 3-7.
96. Smith, C, Marks, A and Lieberman, M, *Basic Medical Biochemistry: A Clinical Approach*, Lippincott William & Wilkins, Philadelphia, **2005**, pp. 493-500.
97. Benyon, S, *Metabolism and Nutrition*, Elsevier Science Ltd, London, **2003**, pp. 1-2.
98. Smith, C, Marks, A and Lieberman, M, *Basic Medical Biochemistry: A Clinical Approach*, Lippincott William & Wilkins, Philadelphia, **2005**, pp. 477-491.
99. Kotz, JC, Treichel, PM and Weaver, GC, *Chemistry and Chemical Reactivity, Vol.* Thomson Brooks/Cole, Toronto, **2006**.
100. *Monosaccharides -- Structure of Glucose*, Chemistry 240, Summer 2001, California State University, Dominguez Hills, **2001**,  
<http://chemistry2.csudh.edu/rpendarvis/monosacch.html#cyclose>.
101. Arnold, SA, Harvey, LM, McNeil, B and Hall, JW, *Employing Near-Infrared Spectroscopic Methods of Analysis for Fermentation Monitoring and Control, Part 1, Method Development*, BioPharm International, **2002**.
102. Mckesson, *Diabetes: Self Blood Glucose Monitoring (SBGM)*, Mckesson Provider Technologies, **2005**,  
[http://www.med.umich.edu/1libr/pa/pa\\_selfgluc\\_hhg.htm](http://www.med.umich.edu/1libr/pa/pa_selfgluc_hhg.htm).
103. McGarraugh, G, Schwartz, S and Weinstein, R, *Glucose Measurement Using Blood Extracted from the Forearm and the Finger*, **2001**.

104. Mukaibo, Y, Shirado, H, Konyo, M and Maeno, T, Development of a Texture Sensor Emulating the Tissue Structure and Perceptual Mechanism of Human Fingers, *International Conference on Robotics and Automation* (Barcelona, Spain) **2005**, pp. 2576-2581.
105. Chen, W, Liu, R, Xu, K and Wang, RK, Influence of contact state on NIR diffuse reflectance spectroscopy in vivo, *Journal of Physics D: Applied Physics*, **38**, **2005**, 2691-2695.
106. Mitri, GM, Lucas, M, Fertig, N, Steen, VD and Medsger, TA, A Comparison Between Anti-Th/To–and Anticentromere Antibody–Positive Systemic Sclerosis Patients With Limited Cutaneous Involvement, *ARTHRITIS & RHEUMATISM*, **48**, **2003**.
107. Moon, SJ and Lee, SS, A novel fabrication method of a microneedle array using inclined deep x-ray exposure, *Journal of Micromechanics and Microengineering*, **15**, **2005**, 903-911.
108. Mason, D, JPG, (Ed. s. structure), TalkHealth Partnership Ltd., [http://www.talkacne.com/image\\_01/products/Skin\\_Structure1.jpg](http://www.talkacne.com/image_01/products/Skin_Structure1.jpg).
109. Hall, JW and Pollard, A, Near-infrared spectrophotometry: a new dimension in clinical chemistry, *Clin Chem*, **38**, **1992**, 1623-1631.
110. Burmeister, JJ and Arnold, MA, *Spectroscopic Considerations for Noninvasive Blood Glucose Measurements with Near Infrared Spectroscopy*, IEEE, **1998**.
111. Hazen, KH, Welch, M, Ruchti, TL, Lorenz, AD and Blank, TB, *Construction of a Family of Tissue Simulating Phantoms for Glucose Determination Using Diffuse Reflectance Near-IR Spectroscopy*, Instrumentation Metrics, Inc., Detroit, **2001**.
112. Troy, TL and Thennadil, SN, Optical properties of human skin in the near infrared wavelength range of 1000 to 2200nm, *Journal of Biomedical Optics*, **6**, **2001**, 167-176.
113. Amerov, AK, Sun, Y, Small, GW and Arnold, MA, Kromoscopic measurement of glucose in the first overtone region of the near infrared spectrum, *Optical Diagnostics and Sensing of Biological Fluids and Glucose and Cholesterol Monitoring II* **2002**, pp. 11-19.

114. Ruchti, TL, Thennadil, SN, Blank, TB, Lorenz, A and Monfre, SL, *Noninvasive measurement of glucose through the optical properties of tissue*, (Ed. U. S. Patent), United States of America, **2006**,  
<http://www.freepatentsonline.com/6990364.html>.
115. Olesberg, JT, Liu, L, Zee, VV and Arnold, MA, In Vivo Near-Infrared Spectroscopy of Rat Skin Tissue with Varying Blood Glucose Levels, *Analytical Chemistry*, **78**, **2006**, 215-223.
116. Malin, SF, Ruchti, TL, Blank, TB, Thennadil, SN and Monfre, SL, Noninvasive Prediction of Glucose by Near-Infrared Diffuse Reflectance Spectroscopy, *Chinical Chemistry*, **45**, **1999**, 1651-1658.
117. Danzer, K, Fischbacher, C, Jagemann, KU and Reichelt, KJ, *Near-Infrared Diffuse Reflection Spectroscopy for Non-Invasive Blood-Glucose Monitoring*, IEEE, **1998**.
118. Blank, TB, Ruchti, TL, Malin, SF and Monfre, SL, *The Use of Near-Infrared Diffuse Reflectance for the Non-Invasive Prediction of Blood Glucose Levels*, IEEE, **1999**.
119. Blank, TB, Ruchti, TL, Lorenz, AD, Monfre, SL, Makarewicz, MR, Mattu, M and Hazen, KH, Clinical Results from a Non-invasive Blood Glucose Monitor, *Optical Diagnostics and Sensing of Biological Fluids and Glucose and Cholesterol Monitoring II* **2002**, pp. 1-10.
120. Liu, R, Chen, W, Gu, X, Wang, RK and Xu, K, Chance correlation in non-invasive glucose measurement using near-infrared spectroscopy, *Journal of Physics D: Applied Physics*, **38**, **2005**, 2675-2681.
121. Tarumi, M, Shimada, M, Murakami, T, Tamura, M, Shimada, M and Yamada, Y, A Monte Carlo Simulation of NIR spectrum Changes Induced by Variations of Glucose Concentration, *Optical Diagnostics and Sensing of Biological Fluids and Glucose and Cholesterol Monitoring II* **2002**, pp. 28-35.
122. Tarumi, M, Shimada, M, Murakami, T, Tamura, M, Shimada, M, Arimoto, H and Yamada, Y, Simulation study of in vitro glucose measurement by NIR spectroscopy and a method of error reduction, *Physics in Medicine and Biology*, **48**, **2003**, 2373-2390.

123. Kawano, S and Abe, H, Development of a calibration equation with temperature compensation for determining the Brix value in intact peaches, *Journal of Near Infrared Spectroscopy*, 3, **1995**, 211-218.
124. Abe, H, A study on the universality of a calibration with sample temperature compensation, *Journal of Near Infrared Spectroscopy*, 8, **2000**, 209-213.
125. Yeh, S-j, Hanna, CF and Khalil, OS, Monitoring Blood Glucose Changes in Cutaneous Tissue by Temperature-modulated Localized Reflectance Measurements, *Clin Chem*, 49, **2003**, 924-934.
126. Khalil, OS, Yeh, S-j, Lowery, MG, Wu, X, Hanna, CF, Kantor, S, Jeng, T-W, Kanger, JS, Bolt, RA and Mul, FFd, Temperature modulation of the visible and near infrared absorption and scattering coefficients of human skin, *Journal of Biomedical Optics*, 8, **2003**, 191-205.
127. McGarraugh, G, Price, D, Schwartz, S and Weinstein, R, Physiological influences on off-finger glucose testing, *Diabetes Technol Ther*, 3, **2001**, 367-376.
128. Burmeister, JJ and Arnold, MA, Evaluation of Measurement Sites for Noninvasive Blood Glucose Sensing with Near-Infrared Transmission Spectroscopy, *Clin Chem*, 45, **1999**, 1621-1627.
129. Burmeister, JJ, Arnold, MA and Small, GW, Noninvasive blood glucose measurements by near-infrared transmission spectroscopy across human tongues, *Diabetes Technol Ther*, 2, **2000**, 5-16.
130. Bina, DM, Anderson, RL, Johnson, ML, Bergenstal, RM and Kendall, DM, Clinical Impact of Prandial State, Exercise, and Site Preparation on the Equivalence of Alternative-Site Blood Glucose Testing, *Diabetes Care*, 26, **2003**, 981-985.
131. Marbach, R, Koschinsky, Th, Gries, FA and Heise, HM, Noninvasive Blood Glucose Assay by Near-Infrared Diffuse Reflectance Spectroscopy of the Human Inner Lip, *Applied Spectroscopy*, 47, **1993**, 875-881.
132. Schrader, W, Meuer, P, Popp, J, Kiefer, W, Menzebach, J-U and Schrader, B, Non-invasive glucose determination in the human eye, *Journal of Molecular Structure*, 735-736, **2005**, 299.

133. Hoskuldsson, A, PLS Regression Methods, *Journal of Chemometrics*, 2, **1988**, 211-228.
134. Arnold, MA, Burmeister, JJ and Small, GW, Phantom glucose calibration models from simulated noninvasive human near-infrared spectra, *Anal Chem*, 70, **1998**, 1773-1781.
135. Jeon, KJ, Hwang, ID, Hahn, S and Yoon, G, Comparison between transmittance and reflectance measurements in glucose determination using near infrared spectroscopy, *Journal of Biomedical Optics*, 11, **2006**, 014022-014021 -014027.
136. *Spectrometer Software Application Manual*, Control Development, Inc., **2003**.
137. Tobias, RD, *An Introduction to Partial Least Squares Regression*, SAS Institute Inc.
138. Davies, AMC and Fearn, T, Back to basics: observing PLS, *SpectroscopyEurope*, 17, **2005**, 28-29.
139. *Partial Least Square (PLS)*, StatSoft, Inc, **2003**,  
<http://www.statsoft.com/textbook/stpls.html>.
140. Trygg, J, *Have you ever wondered why PLS sometimes needs more than one component for a single-y vector?* Homepage of Chemometrics, **2002**.
141. Rosipal, R and Kramer, N, *Overview and Recent Advances in Partial Least Squares*, Springer-Verlag Berlin Heidelberg, **2006**.
142. Kleinknecht, W, *A statistician's view of single-Y PLS problem*, Homepage of Chemometrics, **June 2002**.
143. Jong, Sd, SIMPLS: An alternative approach to partial least squares regression, *Chemometrics and Intelligent Laboratory Systems*, 18, **March 1993**, 251-263.
144. Serneels, S and Espen, PJV, *Sample specific prediction intervals in SIMPLS*, Universiteit Antwerpen.
145. Savitsky, A and Golay, MJE, Smoothing and differentiation of data by simplified least squares procedures, *Anal Chem*, 36, **1964**, p.1639.
146. Gorry, PA, General Least-Squares Smoothing and Differentiation by the Convolution(Savitzky-Golay) Method, *Anal Chem*, 62, **1990**, pp. 570-573.

147. Madden, HH, Comments on the Savitzky-Golay Convolution Method for Least-Squares Fit Smoothing and Differentiation of Digital Data, *Analytical Chemistry*, 50, **1978**, pp. 1383-1386.
148. Ana Herrero, MCO, Piecewise Direct Standardization Method Applied to the Simultaneous Determination of Pb(II), Sn(IV) and Cd(II) by Differential Pulse Polarography, *Electroanalysis*, 10, **1998**, pp. 717-721.
149. Li, B and Gupta, R, Optical Saturation in Continuous-Wave Photothermal Deflection Spectroscopy: Quantitative Investigation of Fundamental and Harmonic Components, *Applied Optics*, 40, **2001**, pp. 1563-1569.
150. Jorgensen, B and Goegebeur, Y, *Multivariate Data Analysis and Chemometrics.*, Department of Statistic, University of Southern Denmark, **2006**.
151. Arimoto, H, Tarumi, M and Yamada, Y, Temperature-Insensitive Measurement of Glucose Concentration Based on Near Infrared Spectroscopy and Partial Least Squares Analysis, *Optical Review*, 10, **2003**, pp. 74-76.
152. Mark, H, *Fundamentals of Near-Infrared Spectroscopy*, Near-Infrared Applications in Biotechnology, Marcel Dekker, New York, **2001**, p. 301.
153. Chen, J, Arnold, MA and Small, GW, Comparison of Combination and First Overtone Spectral Regions for Near-Infrared Calibration Models for Glucose and Other Biomolecules in Aqueous Solutions, *Anal. Chem.*, 76, **2004**, pp. 5405-5413.
154. Bromba, MUA and Zlegler, H, Application Hints for Savitzky-Golay Digital Smoothing Filters, *Anal Chem*, 53, **1981**, pp. 1583-1586.
155. Hampton, KA, Wutzke, JL, Cavinato, AG, Mayes, DM, Lin, M and Rasco, BA, Characterization of Optical Probe Light Penetration Depth for Noninvasive Analysis, *Eastern Oregon science journal*, 18, **2002-2003**.
156. Cui, H, An, L, Chen, W and Xu, K, Quantitative effect of temperature to the absorbance of aqueous glucose in wavelength range from 1200nm to 1700nm, *Optics Express*, 13, **2005**, pp. 6887-6891.
157. Jeon, KJ, Hahn, S, Hwang, ID and Yoon, G, Factor analysis for comparing NIR reflection and transmittance for noninvasive glucose measurement, *Advanced Biomedical and Clinical Diagnostic Systems II* **2004**.

158. FDA, *Glucose Meters & Diabetes Management*, U.S. Food and Drug Administration, **2005**, <http://www.fda.gov/diabetes/glucose.html#2>.
159. Samann, A, Fischbacher, CH, Jagemann, KU, Danzer, K, Schuler, J, Papenkordt, L and Muller, UA, Non-invasive blood glucose monitoring by means of near infrared spectroscopy: investigation of long-term accuracy and stability, *Exp Clin Endocrinol Diabetes*, *108*, **2000**, pp. 406-413.
160. Health, CfDaR, *Draft Guidance for Industry and FDA Staff - Total Product Life Cycle for Portable Invasive Blood Glucose Monitoring Systems*, Food and Drug Administration, **2006**, <http://www.fda.gov/cdrh/oivd/guidance/1603.html>.
161. Yuan, B, Murayama, K, Wu, Y, Tsenkova, R, Dou, X, Era, S and Ozaki, Y, Temperature-Dependent Near-Infrared Spectra of Bovine Serum Albumin in Aqueous Solutions: Spectral Analysis by Principle Component Analysis and Evolving Factor Analysis, *Applied Spectroscopy*, *57*, **2003**, pp. 1223-1229.